DOCUMENT NO. 87SDS-024
CONTRACT NAS1-18032
MAY 1987

THE MULTI-DISCIPLINARY DESIGN STUDY A LIFE CYCLE COST ALGORITHM

R.R. HARDING, J.M. DURAN, AND R.R. KAUFFMAN

GENERAL ELECTRIC COMPANY - ASTRO-SPACE DIVISION
KING OF PRUSSIA, PA 19406

NASA CONTRACTOR REPORT 178192

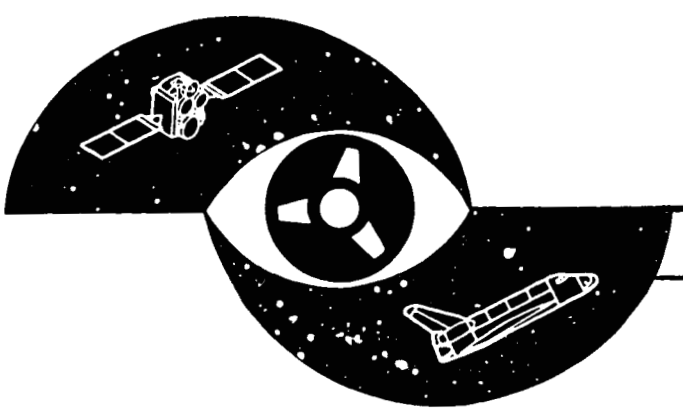

ASTRO-Space Division

GENERAL ELECTRIC

NASA Contractor Report 178192

The Multi-Disciplinary Design Study A Life Cycle Cost Algorithm

R.R. Harding, J.M. Duran, and R.R. Kauffman

General Electric Company - Astro Space Division
King of Prussia. PA 19406

Contract NAS1-18032

May 1987

National Aeronautics and
Space Administration

Langley Research Center
Hampton, Virginia 23665-5225

CONTENTS

1 INTRODUCTION

The Multi-disciplinary Design (MDD) Study investigates three aspects of manned Space Station design; cost, subsystem design parameters, and relationships between cost and design parameters. It is anticipated that complex spacecraft designs will be based on total system costs over the life of the program. An approach to evaluating system design for the complete Life Cycle Costs (LCC) is desirable so that total program costs may be assessed for any given design and, thereby provide a means to trade cost, risk, performance, and maintenance during the design phase. This study develops a model which spans these different disciplines in effort to evaluate LCC, or more importantly, LCC sensitivities to different designs and critical parameters.

First, the cost factors of the system from conceptual design through on-orbit operations are defined so that cost analyses can be estimated within the accuracy of the assumptions. These cost factors include nonrecurring, spares, ground support, etc. which are typical for spacecraft and can be estimated based on historical data or engineering judgement.

Second, the relationships between Space Station subsystem design parameters which define the configuration of the subsystem are examined. For this study, the relationships between the attitude control and structure subsystem designs are investigated by using analysis techniques that have been applied to previous spacecraft designs. For example, the structure mass properties affect controller momentum storage, torque, and bandwidth

requirements which in turn affect hardware and software requirements.

The final phase of this study combined LCC and subsystem design parameters into a set of computations implemented in a single computer program. At this point, the computer program is truly multi-disciplinary. The Multi-disciplinary Design Tool (MDDT) is the name of the computer program which contains the controls and structural design and LCC models. It is capable of performing design studies by evaluating different ACS (Attitude Control System) and structure designs as a function of LCC.

2 SUMMARY

This study developed a multi-disciplinary design model, implemented on the computer, that is used to evaluate attitude control and structure subsystem designs using LCC as a design criteria. Engineering design parameters which define ACS (Attitude Control System) and structure designs are input to the program and resulting LCC and some performance data are output to the user for evaluation.

The Multi-disiplinary Design Study has investigated LCC aspects of the manned Space Station attitude control and structure subsystems designs. The model adresses the major cost aspects for spacecraft in general and the Space Station in particular (for example, costs for Extra Vehicular Activity (EVA), replenishment of expendables, and the latest baseline Space Station hardware). Several example design trades have been performed using the Multi-disciplinary Design Tool which demonstrate the program validity as well as provide some interesting cost saving design approaches.

A summary of the MDD study efforts and cost program flow is shown in Figure 1. It can be seen from this top level diagram that several preliminary analyses and hardware investigations were necessary to define ACS and structure design parameters as well as obtain some basic cost data. These preliminary investigations resulted in general design parameters required to describe ACS and structure configurations as well as representative hardware costs and cost sensitivities (e.g.

$/pound, orbit decay rates, damping material cost estimates, ACS sensor costs, etc.)

The MDDT model architecture spans the following LCC characteristics for the Space Station ACS and structure designs.

Non-recurring design

Launch

Expendable replenishment

Part failure, replacement, and maintenance

Ground support

The architecture of MDDT incorporates the above LCC characteristics in individual subroutines. The MDDT main program is a series of calls to these subroutines so that the ACS and structure costs can be calculated. Each of the above LCC criteria incorporates a number of sub-level cost parameters which can be, and in many cases are, used in other LCC criteria calculations.

Results of specific trade studies (as required in the Statement of Work) and example LCC design trades are summarized in the following paragraphs.

Preliminary Attitude Control Optimization. The ACS (Attitude Control System) did not prove cost sensitive in the preliminary analysis. Instead, optimization of the ACS was based on creating a maximum controller bandwidth for a user

specified fundamental structural resonant frequency. Cost of the ACS as an optimization criteria was accomplished after the MDDT model was sophisticated enough to include active structural damping designs.

Structural Resonance Sensitivity. The controlled Space Station response to crew kick-off and STS docking was performed using a flexible body simulation of the Space Station. The structural response of the lower boom resulting from these disturbances are 12 arcseconds and 1860 arcseconds (0.52 degrees) of deflection for crew and docking disturbances, respectively.

Preliminary Structural Optimization. The five meter bay truss resulted in significant LCC savings over the nine foot bay truss; approximately $47 million saved for the erectable and $67 million for the for the deployable.

Solar Array Feathering. Feathering the solar arrays during umbra in order to reduce propellant expenditures for velocity make-up (orbit adjust) provided a savings of $25 million.

Orbit Adjust. LCC sensitivity analysis to orbit adjust interval showed a $21 million savings by going from a 50 day interval to 10 day interval between orbit adjust firings.

Mono Propellant vs. Bipropellant RCS. The higher Isp of the bipropellant RCS subsystem netted a LCC cost savings of $126 million.

Active vs. Passive Structural Damping. A combination of active control and passive damping material (e.g. SMERD) yielded significant increase in controller bandwidth and reducing space station LCC. Adding 160 pounds of passive damping material resulted in increasing the structural damping ratio from 0.05% to 5% which reduced the number of controlled strucural modes and reduced LCC by $12 million.

Figure 1 MDD Top Level Analysis and Program Flow

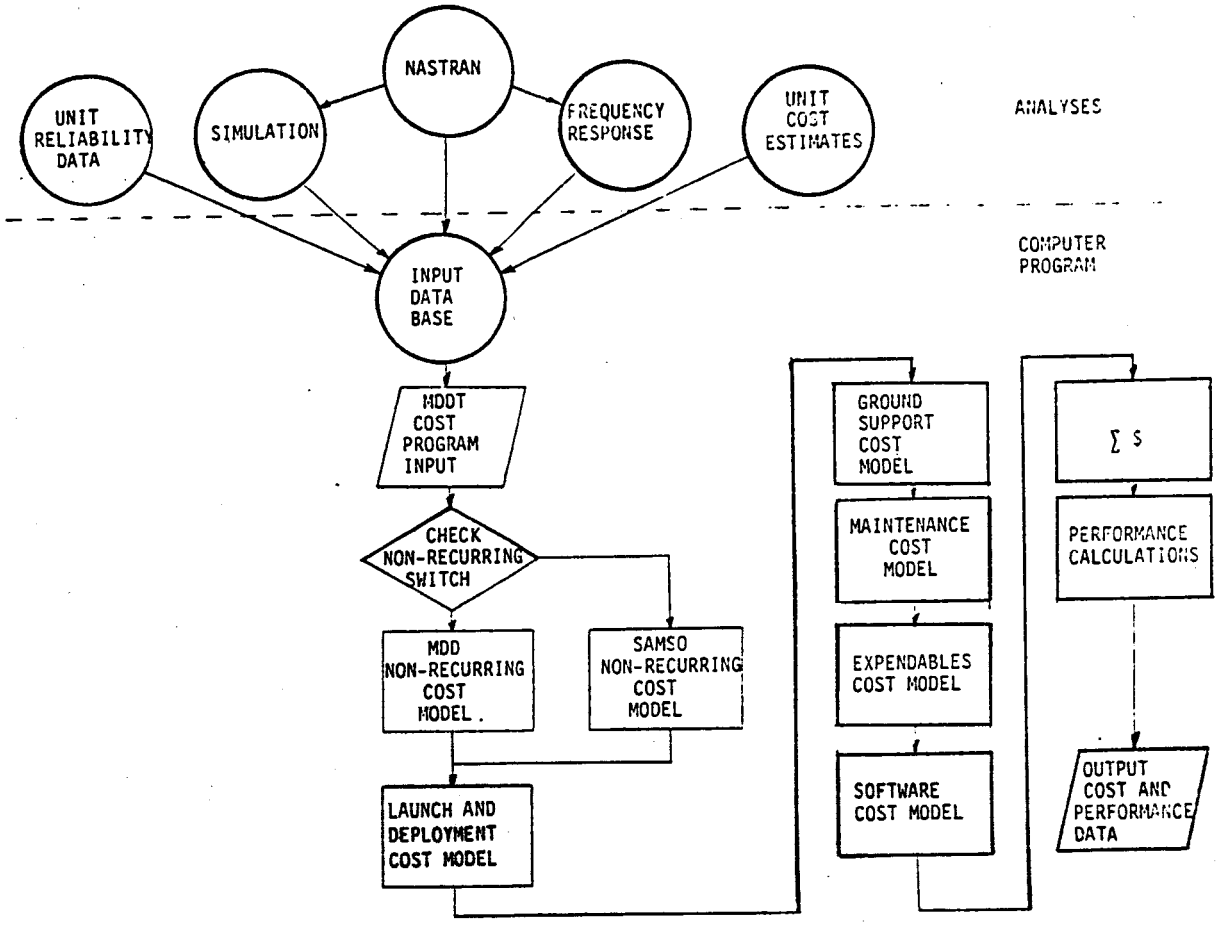

3 MDDT PROGRAM FLOW

3.1 Main Routine

The MDDT computer program consists of a main routine (MDDT.FOR) and eleven subroutines. All input and output variables are defined in this routine. All input data is read in through this routine, and the subroutines are called from here. A flow diagram of the main routine is presented in Figure 2.

3.2 Non-recurring Cost Subroutine

The Non-recurring Cost subroutine (NRC.FOR) calculates the non-recurring cost of the of the ACS (Attitude Control System) and Structures subsystems. Figure 3 illustrates the flow of the subroutine. A choice of two cost calculation approaches is given. Subsystem non-recurring cost may be calculated using SAMSO, a parametric cost model relating cost to subsystem weight (reference 1). The SAMSO cost model is of the form,

$$Y = 1000.0(A + B(WT)^C)$$

where,

Y = Subsystem non-recurring cost

WT = Subsystem weight

A, B, C = Input empirical constants

The values of the parameters A, B, and C are defined in Reference 6. These values may be modified to reflect historical cost data. The SAMSO model costs include the cost of hardware, design, manufacture, and test of the given subsystem. Alternatively, non-recurring cost can be calculated by summing cost per component times number of components for all types of components. In this case, component design, test and manufacturing costs should be included in the component costs, and project engineering costs for the design phase can be calculated by invoking a call from the main routine to the ACS design subroutine (ACSDES). The non-recurring cost is multiplied by the following three complexity factors for both cost models.

CI = Inflation factor from 1979 dollars

CC = Complexity factor from the SAMSO model

CM = Modifier to account for the difference in cost between unmanned and manned spacecraft

For the examples, the SAMSO model was used to calculate the Structures Subsystem non-recurring cost, as SAMSO is a time-proven model and large space structure data was available to calibrate the SAMSO model for structures in this weight range. Valid SAMSO parameters could not be found for the ACS subsystem, so the alternate method of calculation for ACS non-recurring costs was used in all examples.

3.3 ACS (Attitude Control System) Design Subroutine

The ACS Design subroutine (ACSDES), Figure 4, calculates total design cost for the ACS subsystem. Design cost is defined as the total labor cost of engineering personnel involved in design and support of the subsystem throughout all phases of the mission: initial design, initial on-orbit development and check-out and nominal on-orbit ground support. Engineering personnel are catagorized as project engineers, subsytem engineers, component engineers, and analysts. The number of analysts needed during the initial design phase (i.e. number of development analysts) is assumed to equal the number of control modes, a variable which is input by the user, while the number of analysts needed during the on-orbit phase (i.e. number of operations analysts) is assumed to be 20% of the number of development analysts. During the on-orbit development and check-out phase, the number of analysts drops linearly from the number of development analysts to the number of operations analysts.

The number of component engineers required during the initial phase is defined by the number of types of ACS components, and drops linearly during the on-orbit development and check-out phase to half that number in the final on-orbit phase. The number of project engineers is specified by the user and remains constant throughout the mission.

The number of subsystem engineers, like the number of component engineers, is assumed to drop linearly during the on-orbit development and check-out phase to half the number required during the initial design phase. The areas under the curves described above are integrated for the appropriate phase of the mission, summed, and converted from years to manhours of design and project engineering.

The number of engineering personnel is, of course, dependent on the size and scope of the particular program for which the MDDT is being used, and a combination of knowledge of the program and engineering judgement should be used in specifying inputs where required. The numbers used in the example runs described in this report (Section 5) were:

Number of control modes = 15

Number of components = 6

Number of project engineers = 1

Number of subsystem engineers = 2

3.4 Launch Cost Subroutine

The Launch Cost subroutine (LAUNCH.FOR), Figure 5, calculates the cost of launching a subsystem. Launch cost per pound is calculated by dividing the cost to launch the booster by

the maximum weight capability of the booster to the desired orbit, both user-specified inputs. The total subsystem weight is then multiplied by the launch cost per pound. The total launch cost however, also includes the cost of EVA, IVA, and use of the mobile remote manipulator system (MRMS). For this calculation, the number of hours of activity required and cost per hour of activity, user-specified inputs, are multiplied. The total launch cost is calculated by adding EVA, IVA and MRMS costs to the booster launch cost. Values used for this study were, for ACS:

Number of hours of EVA required for assembly on launch = 57
Number of hours of IVA required for assembly on launch = 37
Number of hours of MRMS required for assembly on launch = 35

and for Structures:

Number of hours of EVA required for assembly on launch = 100
Number of hours of IVA required for assembly on launch = 5
Number of hours of MRMS required for assembly on launch = 50

Cost figures used were:

Cost per hour of EVA = $62000 Cost per hour of IVA = $17500
Cost per hour of MRMS = $22000

3.5 Ground Support Cost Subroutine

The Ground Support Cost subroutine (GSUP.FOR) calculates the cost of ground support over the life of the mission for the

structures subsystem based on the user-specified number of manhours and the user-specified cost per manhour of ground support. (For the ACS subsystem, ground support costs are calculated in the on-orbit ground support phase of the ACS Design subroutine.) For this study, the estimated number of structure-required ground support hours over the length of the mission (assumed to be 10 years) was 62000.

3.6 Maintenence Cost Subroutine

The Maintenence Cost subroutine (MAINT.FOR), Figure 6, calculates the cost of maintaining each subsystem over the life of the mission (post-initial assembly), including replacement of parts and regular subsystem inspections. The number of expected failures for each type of component during the mission is computed using the formula:

$$NF = N(1 - \epsilon^{\frac{-ML}{MTBF}})$$

where the user-specified inputs are defined as follows:

N = number of this type of part or component in subsystem =

ML = mission length

$MTBF$ = mean time between failure of the part or component

As an example, for this study, the Control Moment Gyro (CMG) was assumed to be one of the ACS components. For the CMG, the user-specified inputs were,

N = 6

ML = 10 years

$MTBF$ = 84.2 years

The cost to replace a failed part is calculated by summing the cost of a replacement part (input by user), the cost to launch the part (calculated as in Launch Cost subroutine),and the cost of the EVA, IVA and MRMS activity required during replacement (input by user). The cost of subsystem inspections is computed for four possible related types of activity, EVA, IVA, MRMS use and ground support, and the resulting costs summed. Inspection cost per component type, per type of inspection activity (EVA, IVA, MRMS or ground support) is obtained by multiplying the number of units of that type by the cost of the activity per inspection of that type of component and the total number of inspections expected over the mission life (mission length divided by time between inspections, a user-specified input). The total costs over the mission of replacement and inspections per part are summed for all subsystem components to obtain the total cost of subsystem maintenence over the course of the mission.

3.7 Expendables Cost Subroutine

The Expendables Cost subroutine (EXPD.FOR), Figure 7, calculates the cost incurred due to replacement of expendables consumed over the mission life. This routine requires the user to input an initial and final altitude of the spacecraft (in feet), the time (in days) over which the orbit decay occurred, and the specific impulse of the assumed propellent. For this study, an orbit decay from approximately 448 km to 444.6 km (assumed nominal altitude was 450 km) over a period of ten days was used. (See Figure 29.) The subroutine then computes the energy loss per orbit and weight of propellent used per orbit in velocity makeup. The total weight of propellent used over the mission is then computed, using the orbit period and length of the mission. Using the input cost per pound of propellent, the cost due to purchase of replacement fuel is computed. The cost to launch to replacement fuel is computed by a call to the launch cost subroutine. A switch in the routine allows the calculation of expendables cost for either monopropellent fuel or using the user-specified mixture ratio for bipropellent.

3.8 Software Cost Subroutine

The Software Cost subroutine (SOFT.FOR), Figure 8, calculates the cost of subsystem-related software development using either the user-specified number of lines of code and cost per line of code, or the user-specified number of manhours to develop the required software and cost per manhour of software development. For this study, the assumed number of manhours to

develop ACS-related software was 83000 at $80 per manhour. There is no software development associated with the Structures subsystem.

3.9 ASC Steady State Pointing Subroutine

The ACS Steady State Pointing subroutine (ACSPTG), Figure 9, uses the Bode plot produced in the frequency response analysis (Section 4.2.2) to provide a pointing error estimate as a function of natural frequency of the structure, structural damping and disturbance torque. Controller break frequency to structure natural frequency ratios were calculated for six possible structural damping ratios using the baseline Bode plot, in order to assure controller/structure stability. The user supplies the damping ratio (from one of the six possible choices: .1,.05,.01,.005,.001,.0005), structure natural frequency, maximum expected disturbance torque, orbit rate (for a circular orbit at the assumed altitude of 450 km, orbit rate is .00112 rad/sec) and inertias of the structure. The subroutine calculates the controller break frequencies first, based on the predetermined ratios and the given structural damping, and from the break frequencies, the controller gains are calculated. The disturbance torque transfer function is then evaluated at twice orbit rate to determine the rigid body steady-state pointing error.

3.10 Active Control Subroutine

The Active Control subroutine (ACTCON.FOR), Figure 10,

calculates the additional software costs due to algorithms in the flight software which become required for actively compensating the actuator commands due to structural bending. The routine computes how many structural modes are required to be controlled as a function of how close the resonant frequencies are to the rigid body controller bandwith. Additional software costs are computed based on numbers of lines of code or computer operations per cycle using empirical equations contained in the routine.

3.11 Summation Of Costs Subroutine

The Summation of Costs subroutine (SUM.FOR) computes the life cycle cost of the Attitude Control Subsystem and the life cycle cost of the Structures Subsystem by summing the costs output by all of the cost subroutines.

3.12 Print Subroutine

The Print subroutine (PRINT.FOR) converts the ACS and Structures costs output by each cost routine and the total life cycle cost for each of the two subsystems to millions of dollars. The subroutine also sums the ACS costs with the Structures costs for each category (each of the cost subroutines and the total) and outputs individual and total costs in millions of dollars and ACS perfomance data from the ACS Steady State Pointing subroutine.

FIGURE 2 - MDDT PROGRAM FLOW

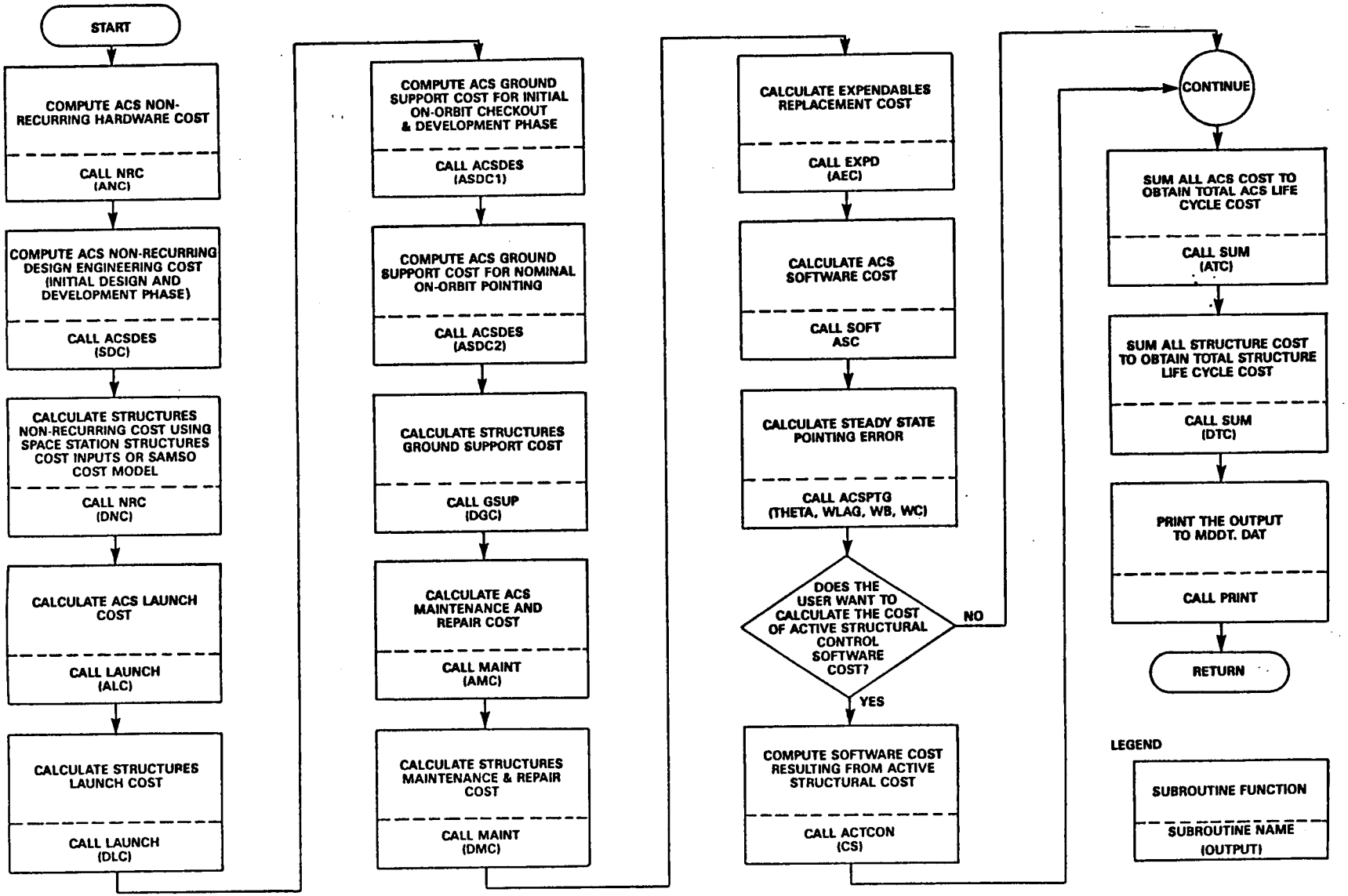

Figure 3

Subroutine NRC

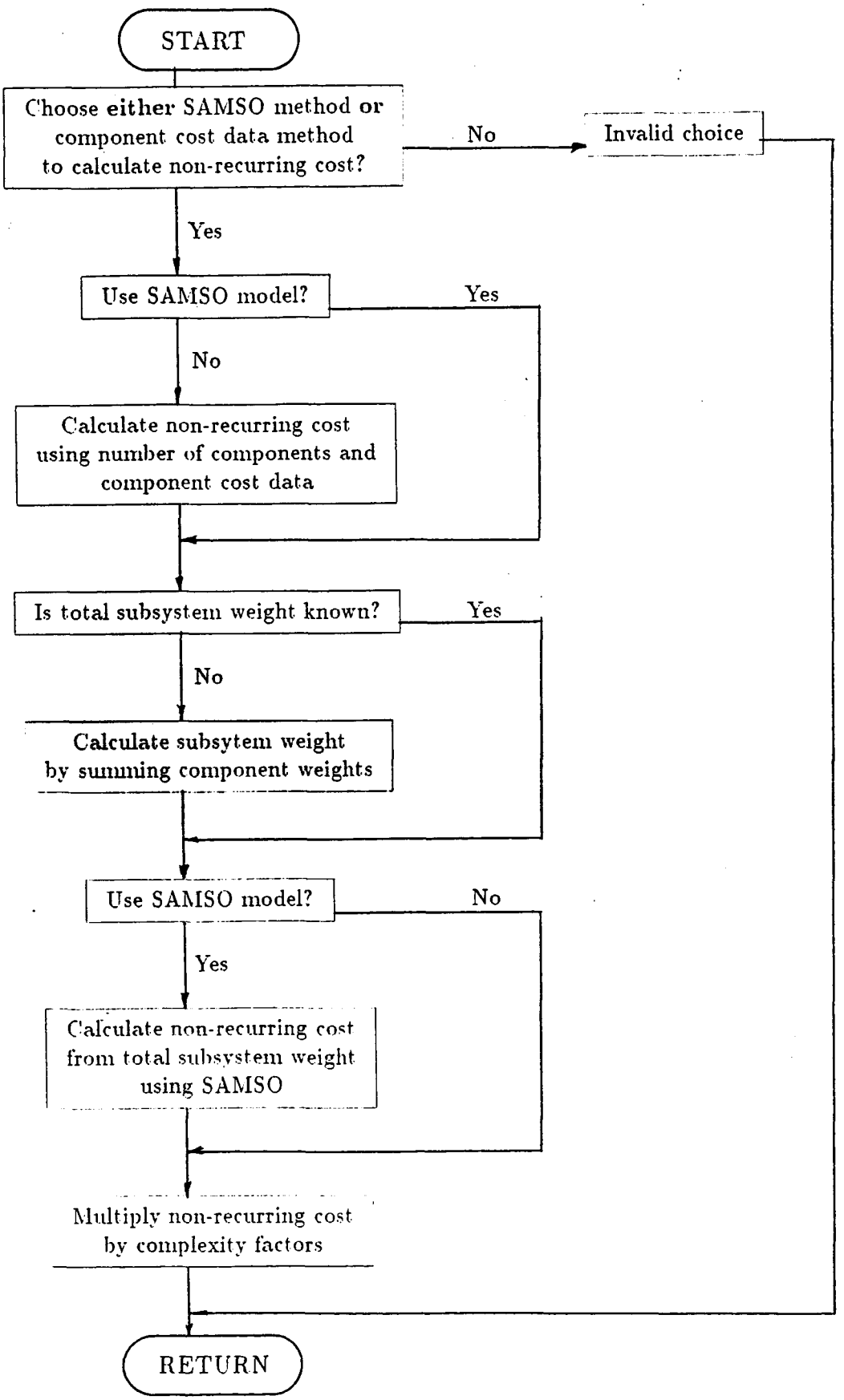

Figure 4

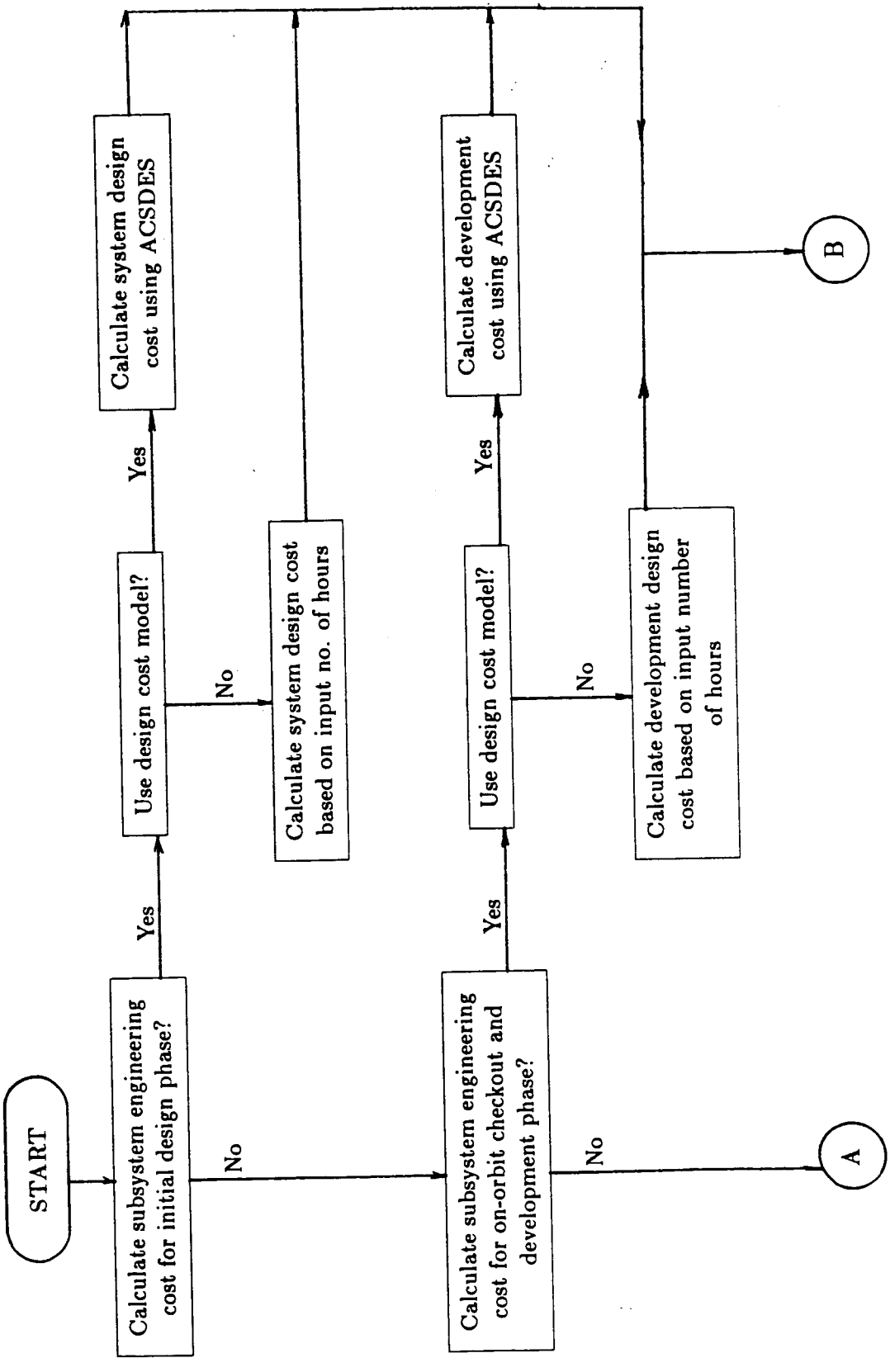
Subroutine ACSDES
START
Calculate subsystem engineering cost for initial design phase?
Yes
No
Use design cost model?
Yes
No
Calculate system design cost using ACSDES
Calculate system design cost based on input no. of hours
Calculate subsystem engineering cost for on-orbit checkout and development phase?
Yes
No
Use design cost model?
Yes
No
Calculate development cost using ACSDES
Calculate development design cost based on input number of hours
A
B

Figure 4

Subroutine ACSDES (continued)

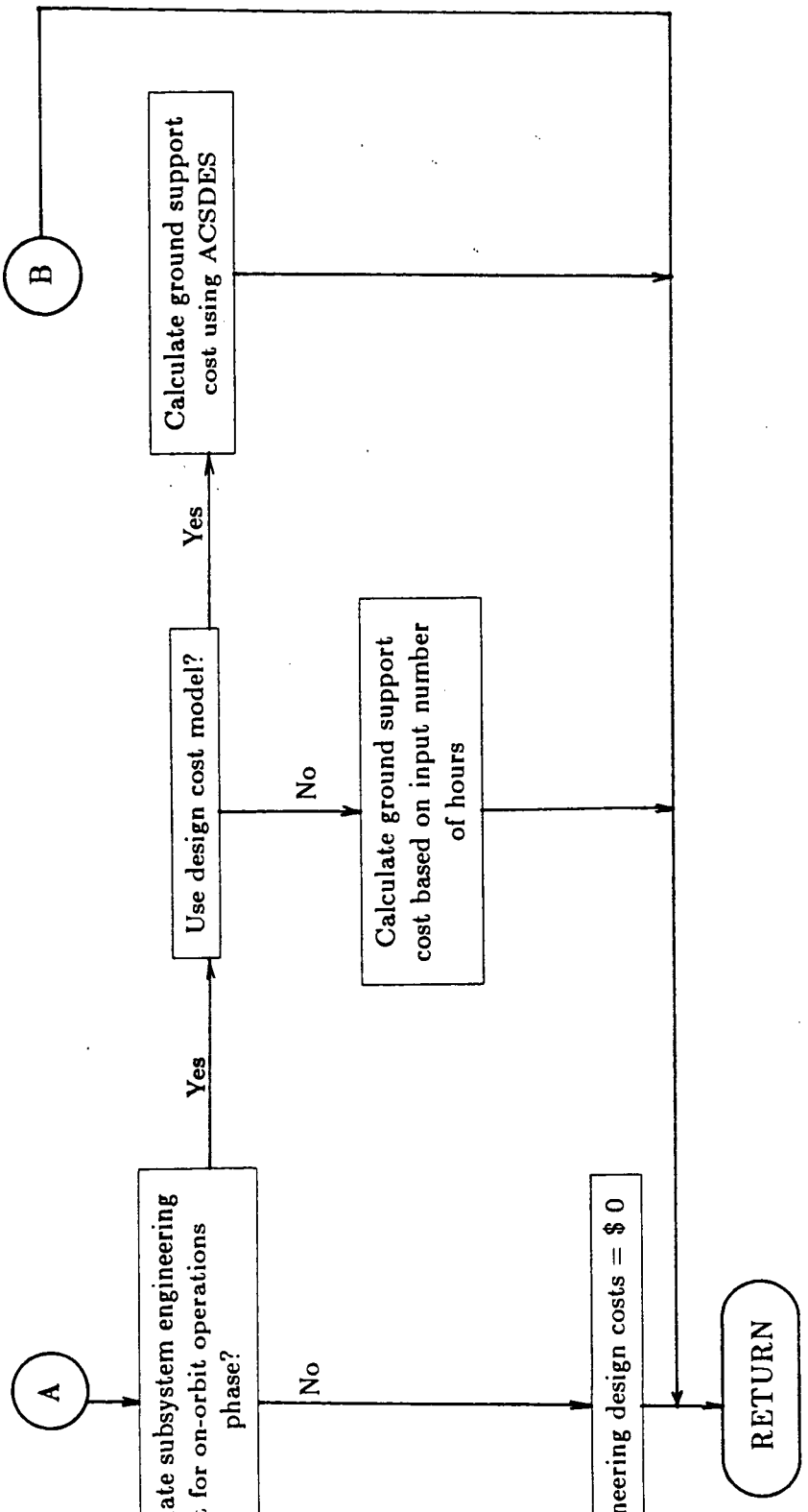

Figure 5

Subroutine LAUNCH

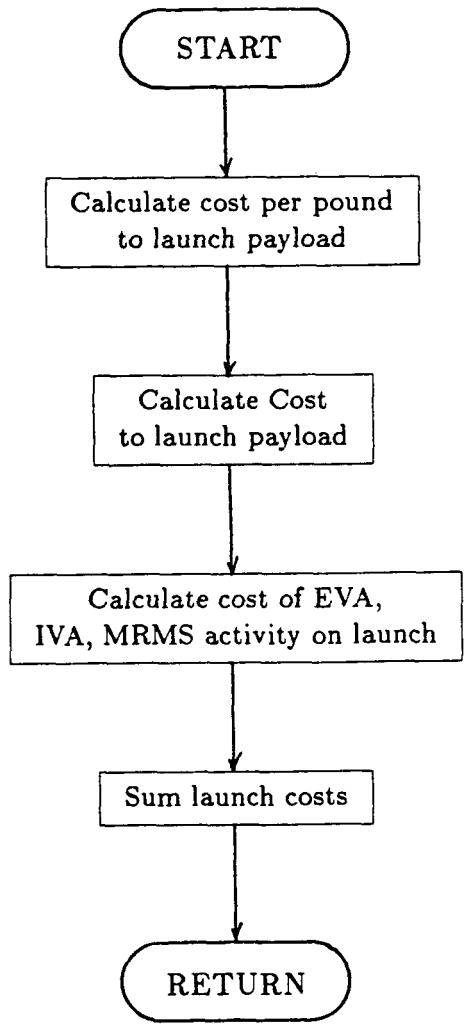

Figure 6

Subroutine MAINT

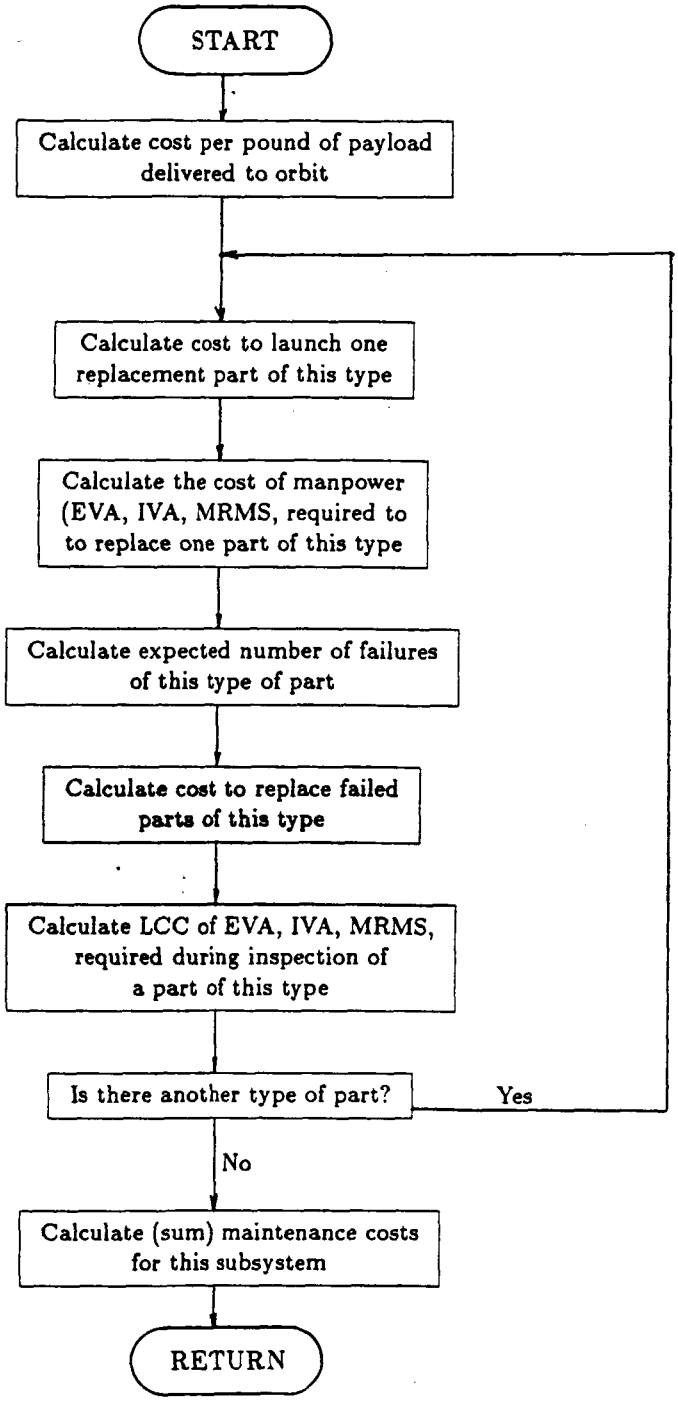

Figure 7

Subroutine EXPD

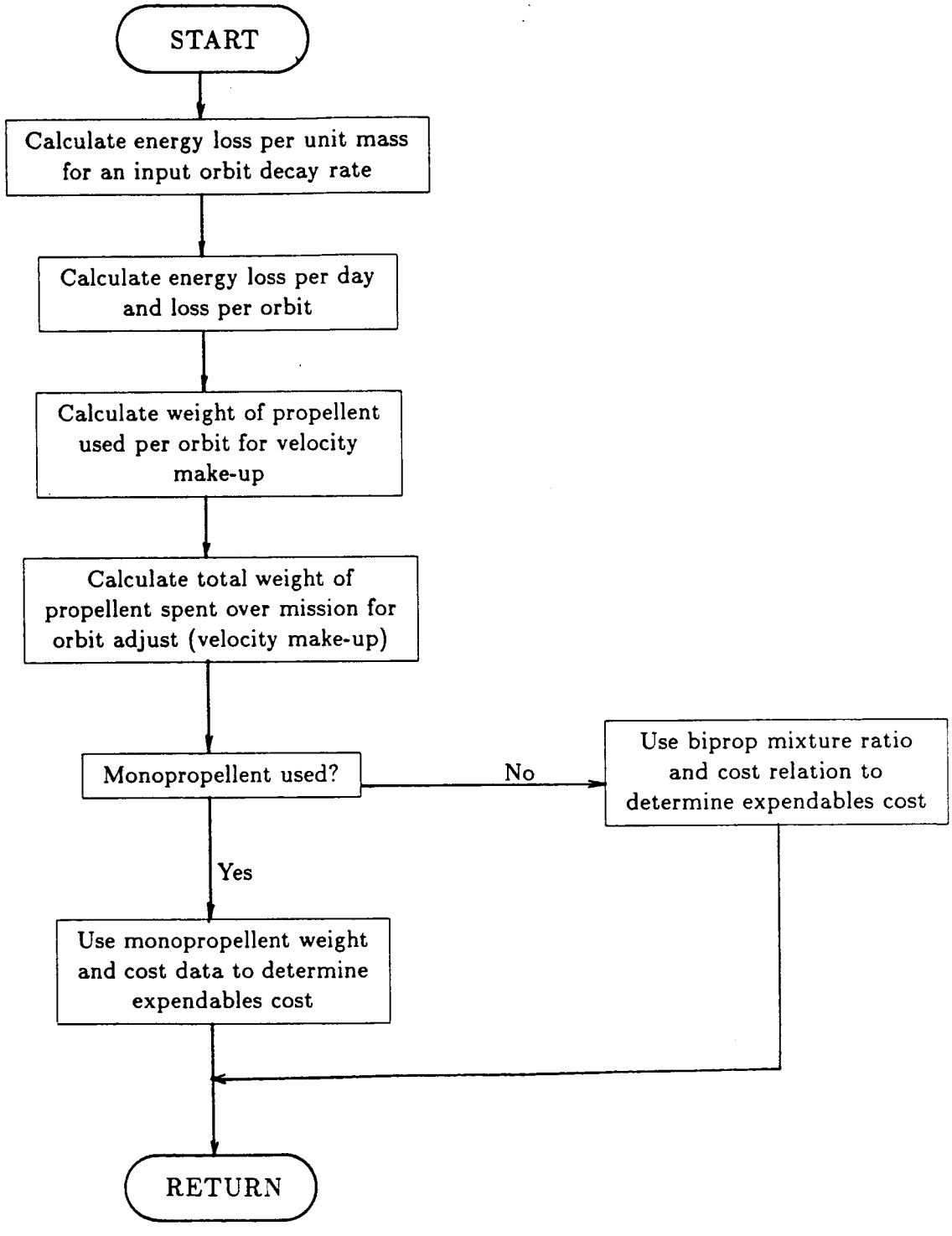

Figure 8

Subroutine SOFT

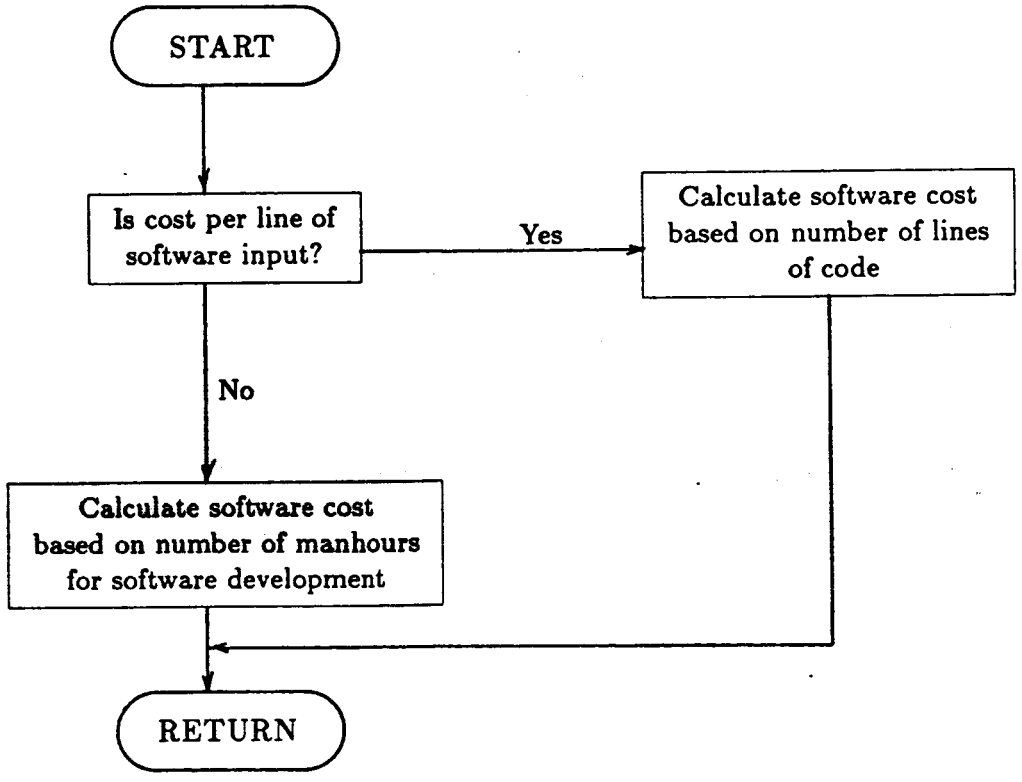

Figure 9

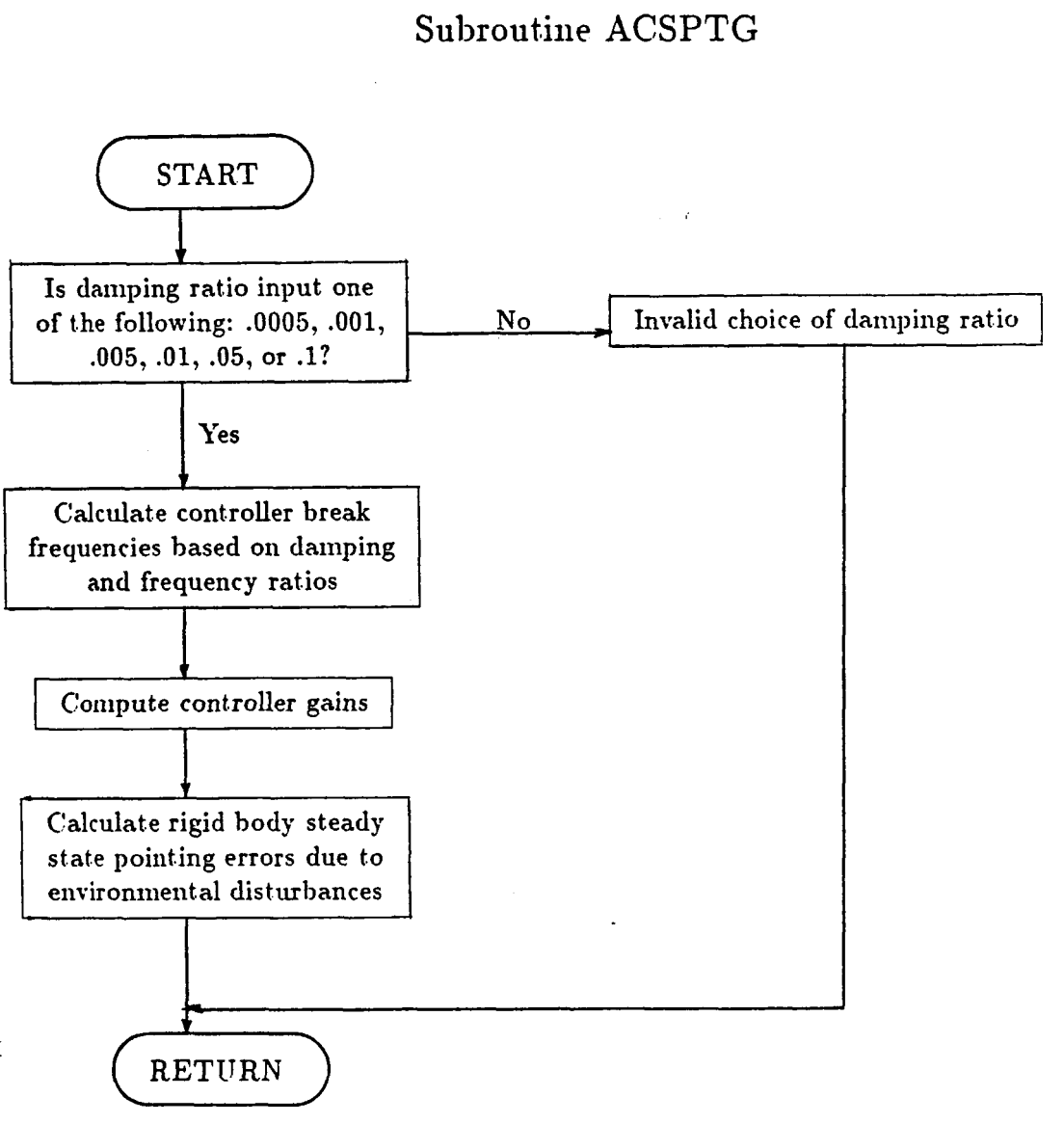
Subroutine ACSPTG
START
Is damping ratio input one of the following: .0005, .001, .005, .01, .05, or .1?
No
Invalid choice of damping ratio
Yes
Calculate controller break frequencies based on damping and frequency ratios
Compute controller gains
Calculate rigid body steady state pointing errors due to environmental disturbances
RETURN

Figure 10

Subroutine ACTCON

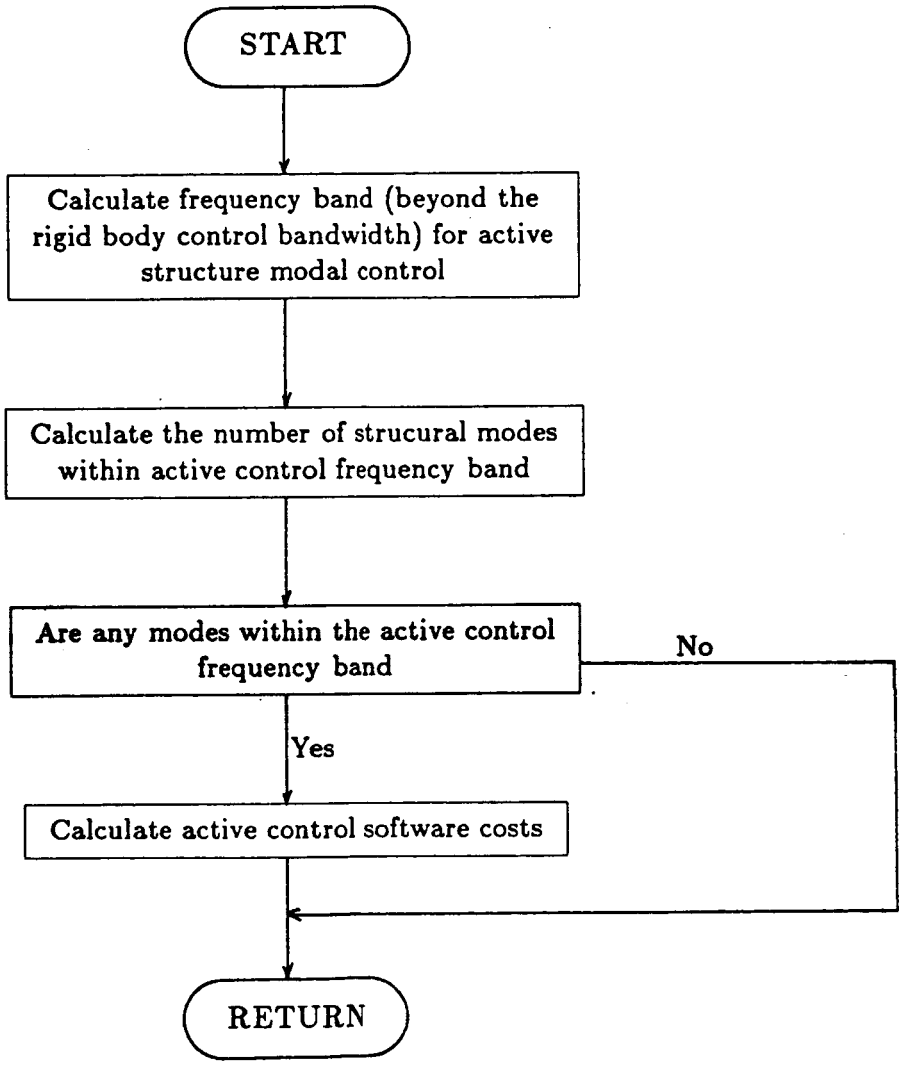

4 MDD STUDY STRUCTURE AND CONTROLS ANALYSES

4.1 Structure

4.1.1 Expendables Analysis For Mass Properties -

4.1.1.1 Expendables Analysis Description -

The mass properties employed in the expendables analysis are taken from reference 2 and consider an Initial Operating Configuration (IOC) space station similar to that shown in Figure 11. These mass properties represent a current best estimate of what the space station's mass properties will be during the early phases of operation. This corresponds to the period of operation when fuel usage will be highest as the space station's ballistic coefficient (weight/frontal area) will be low. This results in large drag effects requiring orbital corrections.

4.1.1.2 Expendables Analysis Assumptions -

These mass properties are for a five meter bay truss dual keel space station with four crew habitation modules. No payloads are included. Various servicing bays are not included. The hybrid power system (four photovoltaic arrays and two solar dynamic engines) is employed. The space shuttle orbiter is not present.

4.1.1.3 Expendables Analysis Results -

The mass properties employed in this analysis are shown in Figure 12. As can be seen, the space station weight used in the expendables analysis is 466354. pounds. The space station also has very large inertias, even during the early build-up phase. Both the mass and inertia of space station will increase as the configuration evolves.

4.1.2 Structural Dynamics -

4.1.2.1 Structural Dynamics Description -

Simple NASTRAN models of two space station configurations were developed. The two configurations considered were a deployable nine foot bay truss and an erectable five meter bay truss dual keel space station. The models included four crew habitation modules and a representative IOC payload compliment. The geometries of the 9-foot and the 5-meter bay models are identical. Figure 13 presents four views of the model. The power system included in the NASTRAN models is comprised of eight photovoltaic solar arrays. The dynamic modes and frequencies of the two configurations were calculated. This data was employed to determine the the Attitude Control System (ACS) performance characteristics.

These models were also employed in a disturbance response analysis. The five meter bay truss space station model was excited by a crew member kickoff forcing function (See Figure 14) and a space shuttle orbiter docking forcing function (See

Figure 15). Selected results of this response analysis are presented in Appendix A. Figures A1 through A10 present the results for the crew kickoff disturbance. Figures A1 through A3 plot the three orthoganal displacements in radians at the ACS package through 100 seconds with the ACS inactive. Figure A4 shows the corresponding Theta y deflections at the tip of the lower boom. Figure A5 presents the corresponding Z axis linear acceleration in g's. Figures A6 through A10 present similar data with the ACS package active. Figures A11 through A20 present the shuttle orbiter docking data in the same order as Figures A1 through A10.

The angular deflection for uncontrolled the kickoff was on the order 60 microrad. The controller reduced this to about 40 microrad. The acceleration levels at the ACS package were about 180 micro-g's both with and without the controller.

The shuttle docking event results in higher response levels. After 100 seconds, the angular deflection for the uncontrolled docking event is approximately 15000 microrad. The controller reduced this to 9000 microrad. The acceleration levels at the ACS package were about 3000 micro-g's both with and without the controller.

4.1.2.2 Structural Dynamics Assumptions -

There were several assumptions employed in this analysis. The space station truss structure was represented as an equivalent beam. This will lead to errors in higher order

eigenvalues and eigenvectors; however, this beam representation is sufficiently accurate for preliminary configuration studies.

Also, it was assumed that the space station acts as a linear structure and that the truss joints are rigid. It has been shown (reference 3) that even small amounts of free play (.0005 inches) in the truss joints will result in significant non-linear behavior (one to three inches of free play in keel). The non-linear characteristics of the keel must be minimized in order to have a well defined predictable stucture. Note that it is more difficult to avoid free play in the joints of deployable trusses than of erectable ones.

4.1.2.3 Structural Dynamics Results -

The results of this analysis are summarized in Figure 16. Listed are flexible mode shape descriptions and the corresponding frequencies through approximately .6 hz for both models. As can be seen from this data, the space station is a highly flexible structure with high modal density.

The fundamental flexible mode is a solar array mode at approximately .17 hz. The fundamental flexible keel modes occur at .197 hz for the nine foot bay configuration and .356 hz for the five meter bay configuration. The low frequencies of the fundamental keel modes will challenge the ability of the ACS to meet orbital performance requirements. The high modal density will also complicate the task of the ACS.

4.1.3 Erectable Vs Deployable Truss LCC Trade Study -

4.1.3.1 Erectable Vs Deployable Truss Description -

A life cycle cost (LCC) trade study was performed between erectable and deployable truss concepts. Also varied were truss bay sizes. Nine foot and five meter bay sizes were considered. Thus there were four cases: a nine foot bay deployable keel, a nine foot bay erectable keel, a five meter bay deployable keel, and a five meter bay erectable keel. All four cases are dual keel space stations with similar overal dimensions.

reference 4 gives the estimated amount (approximately 1 hour) of Extra-Vehicular Activity (EVA) required to deploy/erect each of the four cases considered. The amount of Intra-vehicular Activity (IVA) and Mobile Service Center (MSC) activity required was estimated from the amount of EVA time. The number and types of parts comprising each case were estimated. As would be expected, the nine foot bay cases were comprised of more bays and therefore had significantly more parts than the five meter bay cases (3014 parts for the 9 foot bay design versus 1690 for the five meter design). Also, the deployable cases required various types of deployable joints and therefore required more types of parts than the erectable cases.

4.1.3.2 Erectable Vs Deployable Truss Assumptions -

It was assumed that the ACS (Attitude Control System) required by each of the four cases was identical and that they required the same quantity of expendables. Also, all four cases were assumed to have the same level of structural damping. Finally, it is assumed that the values assigned to all parameters employed in the analysis are correct. Many of the parameters are poorly defined at this stage in space station's development and rough order of magnitude estimates are employed. Any cost study of this nature must be updated as the station's configuration and characteristics become better defined.

4.1.3.3 Erectable Vs Deployable Truss Results - The life cycle costs of the four cases are shown in Figure 17. As can be seen, the five meter bay truss results in significant life cycle cost savings over the nine foot bay truss. Savings of 47.4 million dolars were seen for the erectable cases while savings of 67.4 million dollars were seen for the deployable cases. This results primarily from the reduced number of joints in the larger bay size cases.

Also evident is that the erectable cases are less expensive than the deployable ones. Savings of 52.7 million dollars were seen for the five meter cases while savings of 72.7 million dollars were seen for the nine foot cases. This result occurs even though the erectable cases require more on-orbit manpower to erect/deploy (reference 4). The savings come from the decreased complexity and increased reliability of the erectable designs.

Thus, it was found that the erectable five meter bay truss case had the lowest life cycle cost at 786.5 million dollars while the deployable nine foot bay truss had the highest life cycle cost at 906.6 million dollars. This represents a savings of 120.1 million dollars (fifteen percent) over a ten year mission.

Figure 11 Reference Space Station Design
DUAL KEEL 5-METER CONFIGURATION
Z-Y PLANE

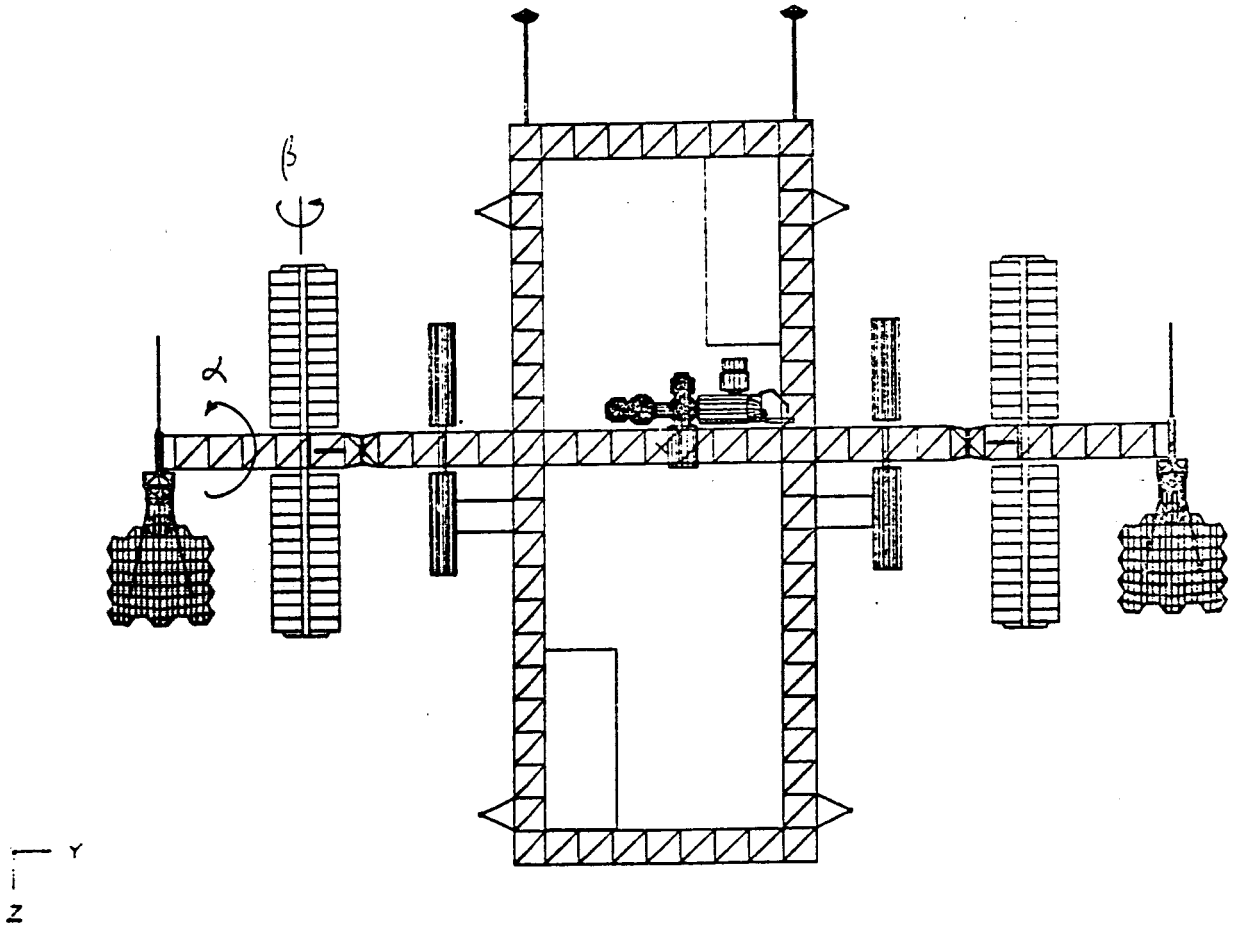

Figure 12 Weight Properties

Weight (lb)	466354.
Inertia(slug-ft**2)	
IXX	1.11E8
IYY	5.22E7
IZZ	7.98E7
IXY	-1.47E4
IXZ	-1.63E6
IYZ	7.80E5

Figure 13 Space Station NASTRAN Model

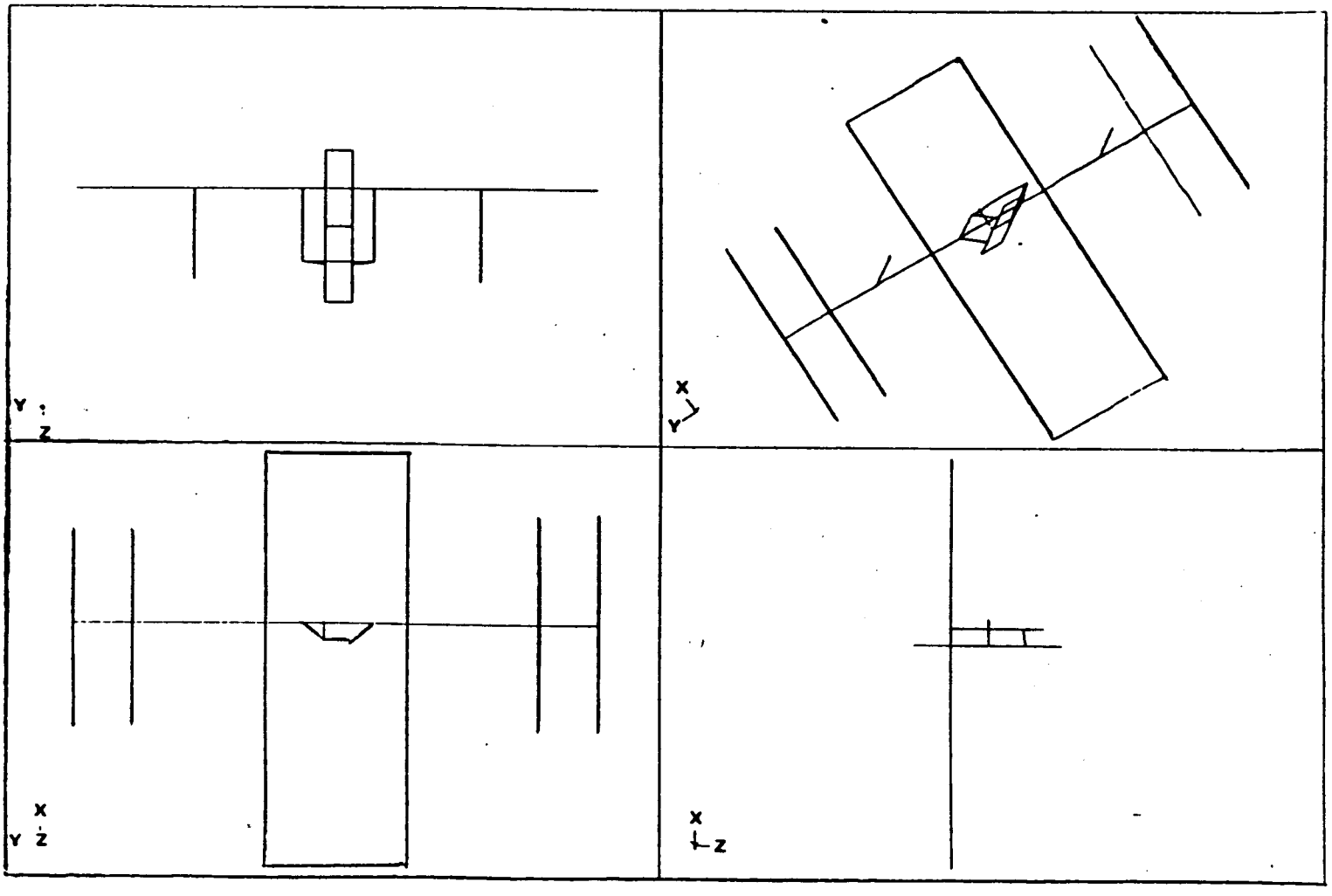

Figure 14 Crew Kickoff Disturbance

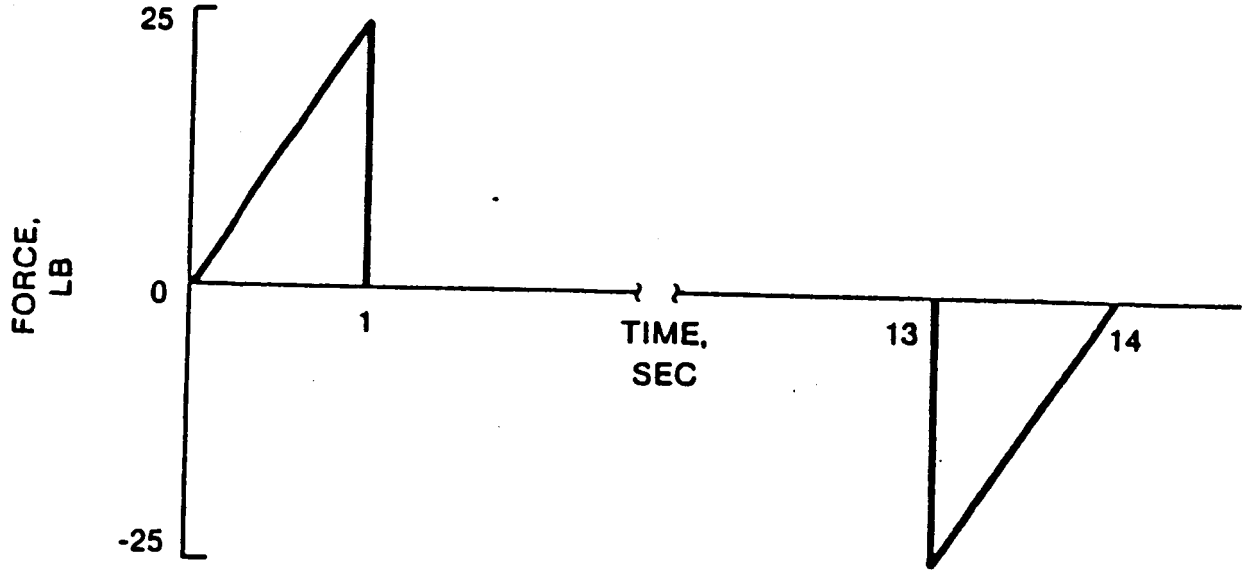

Figure 15 Space Shuttle Orbiter Disturbance

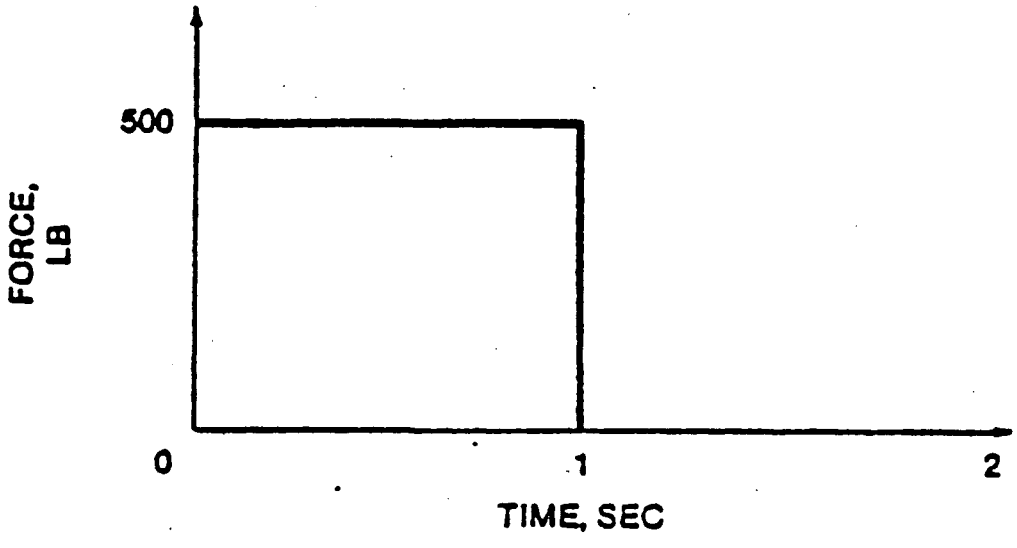

Figure 16 Nine Foot and Five Meter Dual Keel Modal Results

Mode Description	Frequency (hz) Nine Foot	Five Meter
Solar Array Mast	.162	.174
Solar Array Mast	.164	.175
Solar Array Mast	.167	.178
Solar Array Mast	.174	.179
Solar Array Mast	.176	.180
Solar Array Mast	.179	.180
Solar Array Mast	.179	.180
Solar Array Mast	.180	.180
Solar Array Mast	.180	.180
Solar Array Mast	.180	.180
Solar Array Mast	.180	.180
Solar Array Mast	.180	.180
Solar Array Mast	.180	.180
Solar Array Mast	.180	.180
Solar Array Mast	.182	.182
Solar Array Mast	.193	.198
Keel Pitch Bending	.197	.356
Module Support/Keel Pitch Bending	.227	.407
Keel Torsion	.283	.507
Transverse Boom	.354	.631
Keel Roll Bending/Transverse Boom	.378	.680
Transverse Boom/Array Mast	.383	.631
Keel Torsion/Keel Roll Bending	.405	.734
Keel Roll Bending/Keel Torsion/Radiator	.415	.731
Radiator(and Keel Torsion in 5 meter)	.518	.564
Radiator	.521	.548
Radiator	.523	.557
Radiator	.577	.551

Figure 17 Erectable vs Deployable Truss Life Cycle Trade Study

	Cost in Millions of Dollars			
	Five Meter Erectable	Five Meter Deployable	Nine Foot Erectable	Nine Foot Deployable
Type of Cost				
Non-Recurring Cost	153.6	186.0	157.1	195.7
Launch Cost	37.6	40.4	43.1	47.4
Ground Support Cost	20.9	24.8	23.7	29.6
Maintainence Cost	42.0	55.7	73.1	97.3
Expendables Cost	503.6	503.6	503.6	503.6
Software Cost	28.8	28.8	33.2	33.2
Total Cost	786.5	839.2	833.9	906.6

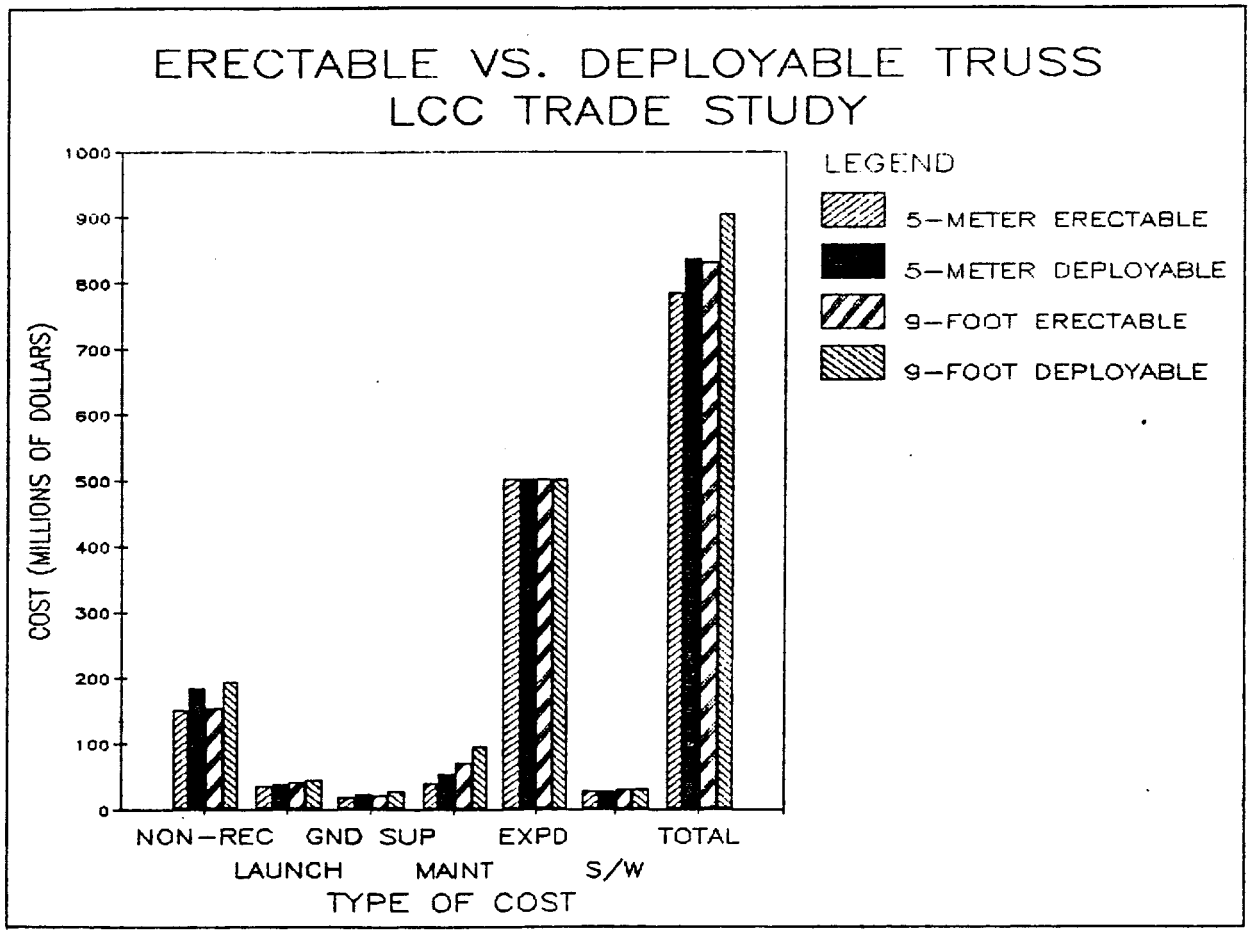

4.2 ATTITUDE CONTROL SUBSYSTEM (ACS) ANALYSES

4.2.1 Disturbance Torques -

4.2.1.1 Disturbance Torque Analysis Description -

The major disturbance torques experienced by low Earth orbiting satellites, such as the Space Station, are gravity gradient torque and aerodynamic torque. Solar pressure torque and residual magnetic dipole were found to be small in comparison, and therefore are not considered here. An independent simulation was run to model these disturbances for use in related analyses.

4.2.1.2 Disturbance Torque Analysis Assumptions -

The disturbance torque analysis assumes that the Space Station configuration is the Dual Keel type with no payloads, 2 satellite service/storage bays, a hybrid power system (four photovoltaic solar arrays and two solar dynamic engines), two solar radiators and five modules Figure 11. A nominal altitude of 450 km is assumed (reference 5 and 6), and mass properties are given in Figure 12. The proposed Torque Equilibrium Attitude pointing scheme is not considered, as it would present complications beyond the scope of this study. It is assumed therefore that the Space Station is Earth-pointed and is flown with no bias attitudes. The controller is modeled as a Proportional-Integral-Derivative (PID) type with,

$$T_c = [KRs + KP + \frac{KI}{s}]\theta$$

where,

T_c = Control torque

KR = Rate gain

KP = Position gain

KI = Integral gain

θ = Pointing error with respect to Earth-pointing reference

s = Laplace operator

A torque is imposed on any Earth-orbiting spacecraft due to the Earth's inverse square gravitational field. This gravity gradient torque is modeled for Space Station in an independent ACS (Attitude Control Subsystem) simulation (Ref. 10) as follows:

$$T_{gx} = 3\omega[(I_{zz} - I_{yy})p_y p_z - I_{xy}p_x p_z + I_{xz}p_x p_y - (p_z^2 - p_y^2)I_{yz}]$$

$$T_{gy} = 3\omega[(I_{xx} - I_{zz})p_x p_z - I_{yz}p_x p_y + I_{xy}p_y p_z - (p_x^2 - p_z^2)I_{xz}]$$

$$T_{gz} = 3\omega[(I_{yy} - I_{zx})p_x p_y - I_{xz}p_y p_z + I_{yz}p_x p_z - (p_y^2 - p_x^2)I_{xy}]$$

where,

ω = orbit rate = 1.12E-03 rad/sec

p_i = direction cosines of the local vertical in the spacecraft reference frame

I_{jk} = moment of inertia (ft-lb-sec)

Aerodynamic torque results from the impact of the Earth's upper atmosphere on the surface of the spacecraft. In this study, aerodynamic force is modeled as a combination of both absorption of and diffuse reflection of atmospheric molecules off the surface of the spacecraft (reference 7). The reference Space Station configuration, Figure 11 was broken down into the following ten planar surfaces and force and torque components were computed for each component surface: 2 satellite storage/service bays, 4 solar array panels, 2 solar concentrators and 2 solar radiators. The trusswork, which accounts for only a small percentage of the total frontal area of the assumed structure, was not considered. The absorptive component of the aerodynamic force acts only in the spacecraft velocity direction, and is described by (reference 8),

$$\vec{F}_{abs} = -\frac{1}{2}\rho V^2 A C_d(\hat{v}\cdot\hat{n})$$

The diffuse component is given by (reference 8),

$$F_{dif} = \frac{2}{3}(\frac{1}{2}\rho V^2 A C_d(\hat{v}\cdot\hat{n}))$$

where,

ρ = Atmospheric density at 450 km. (reference 9)

V = Translational velocity of component surface relative to incident airstream

A = Component surface area

C_d = Coefficient of drag = 2.2 (Ref. 2, 4 and 5)

$\hat{v}$ = Unit vector in the direction of the incident airstream

$\hat{n}$ = Unit vector normal to the component surface and directed outward

A time-varying alpha angle (the array angle in the orbit plane) and an average beta angle (angle the sunline makes with the orbit plane) of 36.73 deg over the orbit were assumed for the aerodynamic torque calculations.

4.2.1.3 Disturbance Torque Analysis Results -

Simulation shows aerodynamic torque to be the most significant environmental disturbance for the assumed space station configuration. A cursory investgation of magnetic dipole and solar pressure torque confirmed that these disturbances are

relatively insignficant. Typical magnitudes are shown in Figures 18 and 19.

4.2.2 Controller Optimization And Design -

4.2.2.1 Controller Optimization And Design Description -

The preliminary design of the ACS is based on baseline ACS design configuration defined in reference 5. (For a list of hardware, see Appendix B.) As a result of the hardware required for a classical control design and it's capability to handle a wide range of controller bandwidths, the ACS did not prove cost sensitive in the preliminary analysis. Optimization of the ACS was based on creating a maximum controller bandwidth for a user specified fundamental structural resonant frequency. The preliminary optimization was, therefore, based on steady state pointing and transient response performance when considering disturbances (i.e. low frequency, step input type, and higher frequency disturbances such as environment, STS docking and crew motion, respectively). Cost of the ACS as an optimization criteria was accomplished after the MDDT model was sophisticated enough to include active structural damping designs.

A frequency response analysis was performed in order to enable the MDD computer program to provide a pointing error estimate as a function of natural frequency of the structure, structural damping and disturbance torque. The frequency response portion of an in-house three-axis control system simulation (reference 10) was run with a variety of controller

break frequencies until a Bode plot exhibiting good stability characteristics was generated. The gain curve shifts in frequency as the structure natural frequency is varied.

A constant ratio is maintained between the structure natural frequency and the controller break frequencies. Ratios of the controller break frequencies have been calculated for the six assumed values of damping ratio; 0.0005, 0.001, 0.005, 0.01, 0.05, 0.1. The ACS pointing routine accepts the fundamental frequency value and the user supplied value of damping for that structural mode as inputs. The routine computes the desired controller gains so that controller/structure stability is assured.

The routine also evaluates the steady state pointing sensitivity to disturbance torques with a frequency content at two times orbital rate via the following sensitivity transfer function.

where,

θ = steady state pointing error

T_d = disturbance torque amplitude

I = moment of inertia

s = Laplace operator

KR = rate gain

KP = position gain

KI = integral gain

Figures 20 through 22 are gain and phase versus frequency plots of pointing sensitivity for the roll, pitch, and yaw axes which have been generated using an in-house linear system analysis computer tool (reference 10). MDDT evaluates the same pointing sensitivity transfer function at two times orbital rate.

Structural mode sensitivity was also investigated to determine the dependence of modal deflection to controller bandwidth. Figure 23 shows the first structural mode sensitivity to disturbances for a relatively low rigid body mode bandwidth (note that the mode shape was largest in this, roll, control axis). Figure 24 is a plot of the same modal sensitivity to disturbances with a higher controller bandwidth. Both cases resulted in a peak modal sensitivity of approximately -22 db. Therefore, structural vibration sensitivity is not dependent on classical controller bandwidth selection. This is expected because the classical controller is designed not to excite the structure.

4.2.2.2 Controller Optimization And Design Assumptions -

The controller optimization and design analysis assumes a classical controller. Evaluation of the disturbance torque transfer function does not take into consideration the effects of flexible modes or the triple lag filter used to roll off the high frequency response. This simplification of the transfer function is used because the low frequency gains are of interest and the higher frequency effects are negligible for this part of the analysis.

4.2.2.3 Controller Optimization And Design Results -

The initial controller design, with relatively high bandwidth (0.0628 rads/sec) results in a very low value of sensitivity i.e. -114, -108, and -110 db in roll, pitch , and yaw, respectively as seen in Figures 20, 21, and 22. The expected steady state pointing error (in radians) is obtained by multiplying these sensitivity values by the input disturbance torque amplitudes.

As a result of this analysis the MDDT computer program provides a means of evaluating attitude perfomance for varying space station configurations. The pointing errors seen for the example cases run are very small (maximum error equals 1.75 arc-sec in pitch with 0.0005 structural damping) due to very small pointing sensitivity to environmental disturbances at twice orbital rate.

Figure 18

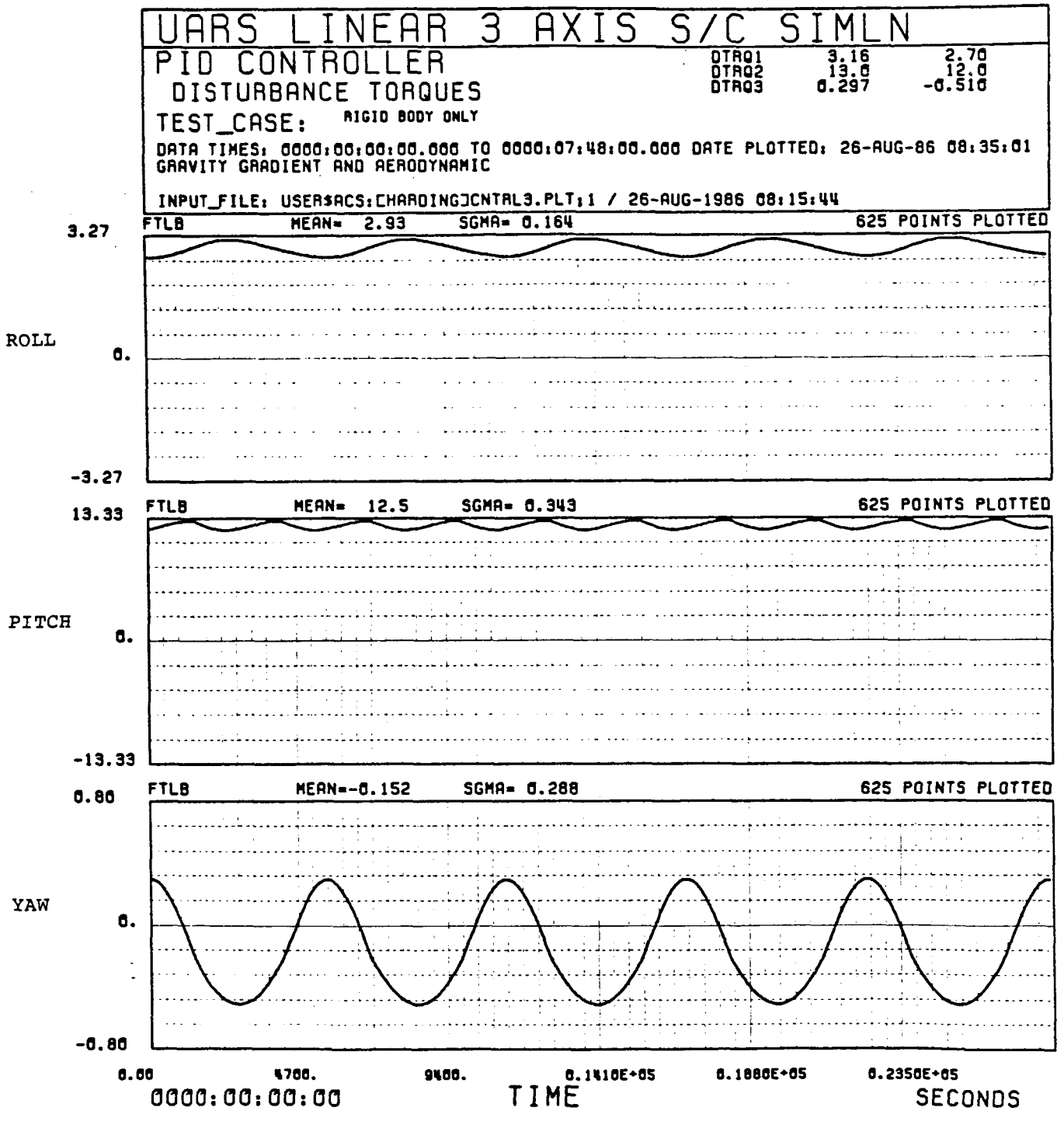
UARS LINEAR 3 AXIS S/C SIMLN
PID CONTROLLER
DISTURBANCE TORQUES
DTRQ1 3.16 2.70
DTRQ2 13.0 12.0
DTRQ3 0.297 -0.510
TEST_CASE: RIGID BODY ONLY
DATA TIMES: 0000:00:00:00.000 TO 0000:07:48:00.000 DATE PLOTTED: 26-AUG-86 08:35:01
GRAVITY GRADIENT AND AERODYNAMIC
INPUT_FILE: USER$ACS:CHARDINGJCNTRL3.PLT;1 / 26-AUG-1986 08:15:44
FTLB MEAN= 2.93 SGMA= 0.164 625 POINTS PLOTTED
3.27
ROLL
0.
-3.27
FTLB MEAN= 12.5 SGMA= 0.343 625 POINTS PLOTTED
13.33
PITCH
0.
-13.33
FTLB MEAN=-0.152 SGMA= 0.288 625 POINTS PLOTTED
0.80
YAW
0.
-0.80
0.00
4700.
9400.
0.1410E+05
0.1880E+05
0.2350E+05
0000:00:00:00
TIME
SECONDS

Figure#19 Expected Environmental Torques

	Gravity Gradient	Aero	GG and Aero	Magnetic	Solar Pressure
Roll (ft-lb) :				1.12E-02	0.00
Max. :	2.93	0.233	3.16		
Mean :	2.93	-4.010E-04	2.93		
Pitch (ft-lb):					1.03E-02
Max. :	6.12	6.90	13.0		
Mean :	6.12	6.37	12.5		
Yaw (ft-lb) :					0.13E-02
Max. :	7.851E-05	0.297	0.297		
Mean :	1.123E-06	-0.152	-0.152		

Figure 20

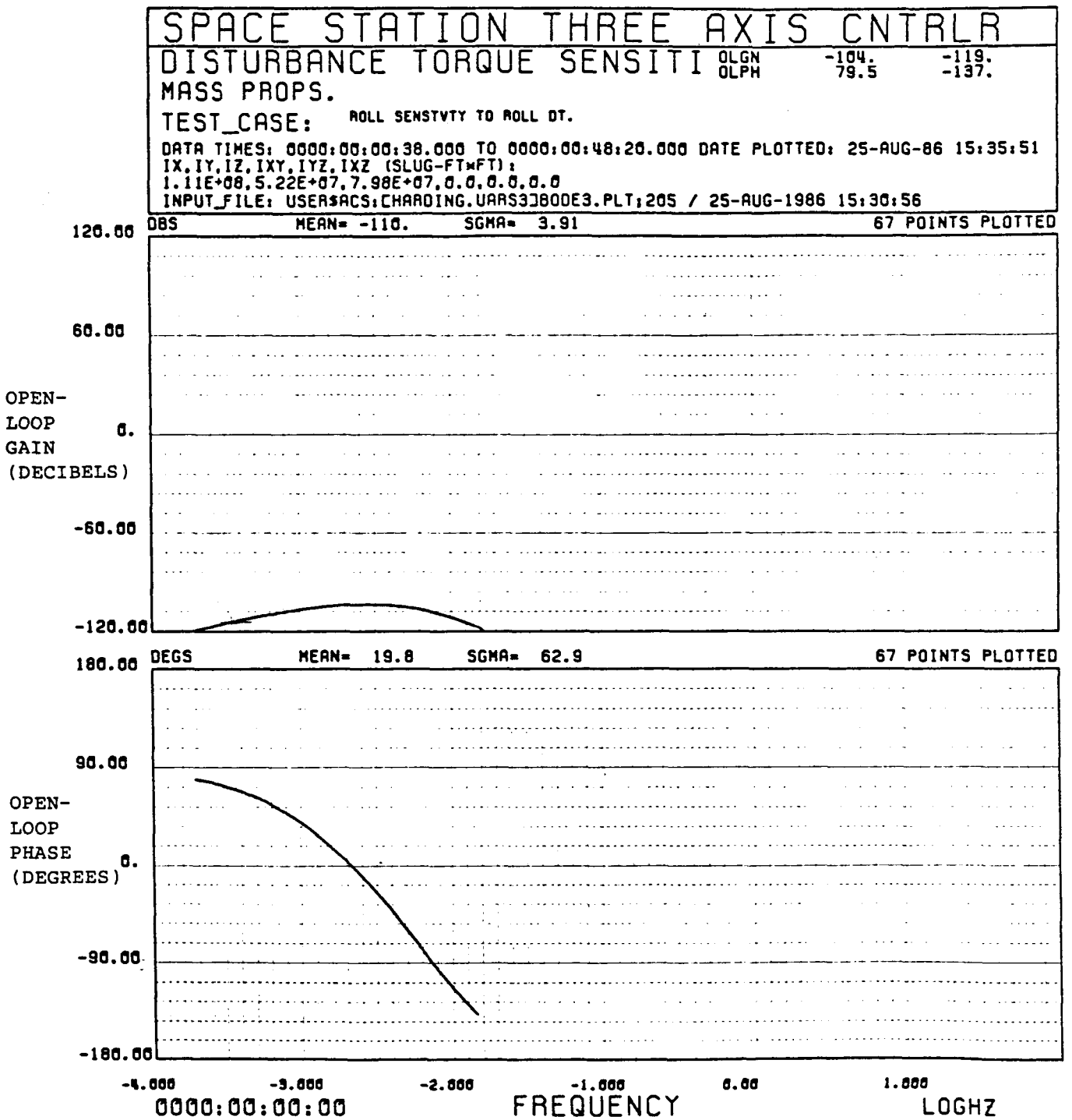
SPACE STATION THREE AXIS CNTRLR
DISTURBANCE TORQUE SENSITI
OLGN -104. -119.
OLPH 79.5 -137.
MASS PROPS.
TEST_CASE: ROLL SENSTVTY TO ROLL DT.
DATA TIMES: 0000:00:00:38.000 TO 0000:00:48:20.000 DATE PLOTTED: 25-AUG-86 15:35:51
IX,IY,IZ,IXY,IYZ,IXZ (SLUG-FT*FT):
1.11E+08,5.22E+07,7.98E+07,0.0,0.0,0.0
INPUT_FILE: USER$ACS:CHARDING.UARS3]800E3.PLT;205 / 25-AUG-1986 15:30:56
OBS MEAN= -110. SGMA= 3.91 67 POINTS PLOTTED
120.00
60.00
OPEN-
LOOP
GAIN
(DECIBELS)
0.
-60.00
-120.00
DEGS MEAN= 19.8 SGMA= 62.9 67 POINTS PLOTTED
180.00
90.00
OPEN-
LOOP
PHASE
(DEGREES)
0.
-90.00
-180.00
-4.000
-3.000
-2.000
-1.000
0.00
1.000
0000:00:00:00
FREQUENCY
LOGHZ

Figure 21

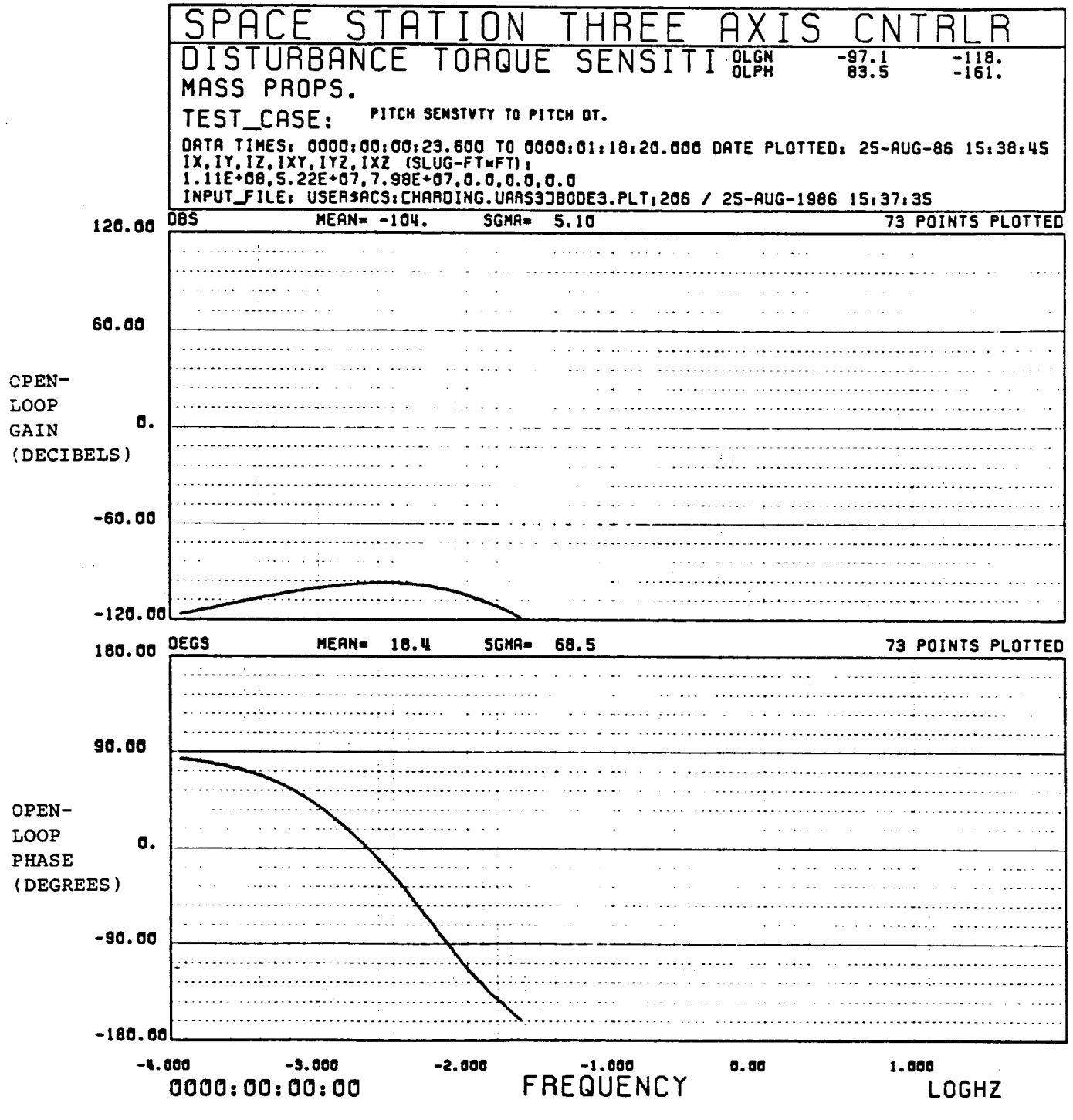
SPACE STATION THREE AXIS CNTRLR
DISTURBANCE TORQUE SENSITI
OLGN -97.1 -118.
OLPH 83.5 -161.
MASS PROPS.
TEST_CASE: PITCH SENSTVTY TO PITCH DT.
DATA TIMES: 0000:00:00:23.600 TO 0000:01:18:20.000 DATE PLOTTED: 25-AUG-86 15:38:45
IX,IY,IZ,IXY,IYZ,IXZ (SLUG-FT*FT):
1.11E+08,5.22E+07,7.98E+07,0.0,0.0,0.0
INPUT_FILE: USER$ACS:CHARDING.UARS3JBODE3.PLT;206 / 25-AUG-1986 15:37:35
OBS MEAN= -104. SGMA= 5.10 73 POINTS PLOTTED
120.00
60.00
OPEN-
LOOP
GAIN
(DECIBELS)
0.
-60.00
-120.00
DEGS MEAN= 18.4 SGMA= 68.5 73 POINTS PLOTTED
180.00
90.00
OPEN-
LOOP
PHASE
(DEGREES)
0.
-90.00
-180.00
-4.000
-3.000
-2.000
-1.000
0.00
1.000
0000:00:00:00
FREQUENCY
LOGHZ

Figure 22

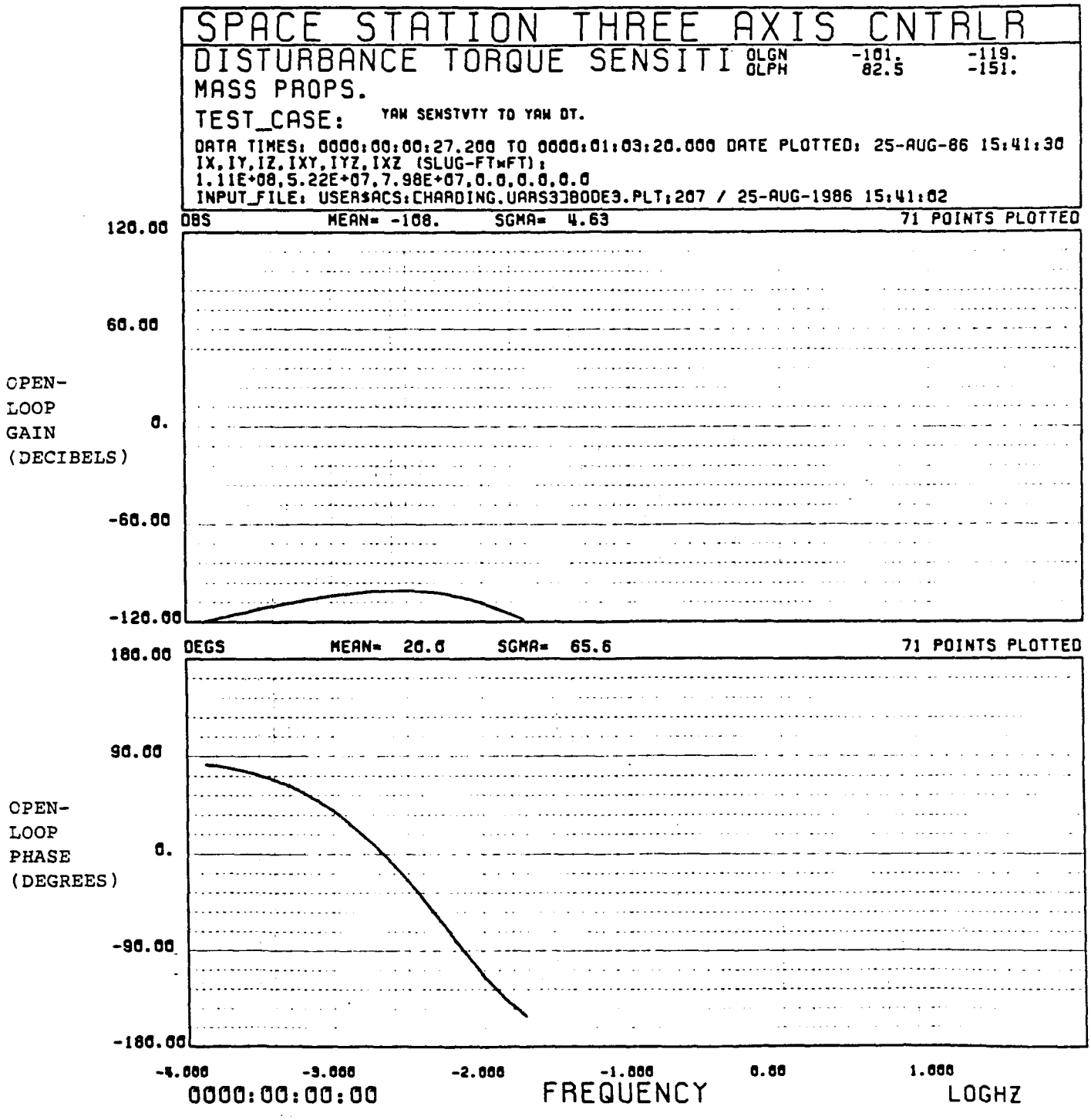
SPACE STATION THREE AXIS CNTRLR
DISTURBANCE TORQUE SENSITI
OLGN -101. -119.
OLPH 82.5 -151.
MASS PROPS.
TEST_CASE: YAW SENSTVTY TO YAW DT.
DATA TIMES: 0000:00:00:27.200 TO 0000:01:03:20.000 DATE PLOTTED: 25-AUG-86 15:41:30
IX,IY,IZ,IXY,IYZ,IXZ (SLUG-FT*FT):
1.11E+08,5.22E+07,7.98E+07,0.0,0.0,0.0
INPUT_FILE: USER$ACS:CHARDING.UARS3]BODE3.PLT;207 / 25-AUG-1986 15:41:02
OBS MEAN= -108. SGMA= 4.63 71 POINTS PLOTTED
120.00
60.00
0.
-60.00
-120.00
OPEN-LOOP GAIN (DECIBELS)
DEGS MEAN= 20.0 SGMA= 65.6 71 POINTS PLOTTED
180.00
90.00
0.
-90.00
-180.00
OPEN-LOOP PHASE (DEGREES)
-4.000
-3.000
-2.000
-1.000
0.00
1.000
0000:00:00:00
FREQUENCY
LOGHZ

Figure 23

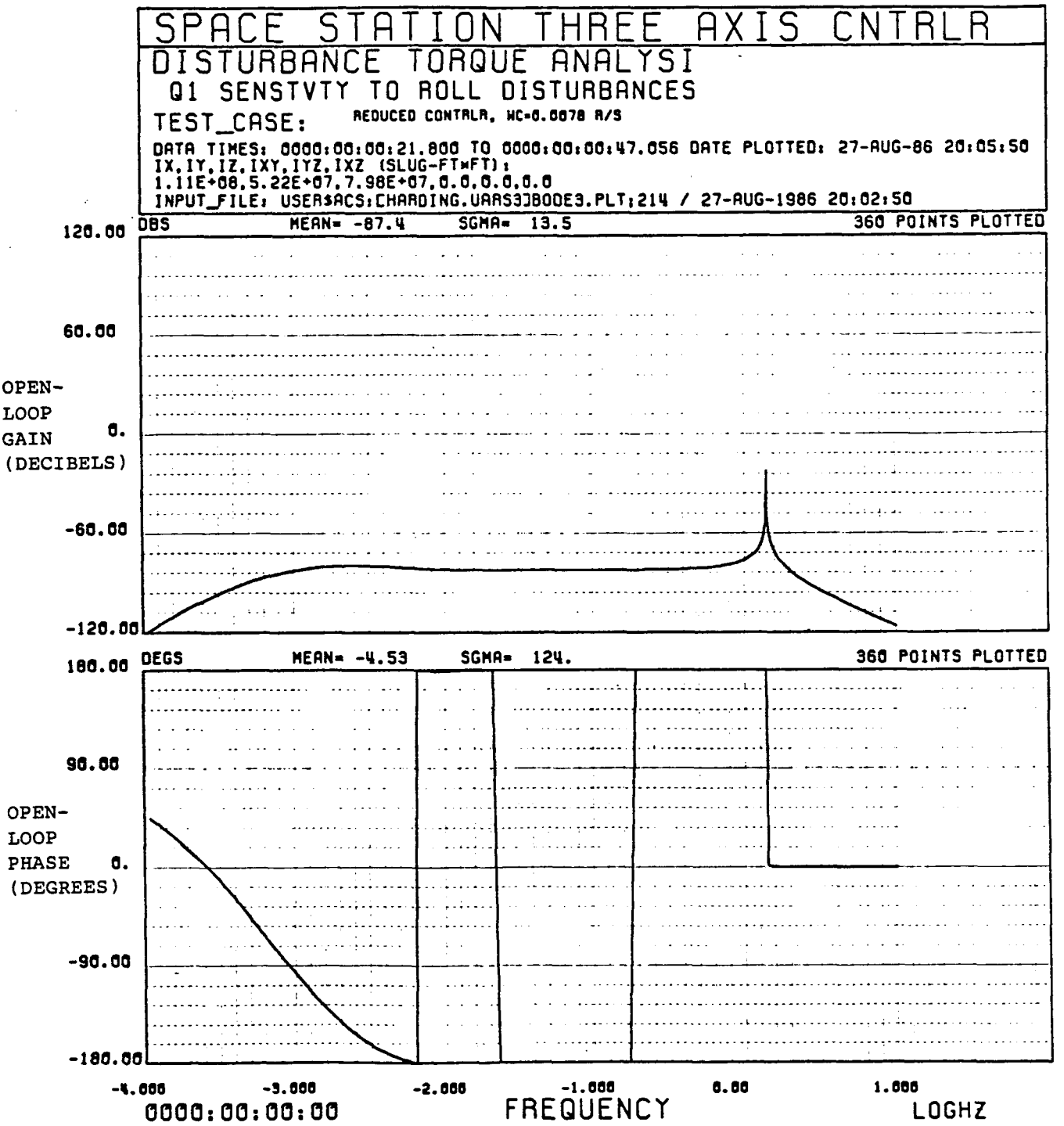
SPACE STATION THREE AXIS CNTRLR
DISTURBANCE TORQUE ANALYSI
Q1 SENSTVTY TO ROLL DISTURBANCES
TEST_CASE: REDUCED CONTRLR, WC=0.0078 R/S
DATA TIMES: 0000:00:00:21.800 TO 0000:00:00:47.056 DATE PLOTTED: 27-AUG-86 20:05:50
IX,IY,IZ,IXY,IYZ,IXZ (SLUG-FT*FT):
1.11E+08,5.22E+07,7.98E+07,0.0,0.0,0.0
INPUT_FILE: USER$ACS:CHARDING.UARS3JBODE3.PLT;214 / 27-AUG-1986 20:02:50
OBS MEAN= -87.4 SGMA= 13.5 360 POINTS PLOTTED
120.00
60.00
OPEN-
LOOP
GAIN 0.
(DECIBELS)
-60.00
-120.00
DEGS MEAN= -4.53 SGMA= 124. 360 POINTS PLOTTED
180.00
90.00
OPEN-
LOOP
PHASE 0.
(DEGREES)
-90.00
-180.00
-4.000
-3.000
-2.000
-1.000
0.00
1.000
0000:00:00:00
FREQUENCY
LOGHZ

Figure 24

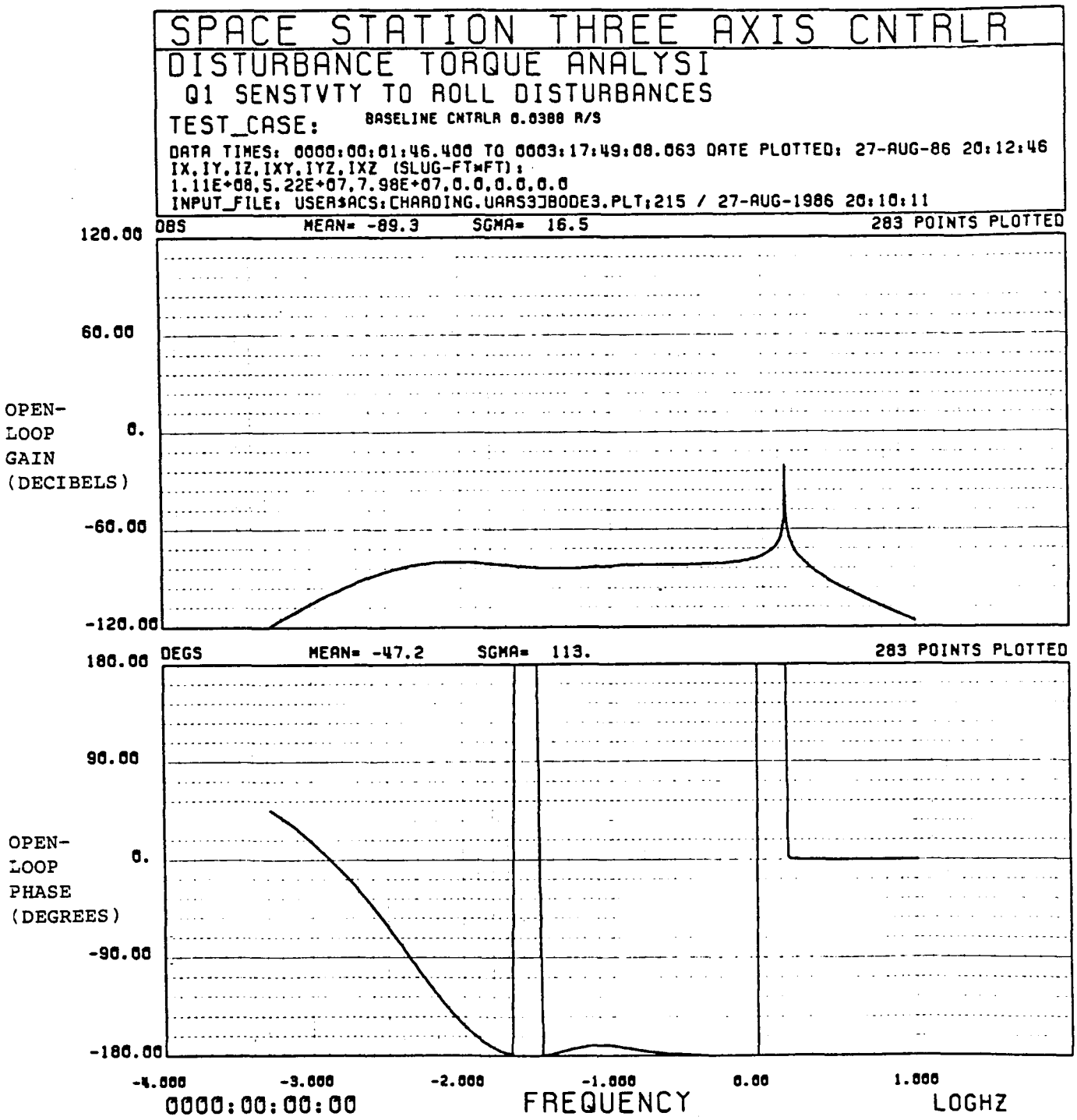
SPACE STATION THREE AXIS CNTRLR
DISTURBANCE TORQUE ANALYSI
Q1 SENSTVTY TO ROLL DISTURBANCES
TEST_CASE: BASELINE CNTRLR 0.0388 R/S
DATA TIMES: 0000:00:01:46.400 TO 0003:17:49:08.063 DATE PLOTTED: 27-AUG-86 20:12:46
IX,IY,IZ,IXY,IYZ,IXZ (SLUG-FT*FT):
1.11E+08,5.22E+07,7.98E+07,0.0,0.0,0.0
INPUT_FILE: USER$ACS:CHARDING.UARS3]BODE3.PLT;215 / 27-AUG-1986 20:10:11
OBS MEAN= -89.3 SGMA= 16.5 283 POINTS PLOTTED
120.00
60.00
OPEN-
LOOP
GAIN
(DECIBELS)
0.
-60.00
-120.00
DEGS MEAN= -47.2 SGMA= 113. 283 POINTS PLOTTED
180.00
90.00
OPEN-
LOOP
PHASE
(DEGREES)
0.
-90.00
-180.00
-4.000
-3.000
-2.000
-1.000
0.00
1.000
0000:00:00:00
FREQUENCY
LOGHZ

5 MDD EXAMPLES

5.1 Solar Array Feathering

5.1.1 Solar Array Feathering Example Description -

The solar array feathering analysis was performed in order to determine the cost savings, if any, resulting from moving the solar array panels into a minimum drag position during each orbit's umbra period. The arrays are rotated about the alpha joint so that they are "edge-on" to the velocity vector during umbra and therby represent zero area for atmospheric drag computations. The MDDT program was run once for the case when the solar arrays are feathered into the mimimum drag configuration and once for the case when the arrays are not feathered. The cost driver for this example is orbit decay rate. Greater atmospheric drag results in a higher orbit decay rate and, consequently, higher propellent-related costs (i.e. the amount of propellent expended and the cost of launching replacement propellent). The MDDT expendables subroutine (SUBROUTINE EXPD) calculates the decay rate using the user-supplied inputs initial altitude, time at measurement of initial altitude, final altitude, and time at measurement of final altitude. For this example, these inputs were derived using an in-house 3-degree of freedom scientific simulation (reference 10). This simulation was excercised for both the feathering case and the no-feathering case with results of the different Space Station array configurations shown in Figures 25 and 26. These plots depict change in semi-major axis versus

time, the inputs required by MDDT, as discussed above, to calculate the energy required to restore the space station to its original orbit. The energy is then translated into pounds of fuel and then into a cost for launch and replenishment.

5.1.2 Solar Array Feathering Example Assumptions -

Some key assumptions were made in calculating the orbit decay using the in-house simulation, and these assumptions are described below. The only user-supplied inputs required by the MDDT program; however, were initial altitude, time at measurement of initial altitude, final altitude, and time at measurement of final altitude.

Orbit altitude. 450 km. is used for a mean orbit altitude. Altitudes may vary from 400 to 500 km. (reference 6).

Inclination. 28.5 degrees.

Mean umbra time. An orbital computer simulation program was run for the baseline Space Station orbit. A mean umbra period of 2071 seconds is calculated. Plots of the umbra data is seen in Figure 27, Umbra Time versus Right Acsension. The computer routine calculates the mean value and prints the mean value at the top of the plot.

Mean array alpha angle. The alpha angle rotates completely around each orbit; however, for the purposes of drag calculations, alpha is assumed to vary from zero to 90 degrees as a sine wave. A mean alpha of 63.64 degrees is assumed as an RMS

value of a sine wave. During umbra the average alpha angle becomes 11.7 degrees.

Mean solar beta angle. A mean solar beta angle can be calculated from geometry of the earth, sun, and orbit inclination. The same program which calculates umbra period also calculates solar beta angles. Results of analysis predict a RMS beta angle of 36.7 derees. The plot of beta angle versus right ascension over the period of a year is shown in Figure 28 with a maximum beta angle of 52 degrees. As in the case of the alpha angle, an RMS value for the beta angle is calculated as 36.8 degrees. This assumes that beta varies as a single sine wave with zero mean and peak value of 52.0 degrees.

Drag coefficient. A value of 2.2 is used for this analysis. Drag coefficients for spacecraft analysis vary from one reference source to the next. The extremes for drag coefficient found in the literature are a low of 2.0 to a high of 2.6 (references 11, 12, and 13). Values of 2.2 seemed to be the most widely used.

Orbit decay time period. Orbit decay rate is non-linear over extended periods of time as seen in Figure 29. For the purposes of this example, a 10 day orbit adjust interval is assumed.

Hydrazine is the assumed propellent. The no-feathering case is approximated by calculating orbit decay assuming a frontal area consisting of the initial reference structure with arrays in

the average beta and umbra average alpha position. The feathering case is approximated using the reference structure area without solar arrays. Orbit adjusts are assumed to occur at 10 day intervals.

5.1.3 Solar Array Feathering Example Results -

The analysis predicts that approximately $25.7 million in propellent cost could be saved by feathering the solar arrays during umbra.

5.2 Expendables Orbit Adjust Interval

5.2.1 Expendables Example Description -

As the frequency of orbit adjust maneuvers increases, orbit decay rate decreases. Thus, the longer the interval between orbit adjusts, the more propellent is consumed over the same time period. To demonstrate this effect, one case was run with an interval of 50 days between orbit adjusts rather than the nominal 10 days used in all other cases.

5.2.2 Expendables Example Assumptions -

Baseline case, with time between orbit adjusts equal to 50 days.

5.2.3 Expendables Example Results -

The savings resulting from performing orbit adjust maneuvers every 10 days rather than every 50 days is $21,270,000. During an interactive program run, it was found that this the majority of this saving (about 96%) can be attributed to savings in the cost of launching the replacment expendables. The saving in propellent cost alone is approximately $82,000.

5.3 Monopropellent Vs. Bipropellent

5.3.1 Monopropellent Vs. Bipropellent Example Description -

Some of the same information used in the solar array feathering analysis was used to predict the more economic propellent, given the choice between monopropellent hydrazine and a bipropellent.

5.3.2 Monopropellent Vs. Bipropellent Example Assumptions -

The propellents used in the comparison are N2H4 (monopropellent hydrazine; ISP=233) and N2H4/N2O4 (ISP=310).

5.3.3 Monopropellent Vs. Bipropellent Example Results -

A significant savings is realized by using a bipropellent in place of monopropellent hydrazine. Over $126,000,000 is saved overall, most of which is due to launch cost savings. Approximately $1,850,000 in propellent cost is saved.

5.4 Active Vs Passive Damping LCC

5.4.1 Active Vs Passive Damping Example Description -

A trade study on the life cycle cost of active vs passive damping of the space station was performed. The configuration considered is an erectable five meter bay truss dual keel space station. Various levels of passive structural damping were considered. The amount of active control required for equivalent performance at each level of passive damping was estimated based on results obtained from previous Independent Research and Development results.

5.4.2 Active Vs Passive Damping Example Assumptions -

It was assumed that the percent damping of the stucture was proportional to the percentage of the structural weight comprised of Visco-Elastic Material (VEM). In an actual structure the majority of the damping occurs in regions of high strain. Thus evenly distributing VEM over all portions of the structure is very inefficient in terms of weight. It is much more efficient to apply VEM only to elements experiencing large strain. The amount of damping required for 1% damping is 1% of the weight of the treated elements. This is a crude first cut approximation of the damping.

For the space station model employed, it is assumed that only the diagonal truss members required treatment with VEM. This assumption was made in order to have an example and it has not been verified that this constitutes an optimal treatment for

the space station. Treating only members with high strain certain elements reduces the weight penalty imposed by passive damping.

It was assumed that the active control of the structure was implemented employing the existing ACS hardware. Changes in the ACS software control law were employed to account for different levels of active control required to achieve similar performance for different levels of damping. The complexity, and therefore cost, of the control law is assumed to be a function of the control system bandwidth, the number of sensors, the number of controllers, and the number of structural modes that have to be controlled. Information from reference 14 and Figure 30 was employed to develop a simple cost model of the active control software. The active control software is asssumed to consist of three functionally distinct processors; the control law, the modal coordinate estimator, and the optimal control gain matrix calculation.

The number of operations/cycle for the control law is included in the table for information purposes. The memory requirements for the compensation is used to determine the cost for the control law. The ops/cycle data is taken directly from a linear quadratic controller used in a prior IRD effort (Internal Research and Development) which investigated active structural control.

Both the estimator and optimal control gain memory requirements are derived from similar Landsat-D software memory requirements. The memory requirements shown here have been scaled from Landsat-D by simple ratios of number of estimated states, numbers of sensors, and numbers of actuators. Numbers of lines of code are derived by an average 2.5:1 ratio of lines of macro code for the NASA standard processor (NSSC-1) to number of words. Again, number of lines of code is included for information only.

Cost has been related to the memory requirement for each processor. A scale of $600/word is typical and is assumed for these calculations.

5.4.3 Active Vs Passive Damping Example Results -

Figure 31 presents the weight of VEM (Visco-Elastic Material) required for each level of damping considered. By treating only the diagonal truss members the weight penalty imposed is significantly reduced. A weight penalty of 340. pounds was incurred in achieving a zeta (percent of critical damping) of ten percent.

Figure 32 presents the results of the life cycle cost trade study done on active verses passive control. Note that as the structural damping increases the amount of active control required to maintain the same ACS performance decreases. As can be seen, a structure with a zeta of ten percent has a life cycle cost of 775.3 million dollars. This is 11.2 million dollars less

than the cost of the case with zeta equal to .05 percent. The savings are due to a reduction in the cost of the active control software and occur in spite of an increase in the cost of the structure.

Figure 25

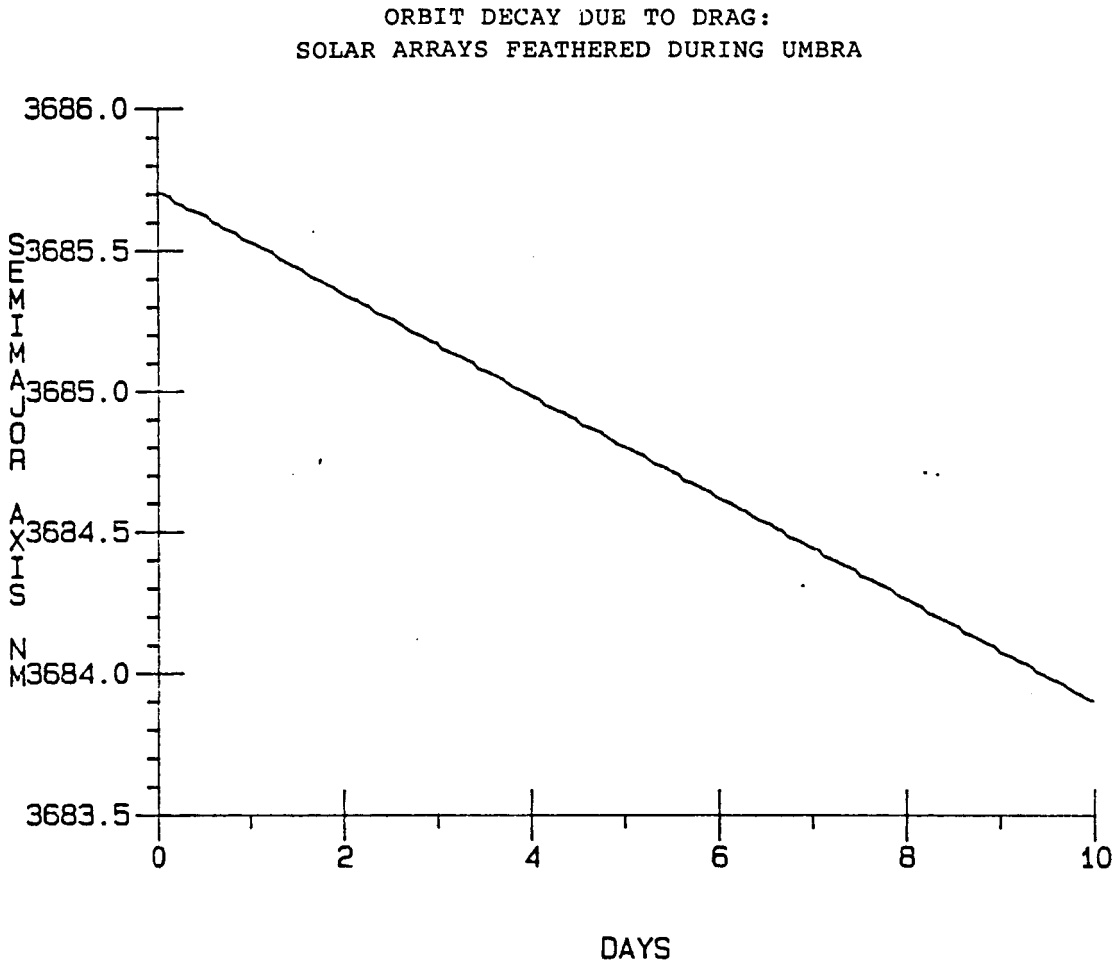
ORBIT DECAY DUE TO DRAG:
SOLAR ARRAYS FEATHERED DURING UMBRA
3686.0
3685.5
3685.0
3684.5
3684.0
3683.5
SEMIMAJOR AXIS NM
0
2
4
6
8
10
DAYS

Figure 26

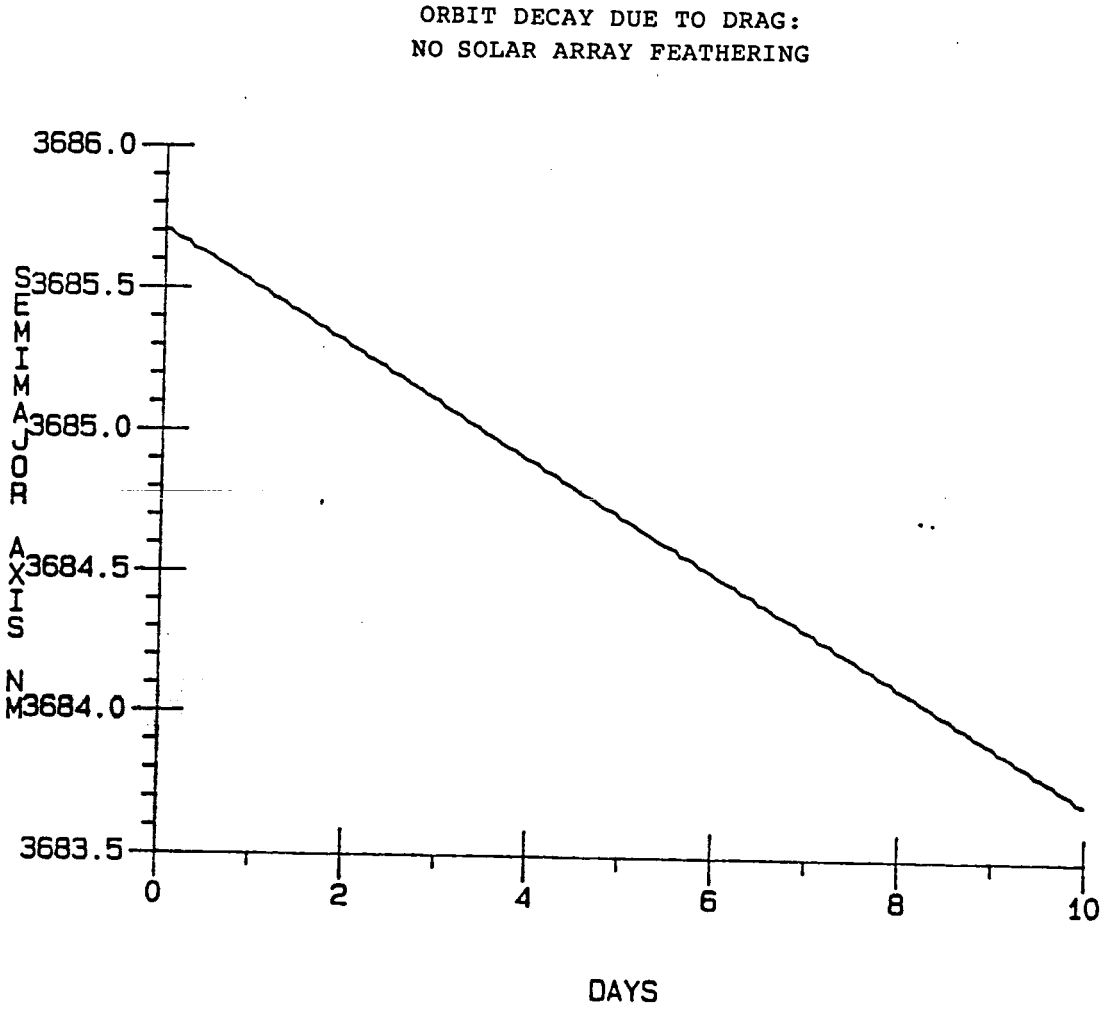
ORBIT DECAY DUE TO DRAG:
NO SOLAR ARRAY FEATHERING
3686.0
3685.5
3685.0
3684.5
3684.0
3683.5
SEMIMAJOR AXIS NM
0
2
4
6
8
10
DAYS

Figure 27

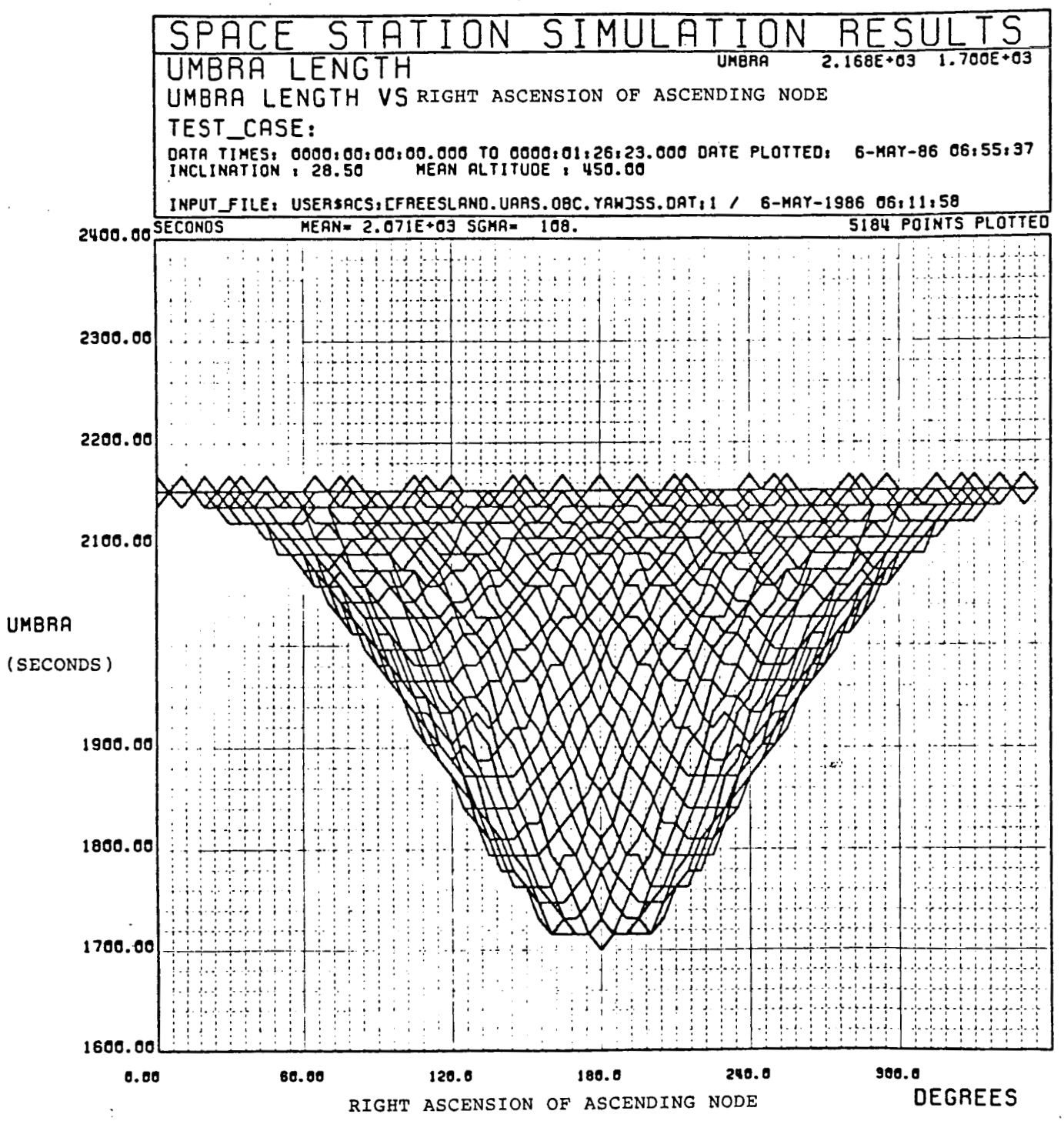
SPACE STATION SIMULATION RESULTS
UMBRA LENGTH
UMBRA 2.168E+03 1.700E+03
UMBRA LENGTH VS RIGHT ASCENSION OF ASCENDING NODE
TEST_CASE:
DATA TIMES: 0000:00:00:00.000 TO 0000:01:26:23.000 DATE PLOTTED: 6-MAY-86 06:55:37
INCLINATION : 28.50 MEAN ALTITUDE : 450.00
INPUT_FILE: USER$ACS:[FREELAND.UARS.OBC.YAWJSS.DAT;1 / 6-MAY-1986 06:11:58
SECONDS MEAN= 2.071E+03 SIGMA= 108. 5184 POINTS PLOTTED
2400.00
2300.00
2200.00
2100.00
UMBRA
(SECONDS)
1900.00
1800.00
1700.00
1600.00
0.00
60.00
120.0
180.0
240.0
300.0
RIGHT ASCENSION OF ASCENDING NODE
DEGREES

Figure 28

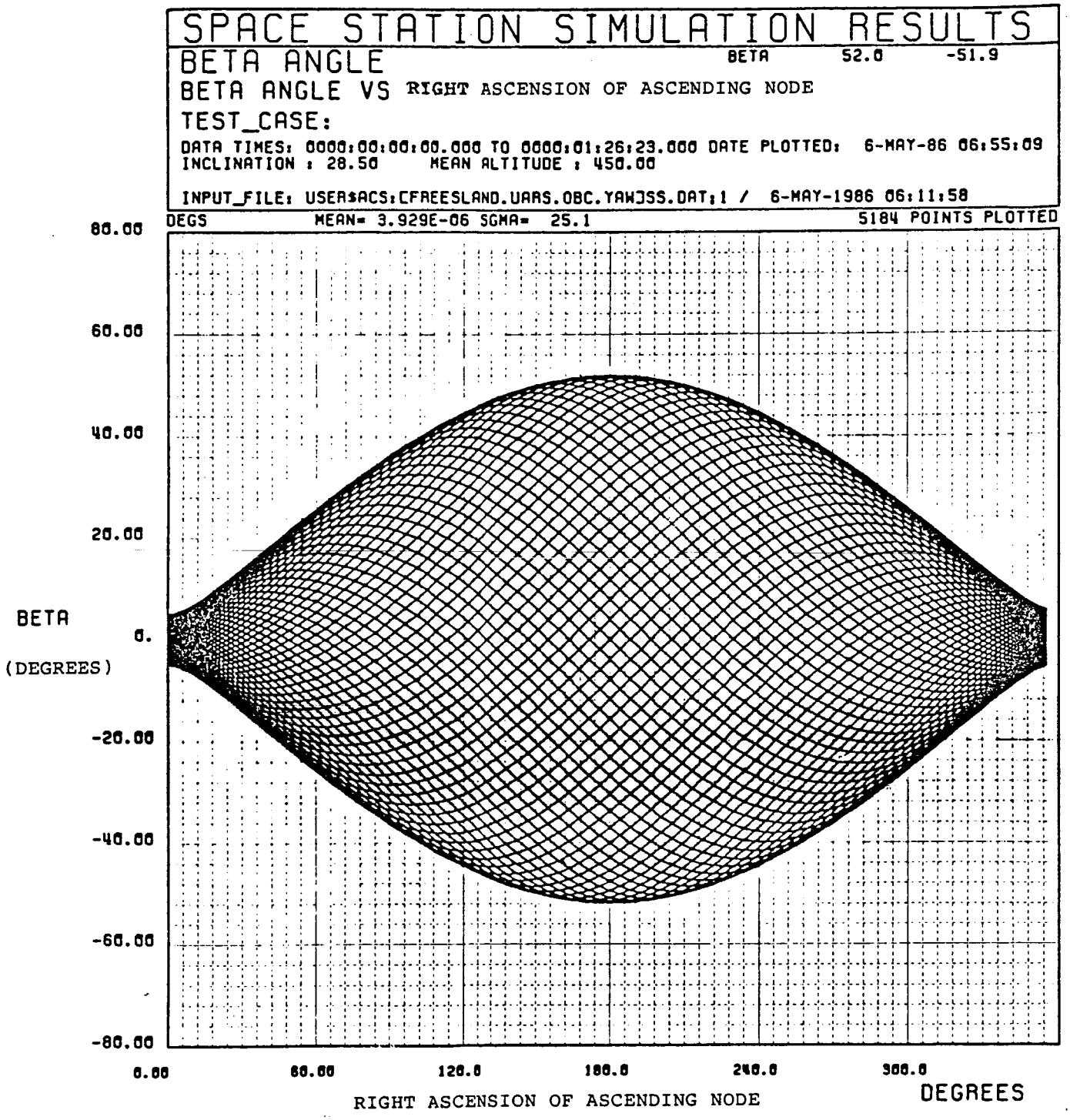

Figure 29

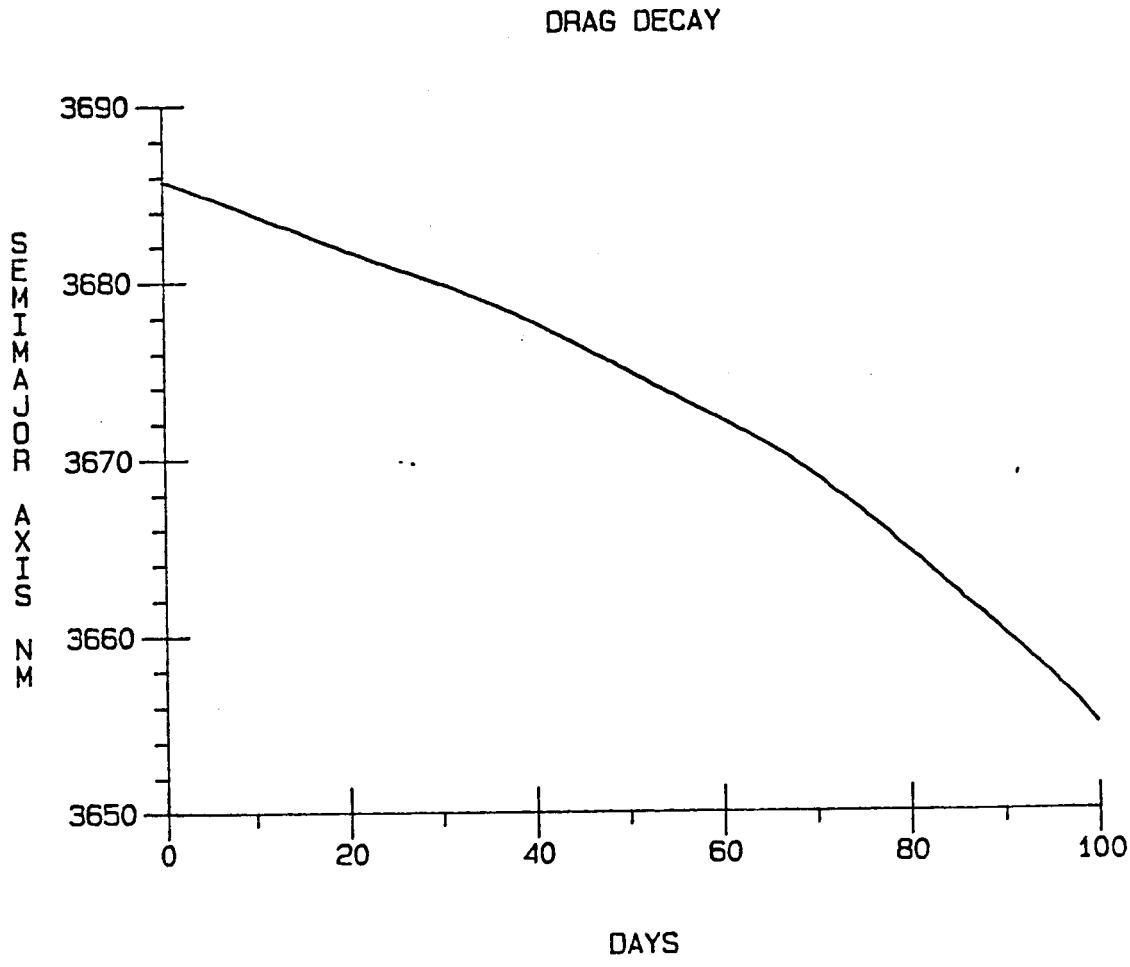
DRAG DECAY
SEMIMAJOR AXIS NM
3690
3680
3670
3660
3650
0
20
40
60
80
100
DAYS

Figure 30

Active Structure Modal Damping
Computational Requirements and Cost

PROCESSOR NAME	NUMBER of OPS/CYCLE[2]	NUMBER of WORDS[3]	NUMBER of LINES of CODE[4]	SOFTWARE COST[1] ($ K)
Control Law		$230xn$	$92xn$	$138xn$
assignments	$8n^2 + 24n + 8nx + 8nm + 3(x + m)$			
counters	$n^2 + 4n + 2(nm + xn) + x + m$			
additions	$n^2 + 4n + 2nm + xn + x$			
multiplies	$n^2 + 2nm + 2xn$			
Kalman State Estimation Gains	*not available*	$500xn$	$200xn$	$300xn$
Optimal Control Gains	*not available*	$500nm$	$200xn$	$300nm$
TOTAL Active Control S/W Cost				$438xn + 300nm$

Legend: x = no. of sensors; n = no. of modes; m = no. of actuators

1. Cost is based on $600/word from DSCS flight software cost data.
2. The number of operations/cycle is shown for information only.
3. Number of words is based on similar Landsat softare scaled for sensors and actuators.
4. Number of words ≈ 2.5 lines of NSSC-1 Macro.

Figure 31 Weight of Passive Damping Treatment

Zeta (Percent)	Weight Penalty (Pounds)	Weight Penalty (Percent of Total Structural Weight)
0.1	<1.	0.04
0.5	10.	0.20
1.0	30.	0.38
5.0	160.	2.0
10.	340.	4.3

Figure 32 Active vs Passive Control Life Cycle Trade Study

	Structural Damping (Zeta in percent)					
	.05	.1	.5	1.	5.	10.
Type of Cost						
Non-Recurring Cost	153.6	153.6	153.7	153.7	154.3	154.9
Launch Cost	37.6	37.6	37.6	37.6	37.9	38.3
Ground Support Cost	20.9	20.9	20.9	20.9	20.9	20.9
Maintainence Cost	42.0	42.0	42.0	42.0	42.0	42.0
Expendables Cost	503.6	503.6	503.6	503.6	503.6	503.6
Software Cost	28.8	28.8	24.4	24.4	15.5	15.5
Total Cost	786.5	786.6	782.2	782.3	774.2	775.3

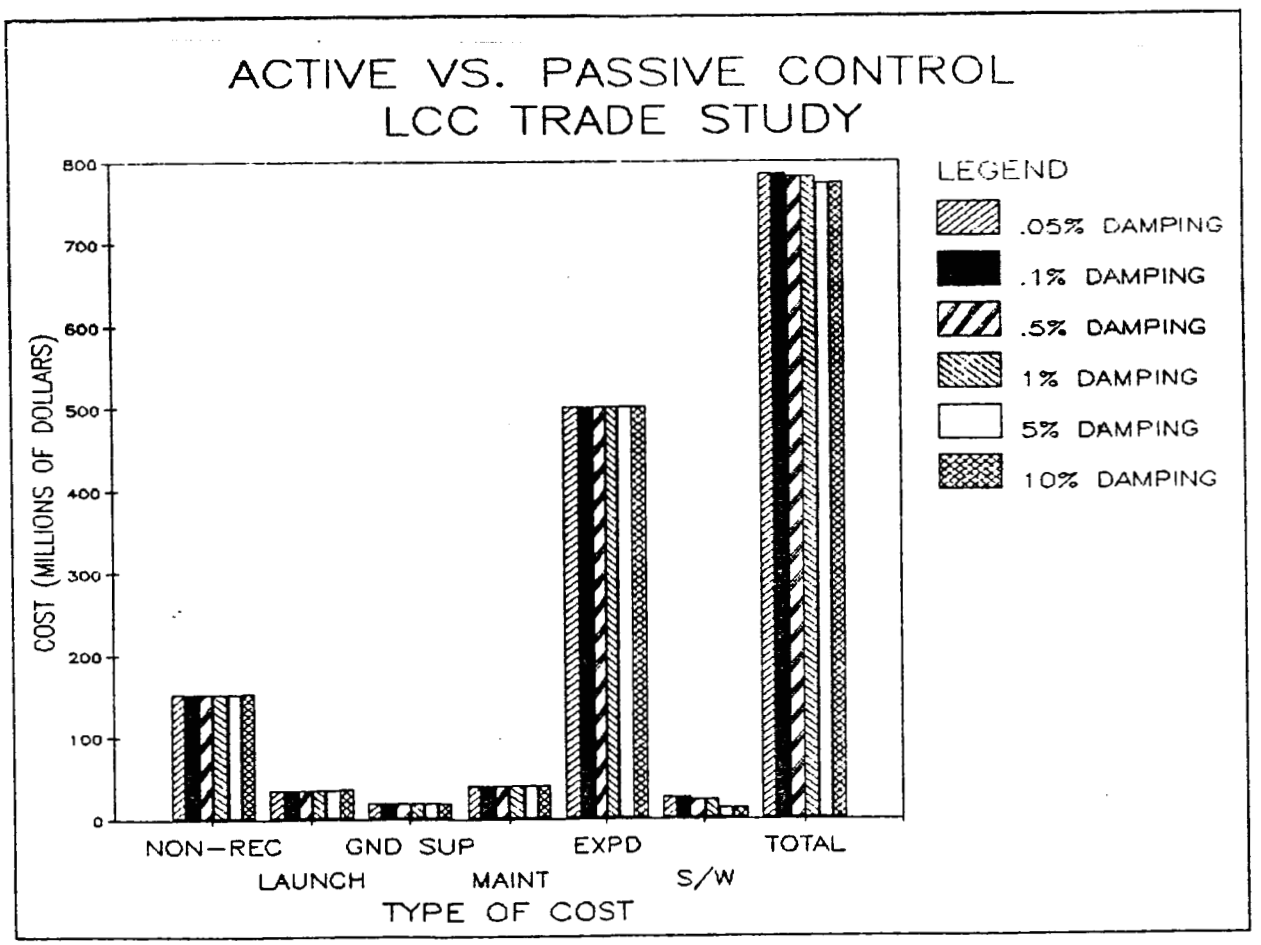

6 CONCLUSIONS

In light of the increasing complexity of spacecraft designs, a need for a design criterion which can be applied to a broad range of design disciplines is readily recognized. The MDD Study investigates the use LCC as a comprehensive design criterion to interrelated spacecraft subsystems design such as controls and structures. The Multi-Disciplinary Design Tool developed as part of the study, uses the relationships between cost and subsystem design parameters to provide a means for evaluating LCC sensitivity to design parameters and, therefore, to different space system designs.

6.1 Advantages Of MDDT

The MDDT computer program is a useful tool for investigating LCC sensitivities and for conducting subsystem design trades using LCC as the design criteria. The examples show that MDDT is a fully operational program capable of performing such analyses. The examples also show that LCC is an important aspect of system design and that analyses such as this one can provide significant cost savings which may outweigh other design criteria.

A program such as MDDT also formalizes the LCC computations so that a variety of system design trades can be accomplished with a high degree of confidence that the same cost consideration is given to each set of design parameters for any given subsystem configuration.

Much of the study was directed toward deriving representative values for the input parameters so that it is possible to use the existing program for cost sensitivities to these parameters with simple changes to the input file.

The architecture of MDDT has proven to be flexible and general. MDDT is modular in design which allows the user to change the program flow easily. This is essential for modifying the program to do LCC studies beyond the current capability of MDDT. This was especially appreciated when the example cases were investigated.

6.2 General User Information

As with any computer tool, the usefulness of the results depends on the assumptions of the programmer and accuracy of the model. In the case of MDDT, care should be taken when interpreting the results. In general, assumptions are made in the LCC model which tend to degrade the accuracy of the predicted costs. This is why the major assumptions are explicitly stated in this report. The user is further cautioned that the model has other inherent inaccuracies. In reality, the design variables tend to be coupled so that a small change in some variables create large variations in the final result. In the MDDT, all design parameters tend to be dependent on less than two other parameters (some of the paramters are independent so that LCC will vary 1:1 with that independent parameter which is due to the difficulty in creating a high fidelty model at this point of the MDDT's development). The aim of the MDD study was to identify

those relations where parameter interdependence was greatest or at least most obvious.

The investigators have noted the following additional comments which are directed to the user or potential user.

The MDDT program is relatively well commented with most parameters defined within the subroutines where they are used.

The MDDT has numerous input parameters; more parameters than we originally anticipated. This seems to be due to the very broad nature of the cost aspects of the LCC design criteria.

Reducing the number of input parameters would require further analysis to define more comprehensive cost relationships. Reduction could also be achieved by including some form of the analysis tools (simulations) which were used to generate some of the parameters.

7 REFERENCES

1. Fong, F.K., et al, "Space Division Unmanned Spacecraft Cost Model", Fifth Edition, Space Division/ACC, June 1981.

2. Bordano,A.,"Space Station Flight Mode",Presentation at Lyndon B. Johnson Space Center, February 20, 1986.

3. Mikulas,Jr.,M.M.,et al,"Deployable/Erectable Trade Study For Space Station Truss Structures", NASA Techical Memorandum 87573, July 1985.

4. McCutchen, D.K., "Minutes for the Structures/ Dynamics Technical Integration Panel Meeting", Lyndon B. Johnson Space Center Memo, January 1986.

5. "Space Station Definition and Preliminary Design, WP-02, Preliminary Analysis and Design Document (DR-02), Book 8, Guidance, Navigation, and Control (Section 4.5)", December 1985.

6. "Space Station 5-meter Truss Configuration (Z-Y Plane View)", Developed from work done at General Electric Space Systems Division, Valley Forge Space Center, for Space Station WP-03 Contract.

7. Foulke, H.F., "DISTOR Equations", Control Systems Engineering, General Electric Space Systems Division, Valley Forge Space Center.

8. Freesland, D.C., Computer programs "DENVAR.FOR", "UMBRA.FOR",

Control Systems Engineering, General Electric Space Systems Division, Valley Forge Space Center.

9. Harding, R.R., Duran, J.M, Computer program "SPSTA.FOR", Control Systems Engineering, General Electric Space Systems Division, Valley Forge Space Center.

10. Wertz, James R., editor, "Astrophysics and Space Science Library: Spacecraft Attitude Determination and Control", Dordrecht, Holland: D. Reidel Publishing Company, 1985.

11. Cook, G.E., "Satellite Drag Coefficients", Royal Aircraft Establishment, Farnborough, Hants.

12. Davison, Paul H., "Passive Aerodynamic Attitude Stabilization of Near Earth Satellites", WADD Technical Report 61-133, Volume II, Flight Dynamics Laboratory, Aeronautical Systems Division, Air Force Systems Command, Wright-Patterson Air Force Base, Ohio, July 1961.

13. DeBra, D.B., "The Effect of Aerodynamic Forces on Satellite Attitude", The Journal of the Astronautical Sciences.

14. Gehling,R.N.,"Effect of Passive Damping on Active Energy Requirements",Work performed under PACOSS Contract F33615-82-C-3222, March 1986.

15. Covault, Craig, "Orbiter Crew Restores Solar Max", Avation Week & Space Technology, April 16, 1984.

16. James, T.R., Computer Program "BOEDT.FOR", Software

Engineering, General Electric Space Systems Division, Valley Forge Space Center.

17. Miller, John, Computer program "JMFSE1.FOR", Systems Requirements and Analysis, General Electric Space Systems Division, Valley Forge Space Center.

18. "Space Station Reference Configuration Description", Systems Engineering and Integration, Space Station Program Office, August 1984.

APPENDIX A

SPACE STATION DISTURBANCE SIMULATIONS

Figure A-1: Crew Kickoff, ACS Inactive, ACS X-axis Deflection.

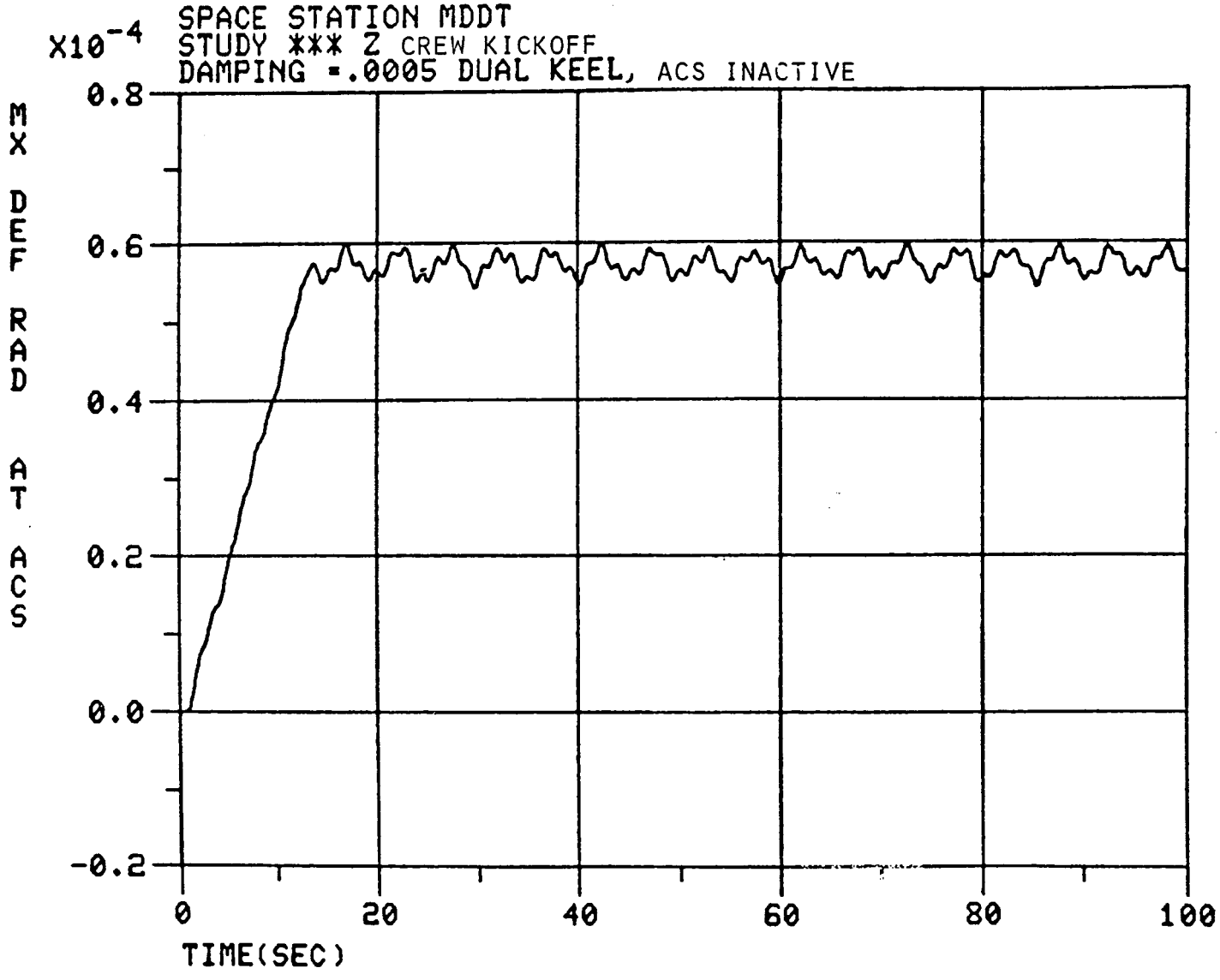

Figure A-2: Crew Kickoff, ACS Inactive, ACS Y-axis Deflection.

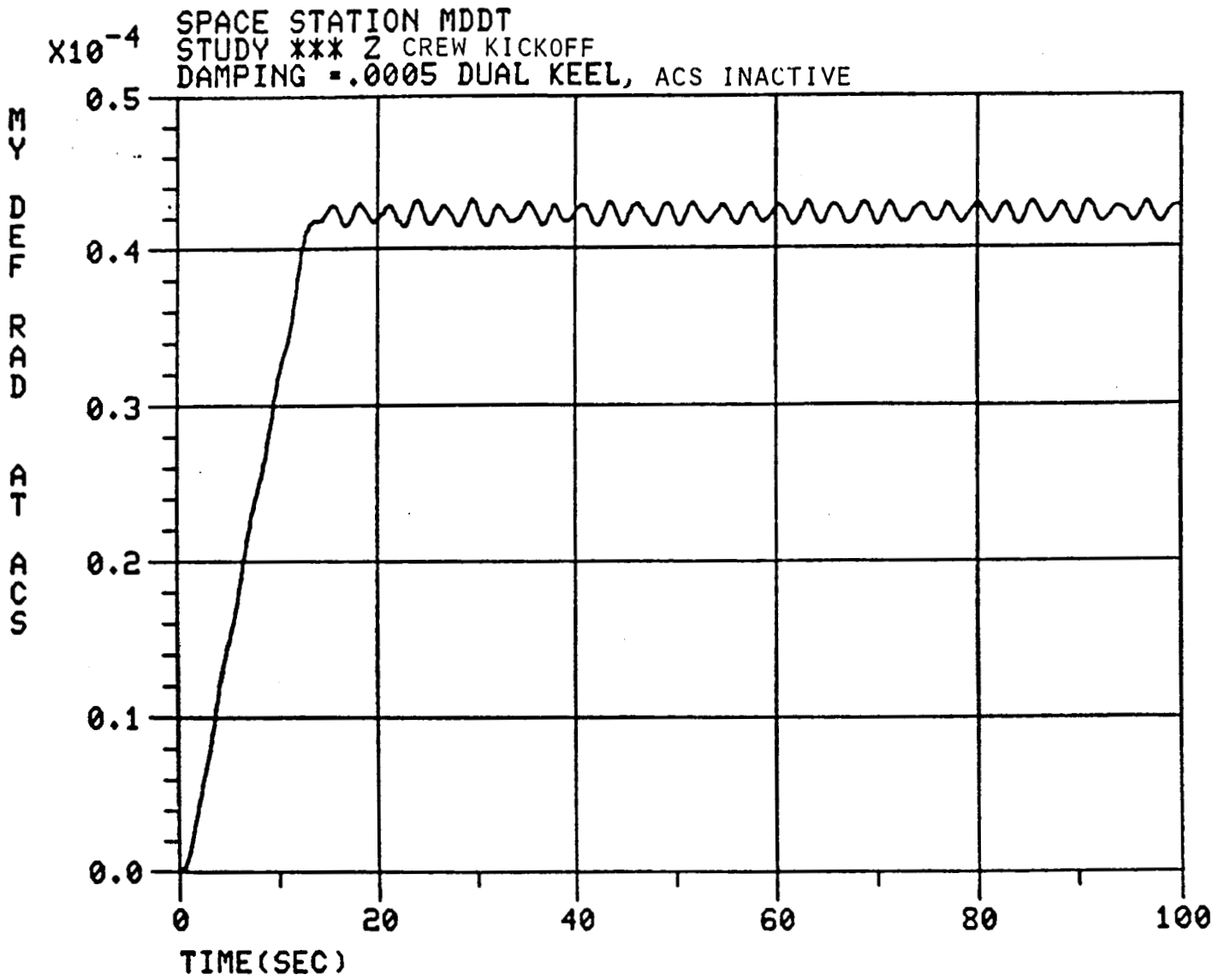

Figure A-3: Crew Kickoff, ACS Inactive, ACS Z-axis Deflection.

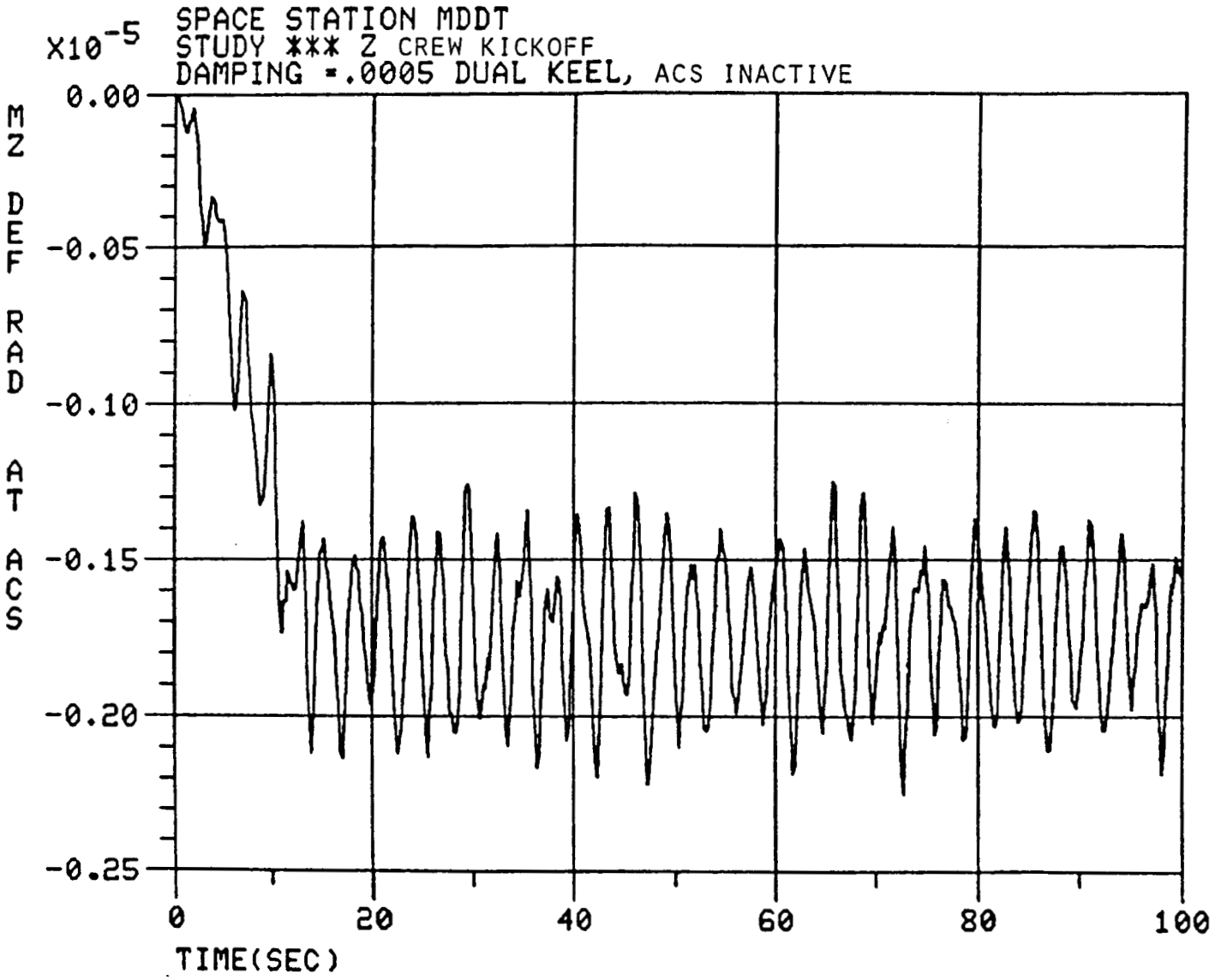

Figure A-4: Crew Kickoff, ACS Inactive, Lower Boom Tip.
Y-axis Deflection.

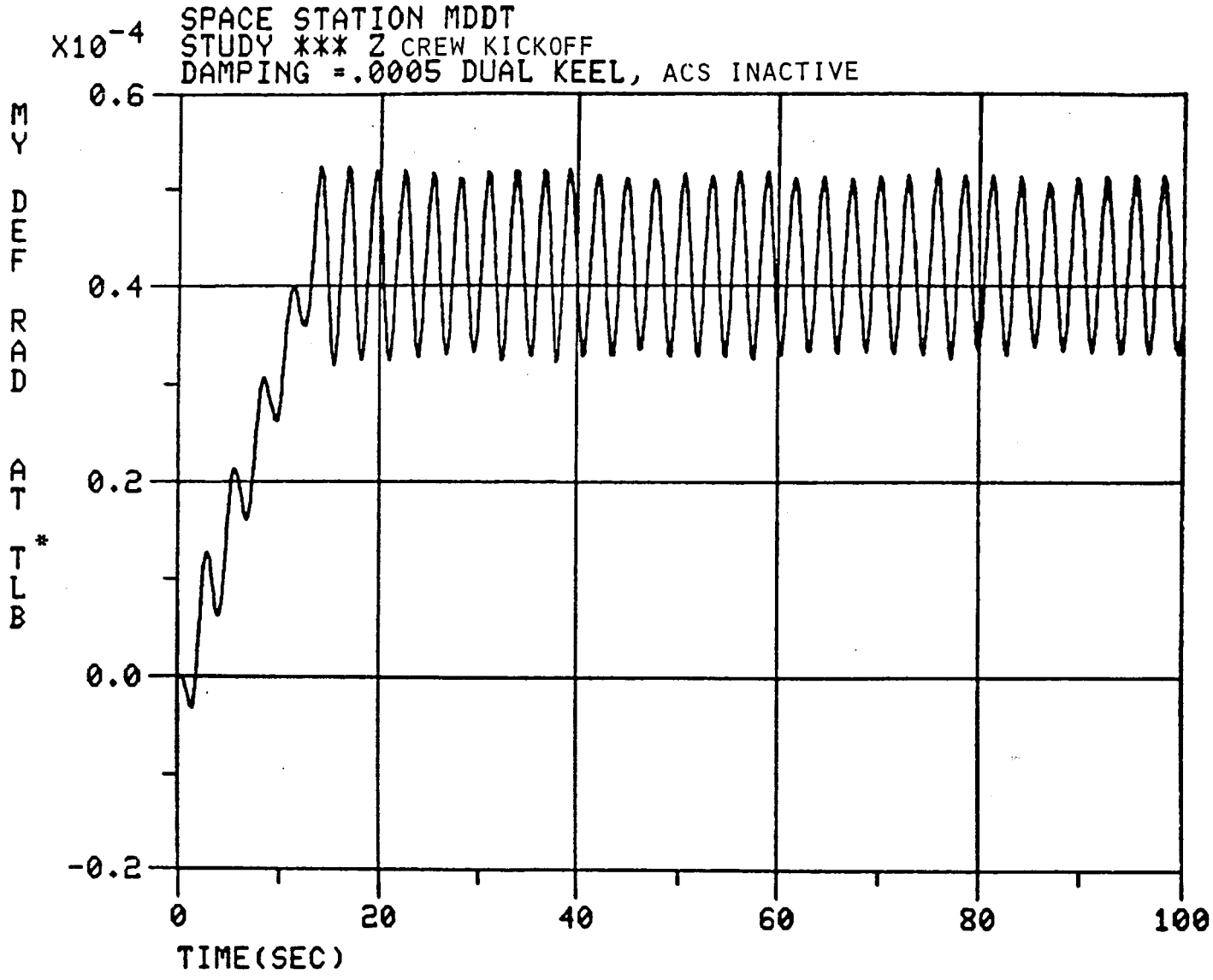

*TLB: TIP OF LOWER BOOM

Figure A-5: Crew Kickoff, ACS Inactive, Lower Boom Tip.
Z-axis Acceleration.

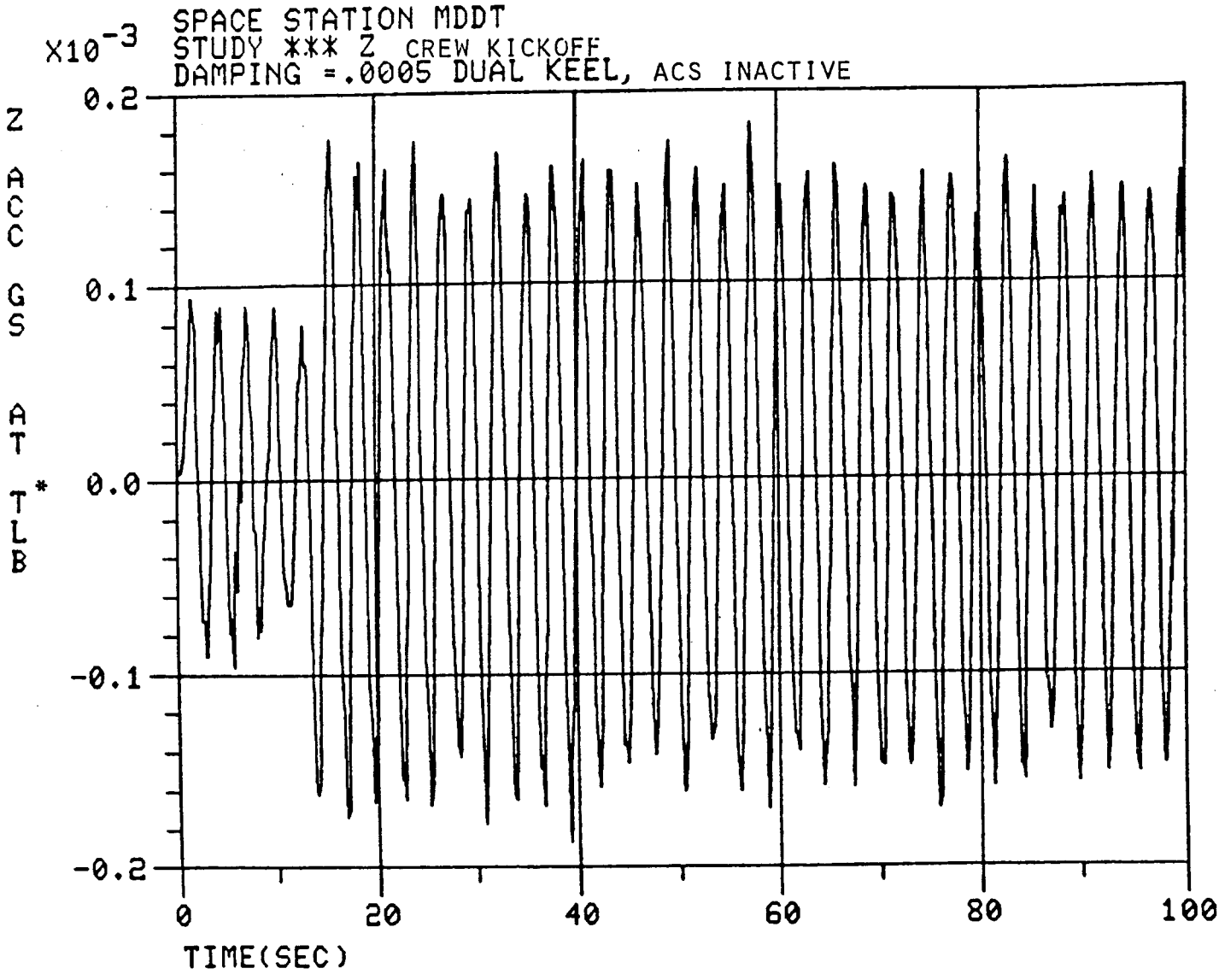

*TLB: TIP OF LOWER BOOM

Figure A-6: Crew Kickoff, ACS Active, ACS X-axis Deflection.

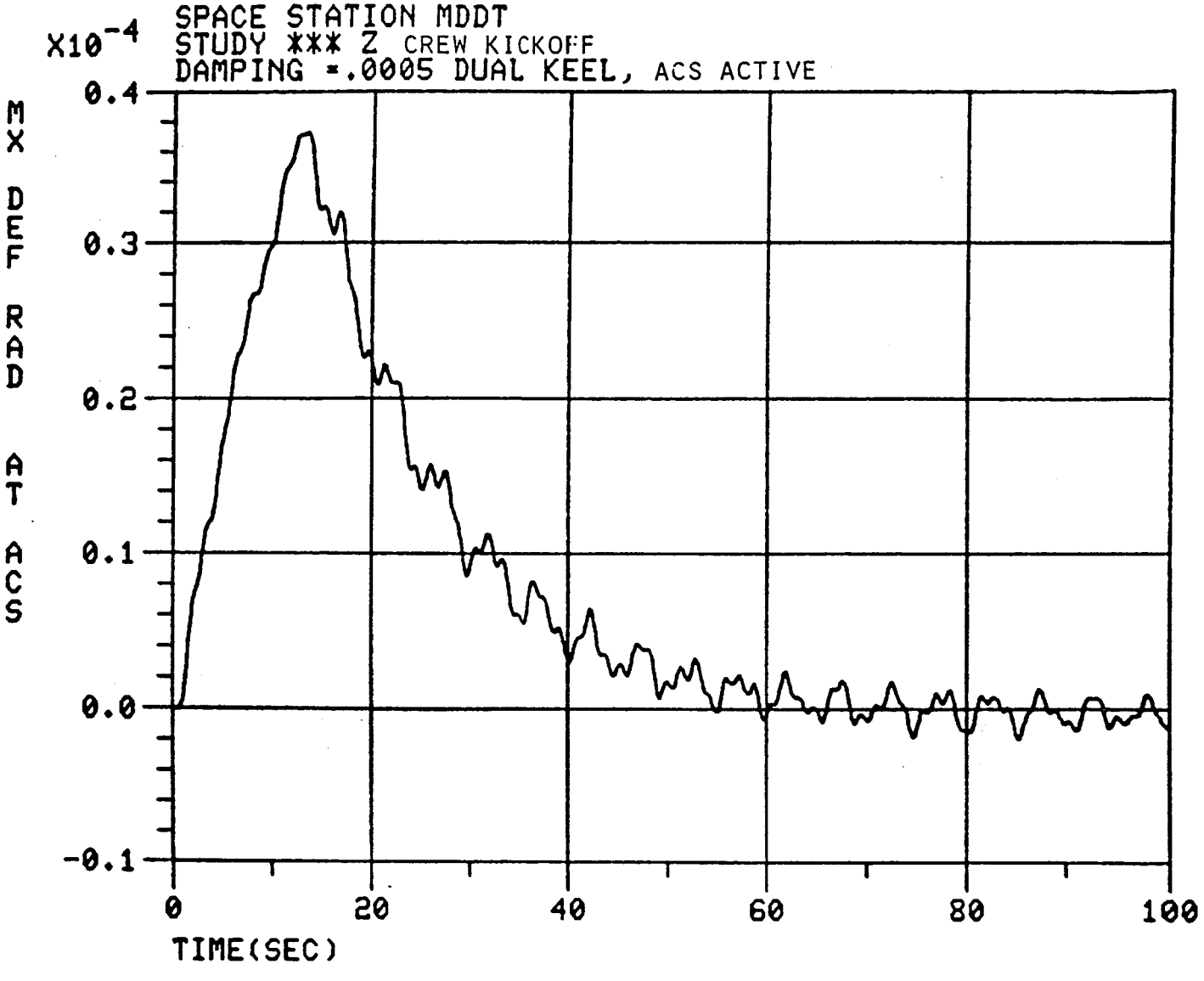

Figure A-7: Crew Kickoff, ACS Active, ACS Y-axis Deflection.

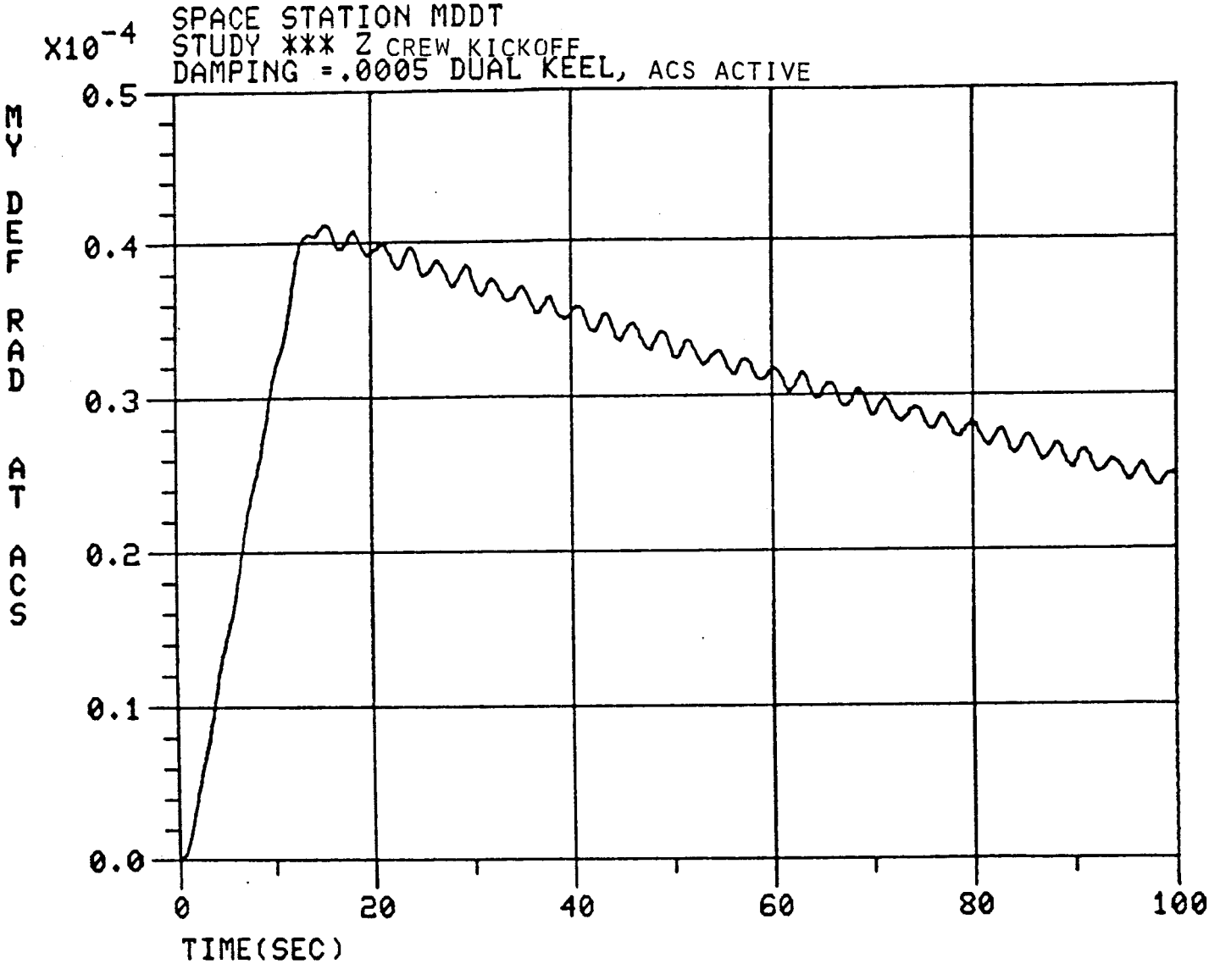

Figure A-8: Crew Kickoff, ACS Active, ACS Z-axis Deflection.

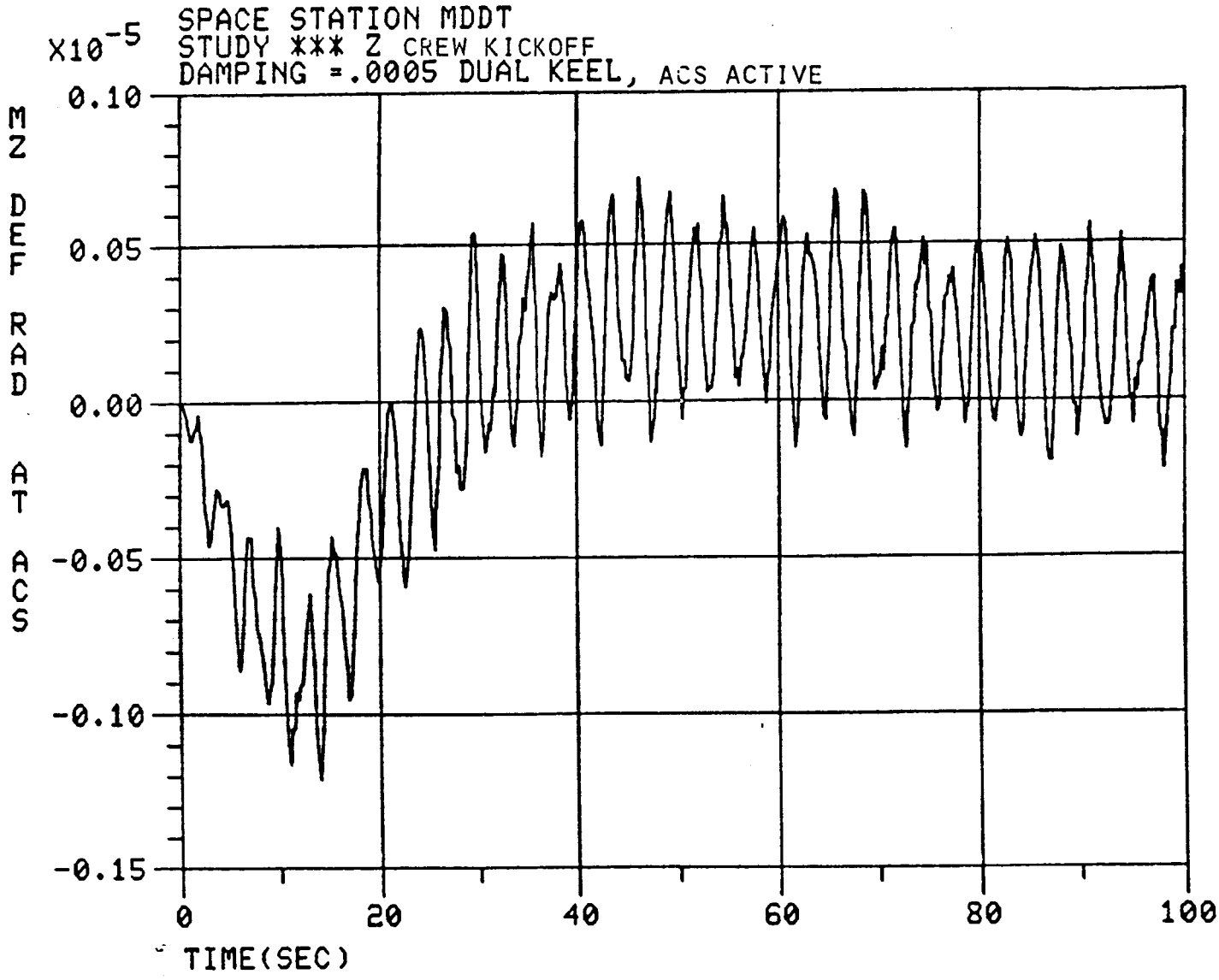

Figure A-9: Crew Kickoff, ACS Active, Lower Boom Tip.
Y-axis Deflection.

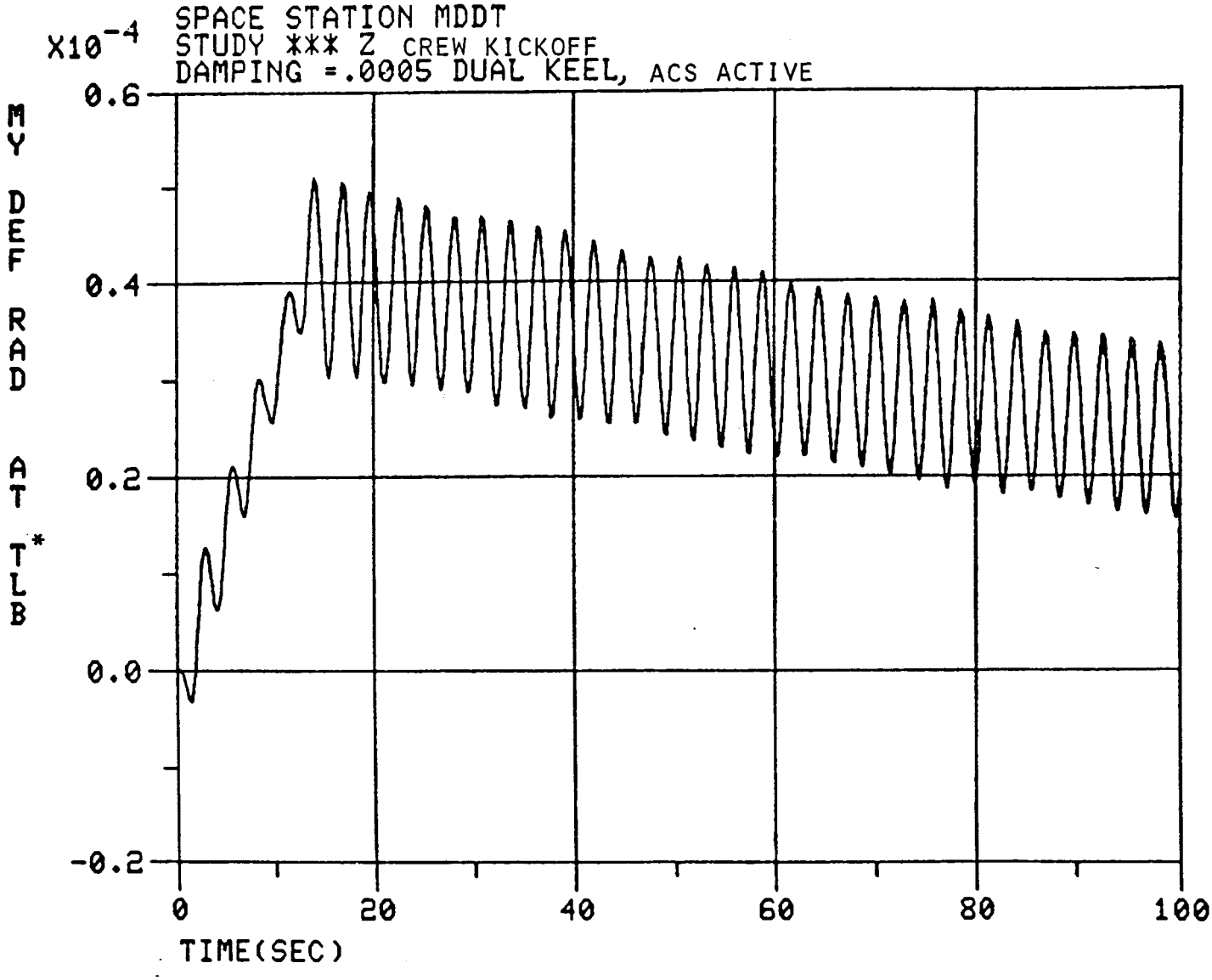

*TLB: TIP OF LOWER BOOM

Figure A-10: Crew Kickoff, ACS Active, Lower Boom Tip.
Z-axis Acceleration.

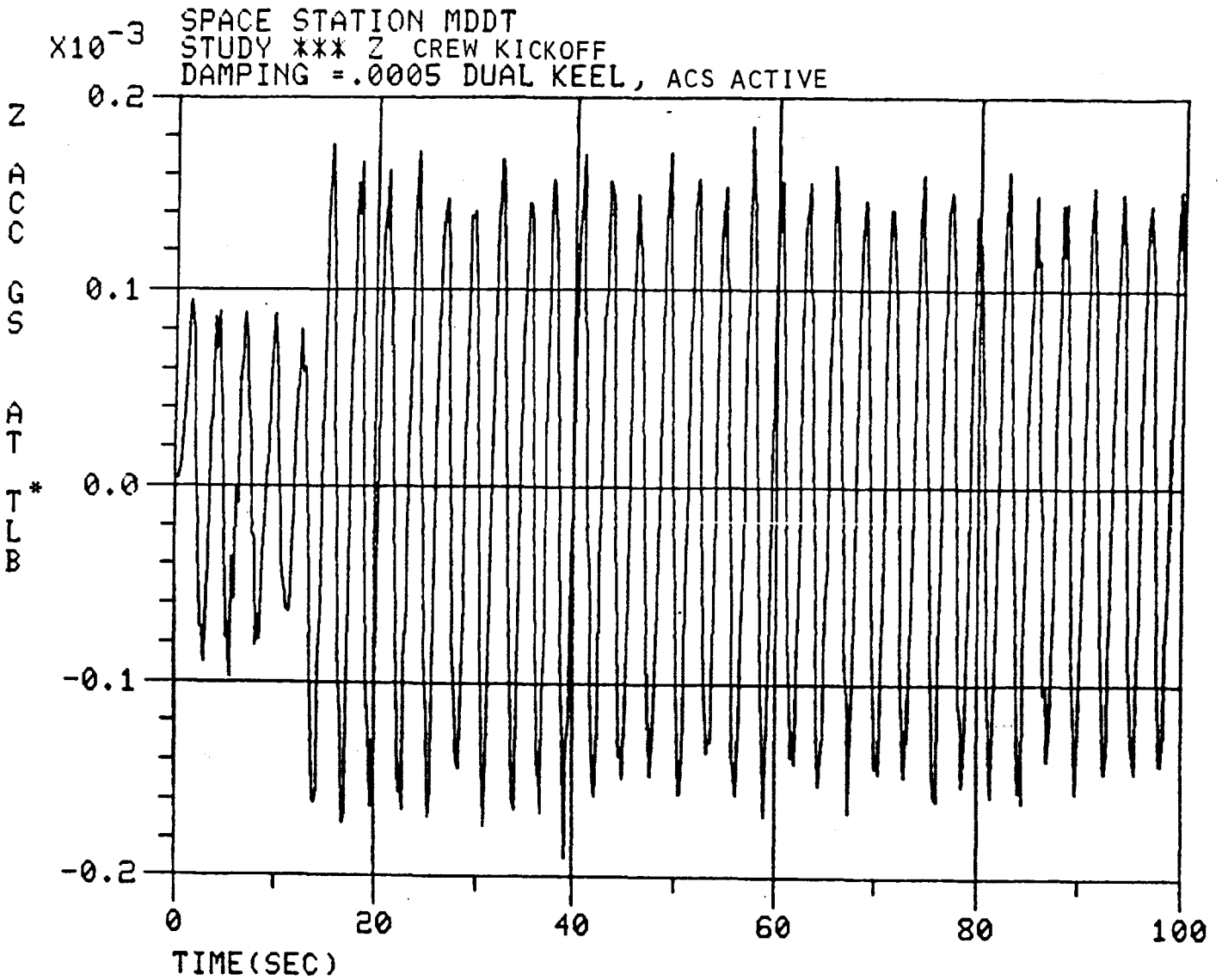

*TLB: TIP OF LOWER BOOM

Figure A-11: Shuttle Docking, ACS Inactive, ACS X-axis Deflection.

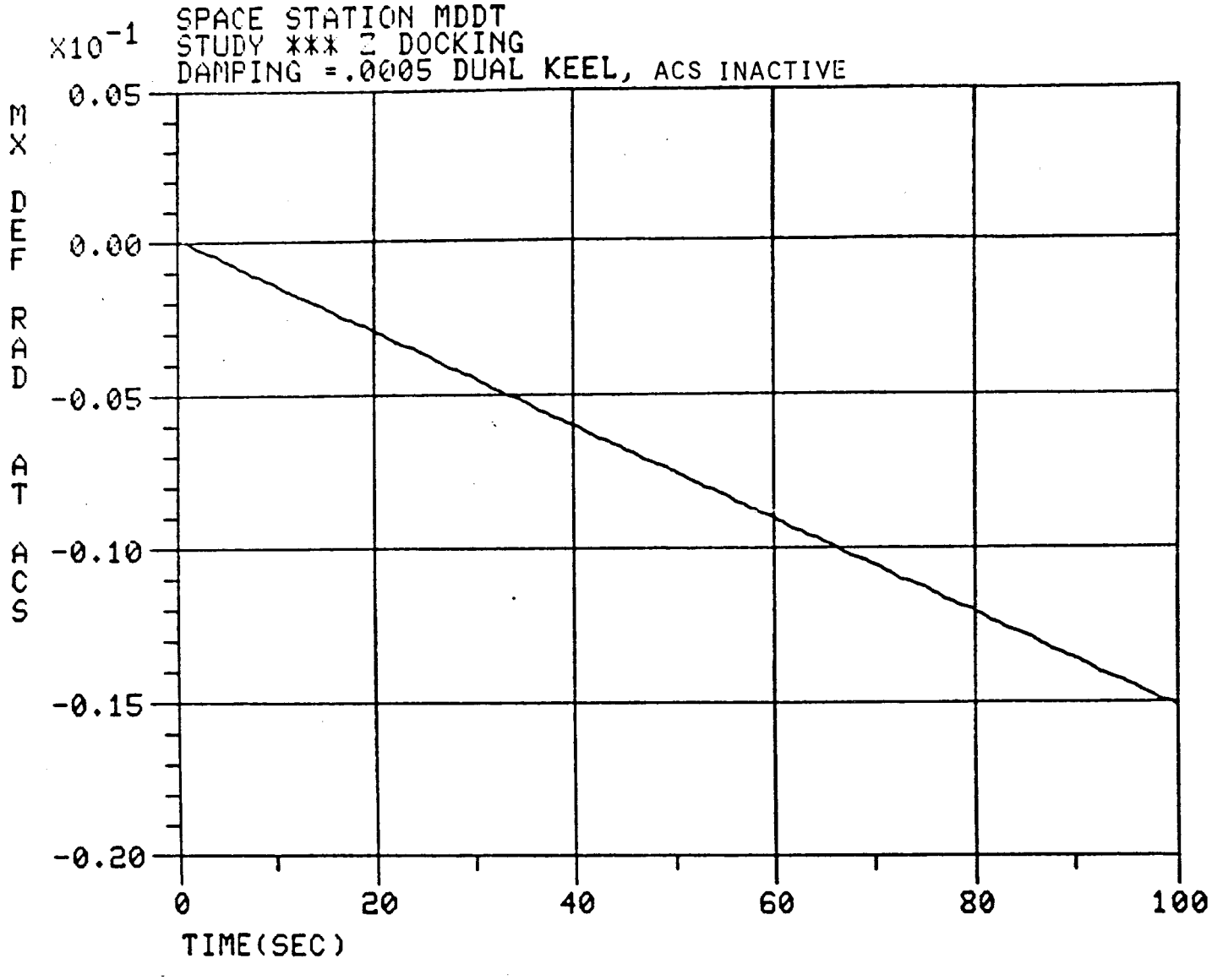

Figure A-12: Shuttle Docking, ACS Inactive, ACS Y-axis Deflection.

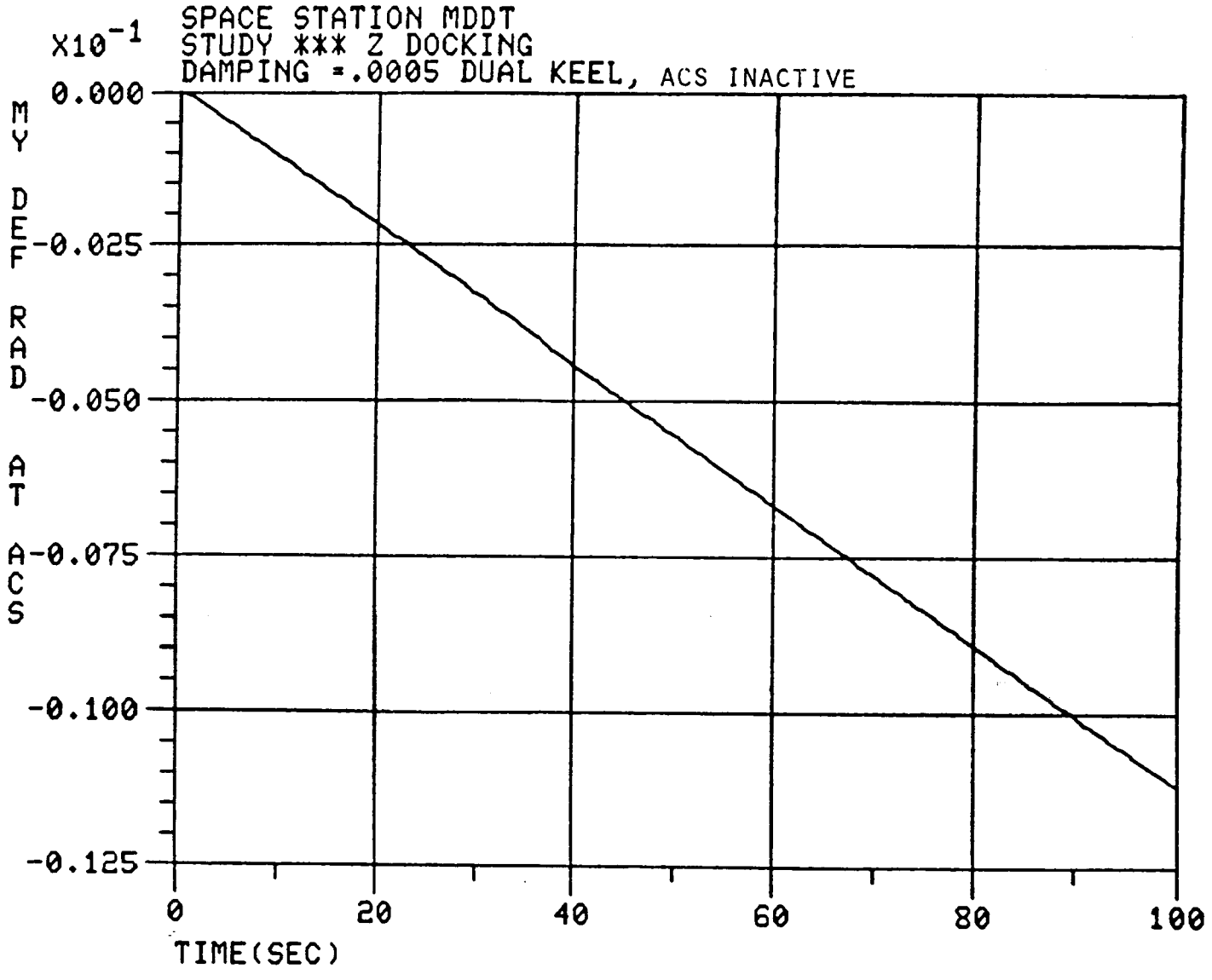

Figure A-13: Shuttle Docking, ACS Inactive, ACS Z-axis Deflection.

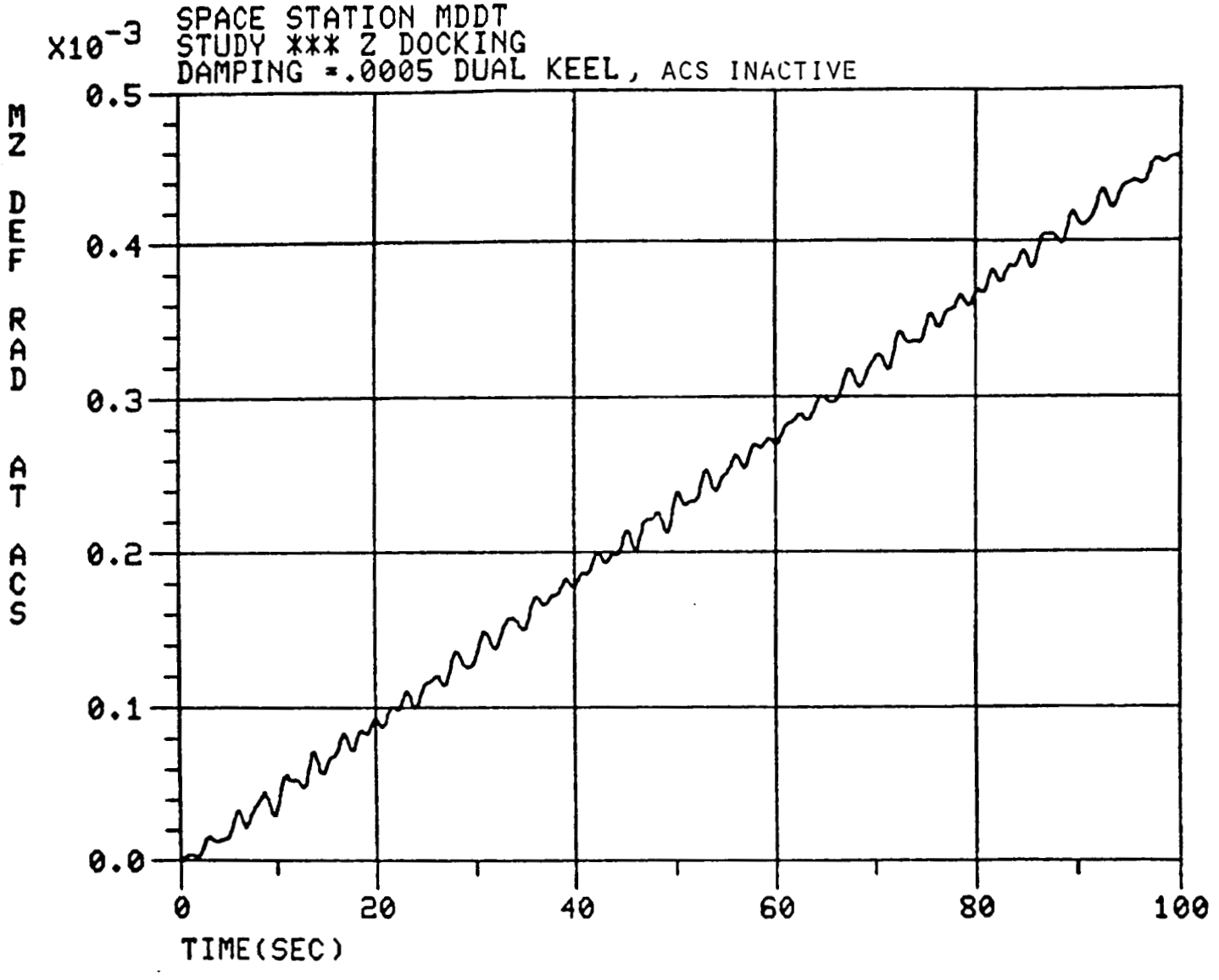

Figure A-14: Shuttle Docking, ACS Inactive, Lower Boom Tip.
Y-axis Deflection.

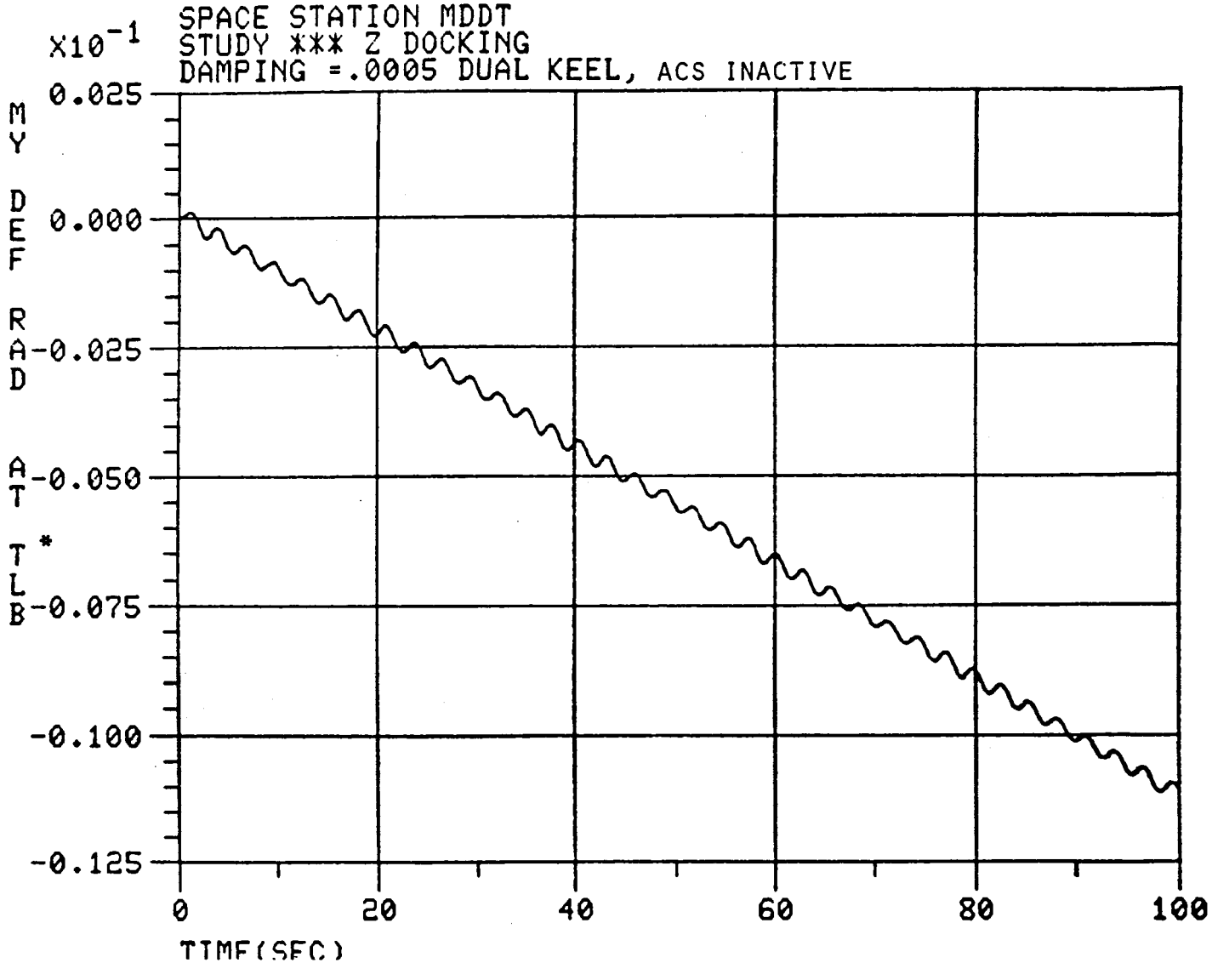

*TLB: TIP OF LOWER BOOM

C-2

Figure A-15: Shuttle Docking, ACS Inactive, Lower Boom Tip. Z-axis Acceleration.

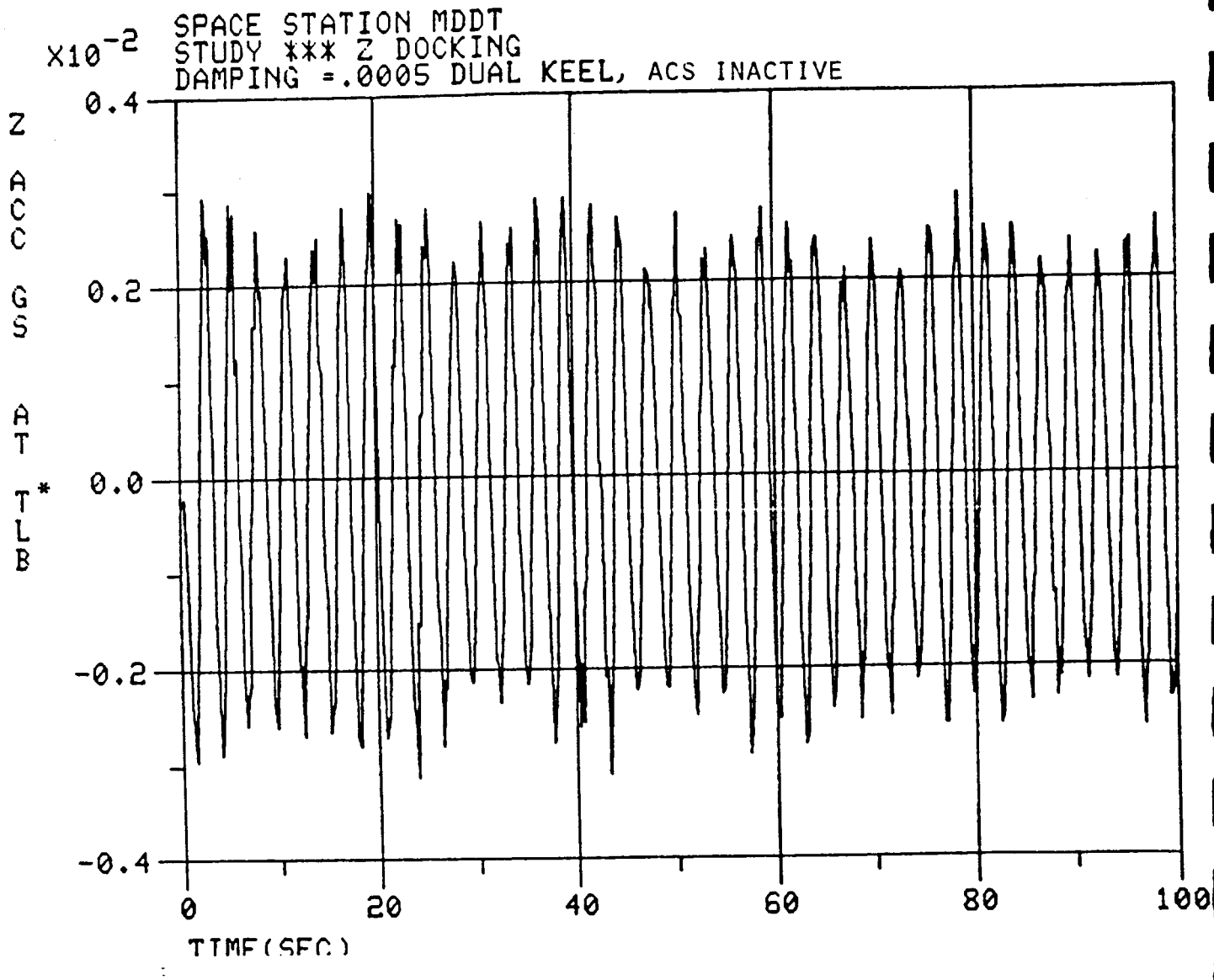

*TLB: TIP OF LOWER BOOM

Figure A-16: Shuttle Docking, ACS Active, ACS X-axis Deflection.

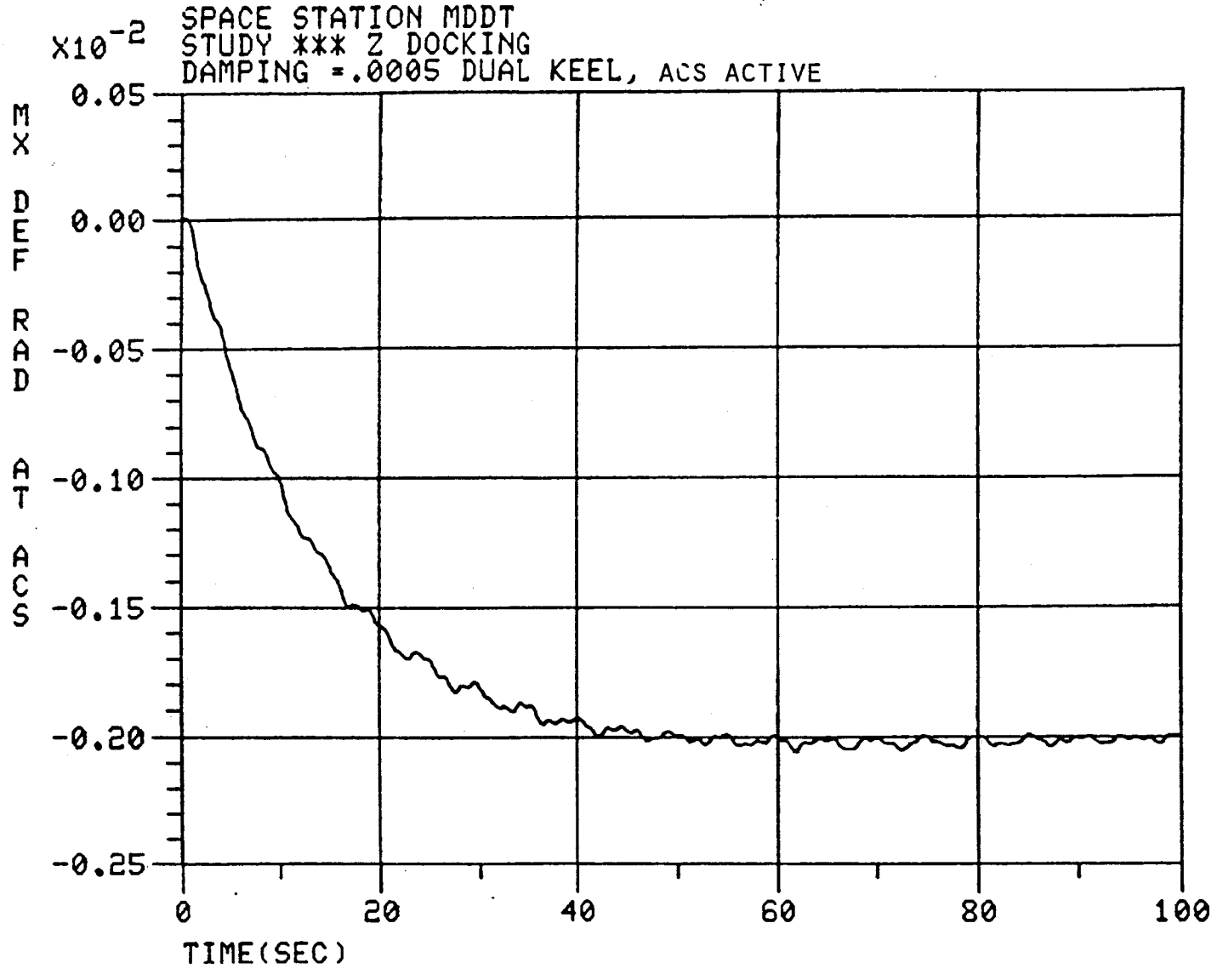

Figure A-17: Shuttle Docking, ACS Active, ACS Y-axis Deflection.

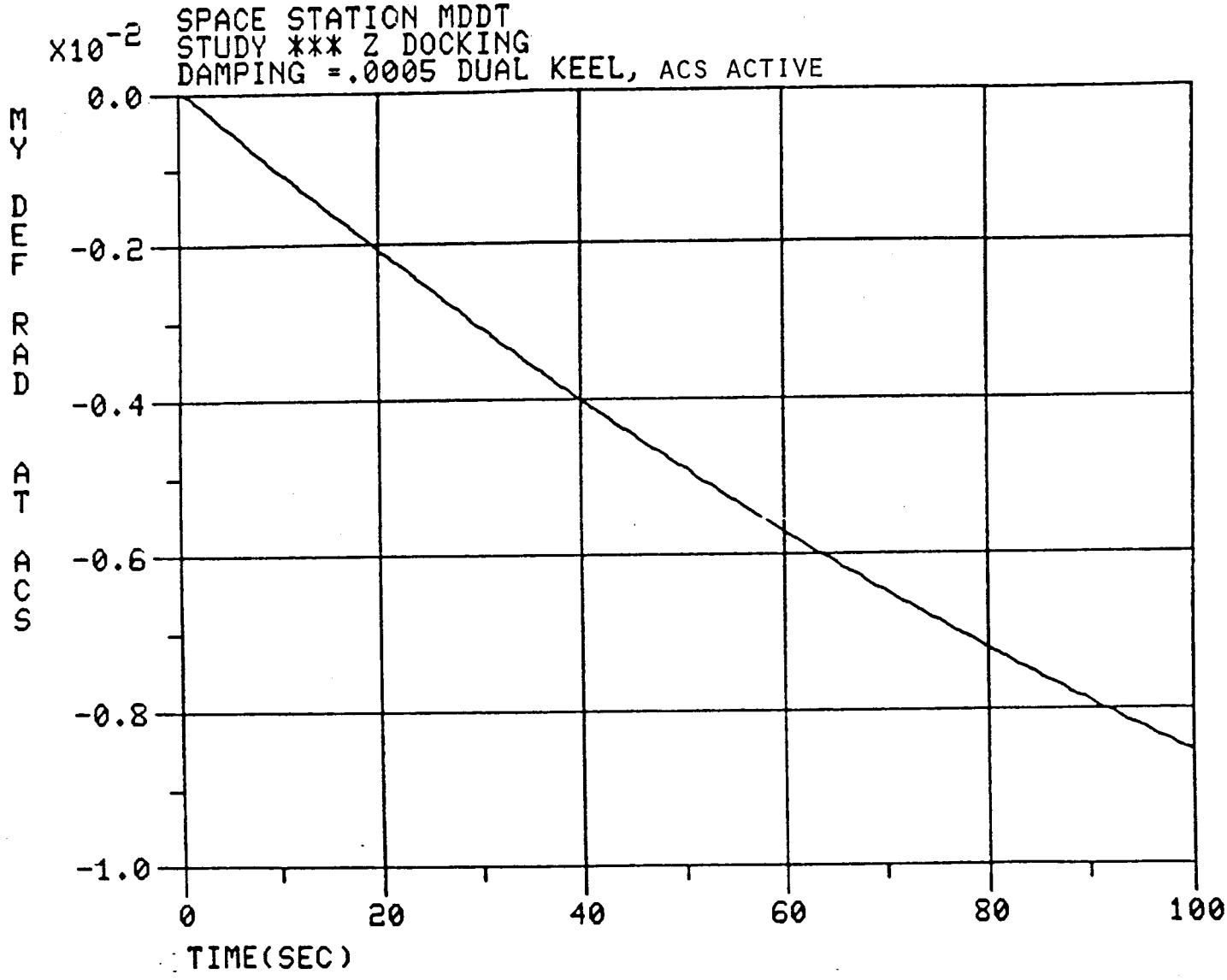

Figure A-18: Shuttle Docking, ACS Active, ACS Z-axis Deflection.

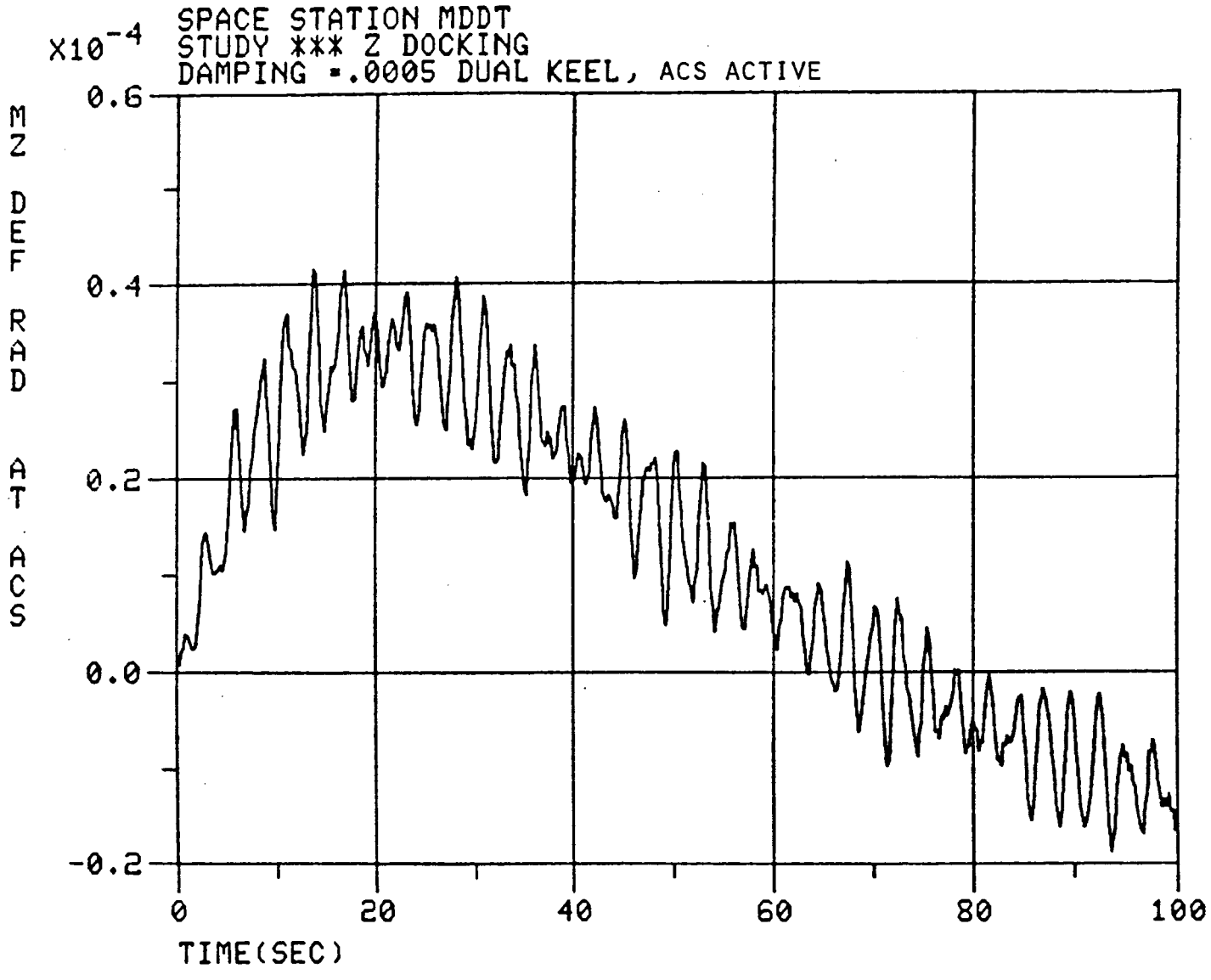

Figure A-19: Shuttle Docking, ACS Active, Lower Boom Tip.
Y-axis Deflection.

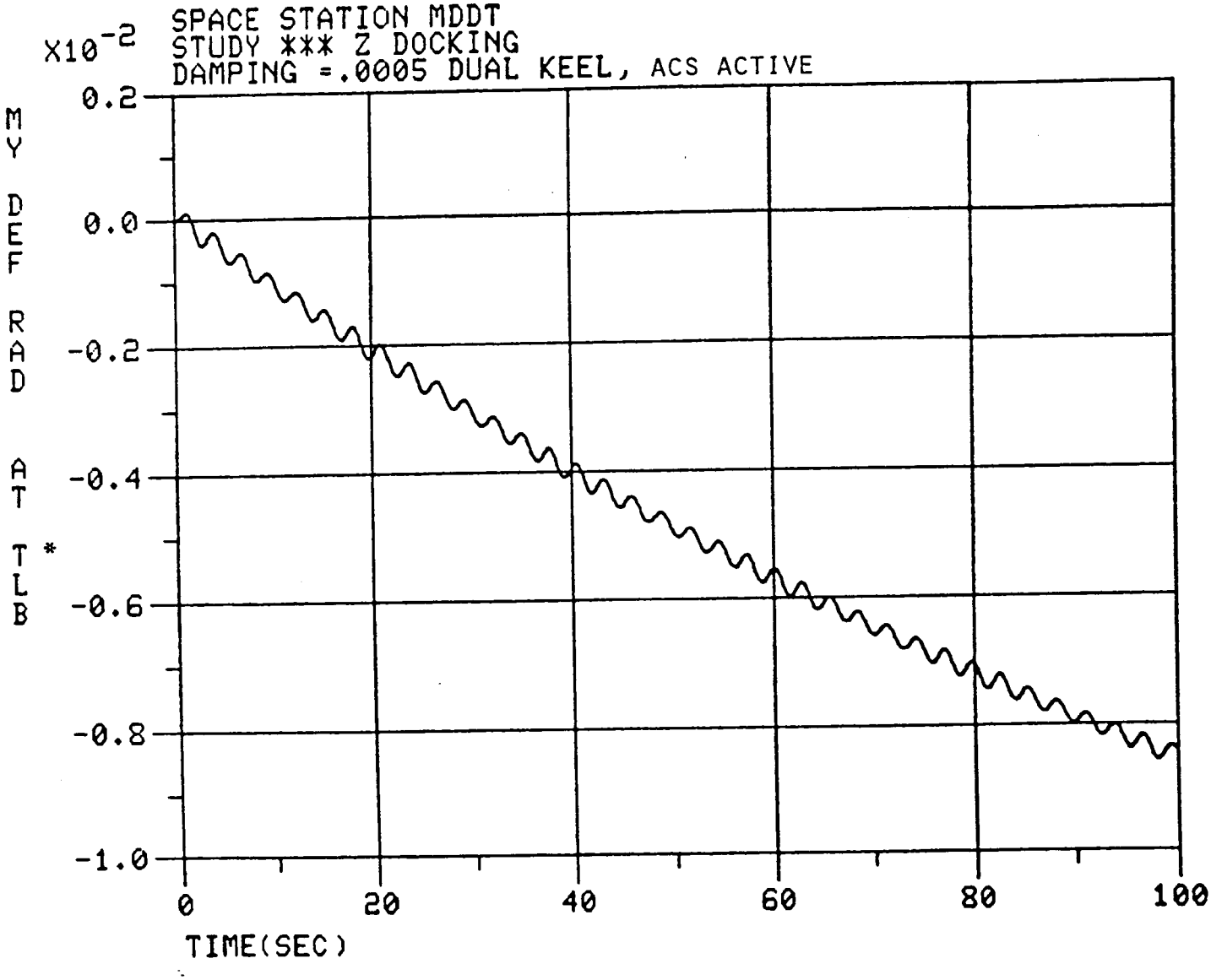

*TLB: TIP OF LOWER BOOM

Figure A-20: Shuttle Docking, ACS Active, Lower Boom Tip.
Z-axis Acceleration.

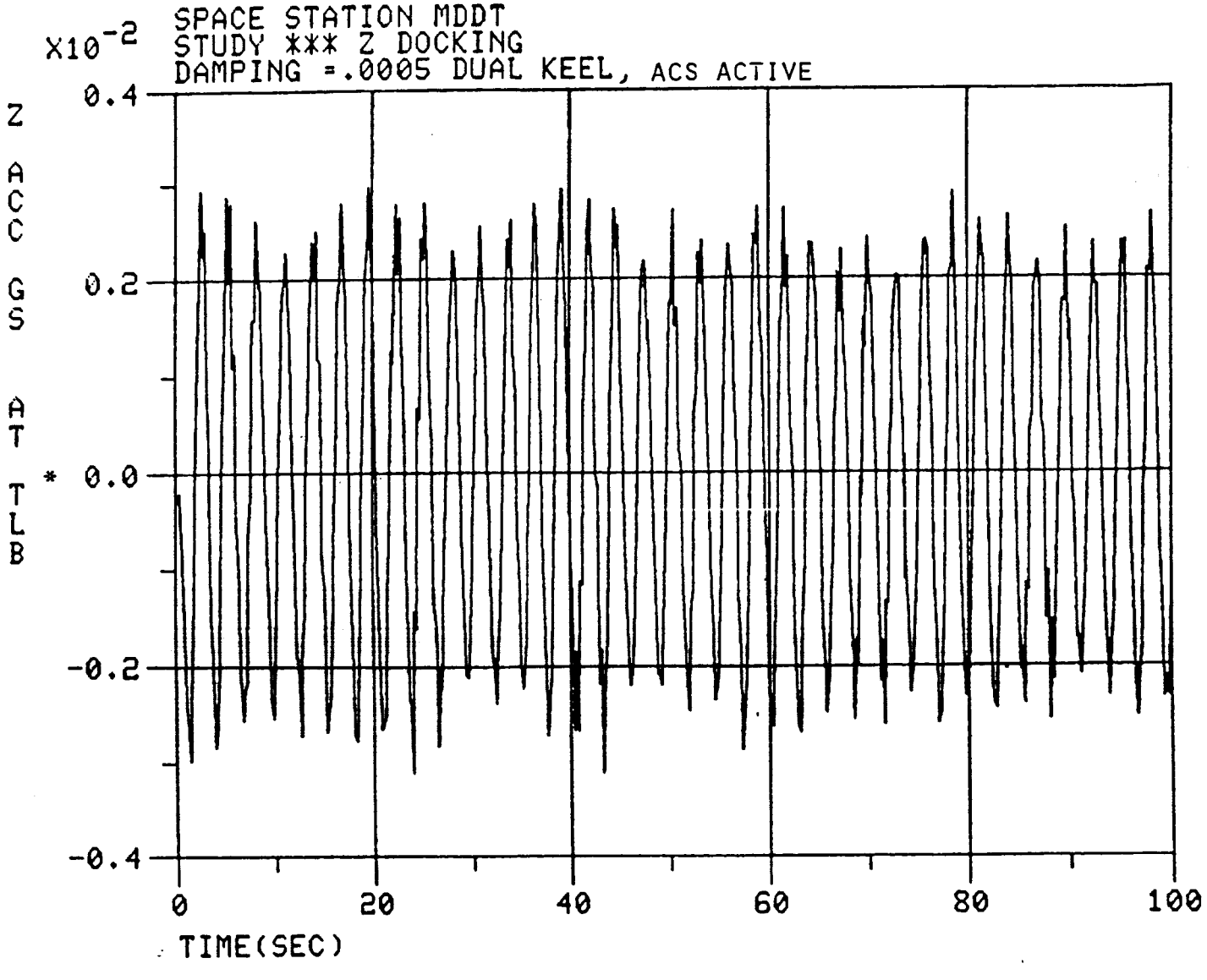

*TLB: TIP OF LOWER BOOM

APPENDIX B

DUAL KEEL REFERENCE CONFIGURATION ACS EQUIPMENT CHARACTERISTICS

FIGURE B-1: DUAL KEEL REFERENCE CONFIGURATION
ACS EQUIPMENT CHARACTERISTICS*

WP-02 EQUIPMENT LIST IDENTIFICATION	UNIT	NO. OF UNITS [3]	DIMENSIONS PER UNIT (INCHES)	VOLUME TOTAL (CU FT)	WEIGHT TOTAL (LBS)	AVG PWR TOTAL [3] (WATTS)	PEAK PWR TOTAL [3] (WATTS)
1.1.2.3.22.A.A	CMG(3500 FT LB SEC) [5]	12 (0)	53(SPHERE)	541.32	6613.20	1908.00	2200.00
1.1.2.3.22.A.G	STAR TRACKER TRIAD [4]	1 (1)	13x13x12	2.34	40.00	12.00	15.00
1.1.2.3.22.A.E	ISA (HEXAD)	1 (0)	12x12x12	1.00	100.00	120.00	150.00
1.1.2.3.22.A.F	ISA (TRIAD)	2 (0)	12x8x12	1.34	75.00	100.00	120.00
1.1.2.3.22.A.H	HORIZON SCANNER	2 (2)	3x3x5	0.10	9.00	2.00	2.50
1.1.2.3.22.A.D	OPT ALIGN TRANS SYS	6 (0)	TBD	0.00	0.00	0.00	0.00
1.1.2.3.22.A.B	RCS ELETRONICS	4 (0)	18x9x6	2.25	104.00	80.00	120.00
1.1.2.3.22.A.L	GN&C PROCESSOR [4]	3 (1)	7x9x9	1.31	80.00	133.33	173.33
1.1.2.3.22.B.A	TRAF CONT PROCESSOR [4]	3 (1)	7x9x9	1.31	80.00	133.33	173.33
1.1.2.3.22.A.C	PAYLOAD CMD PROCESSOR	2 (0)	18x8x6	1.00	48.00	50.00	70.00
1.1.2.3.22.A.J	SENSOR ELECTRONICS	1 (1)	7x7x3.2	0.18	7.90	10.00	12.00
1.1.2.3.22.A.M	GN&C DATA BUS	TBD	TBD	0.00	0.00	0.00	0.00
				552.15	7157.10	2548.67	3036.16

NOTES:
1 OPTICS AND SENSOR PROCESSING, NO SUN SHADES
2 THE FIRST NUMBER IS THE NUMBER OF ACTIVE UNITS, THE SECOND NUMBER IS THE NUMBER OF COLD SPARES
3 POWER FOR ACTIVE UNITS ONLY
4 REFERENCE SPACE STATION DEFINITION AND PRELIMINARY DESIGN WP-02, DATA PACKAGE 2.3 (DR-19), BOOK 1 PARAGRAPH 2.2 DMS
5 SPIN UP POWER 320 WATTS PER CMG; PEAK TRANSIENT POWER 1083 WATTS PER CMG (SPIN MOTOR, IGA, AND OGA DRIVE MAXIMUN RATE; AND HEATERS ON)

*REFERENCE 5

Standard Bibliographic Page

1. Report No.	2. Government Accession No.	3. Recipient's Catalog No.
NASA CR-178192		

4. Title and Subtitle	5. Report Date
The Multi-Disciplinary Design Study - A Life Cycle Cost Algorithm	May, 1987
	6. Performing Organization Code
7. Author(s)	8. Performing Organization Report No.
R.R. Harding, J.M. Duran, R.R. Kauffman	87SDS024
9. Performing Organization Name and Address	10. Work Unit No.
General Electric Company - Astro Space Division 230 Goddard Boulevard King of Prussia, PA 19406	11. Contract or Grant No. NAS1-18032
12. Sponsoring Agency Name and Address	13. Type of Report and Period Covered
National Aeronautics and Space Administration Washington, D.C. 20546	Contractor Report
	14. Sponsoring Agency Code

15. Supplementary Notes

Langley Technical Monitor: James L. Williams
Final Report

16. Abstract

Life-cycle cost (LCC) is investigated as a comprehensive design criterion for two major interrelated spacecraft subsystems, Controls and Structures. A Multi-Disciplinary Design Tool (MDDT) is developed to evaluate the sensitivity of LCC to subsystem design parameters. Major costs addressed are: non-recurring; launch; ground support; maintenance; expendables; and software. Examples and results from the MDDT are described, including a structural optimization study between different truss designs; a solar array feathering trade for a minimal drag configuration during umbra; and the cost of active control of a flexible structure is compared against the cost of passive damping using visco-elastic material.

17. Key Words (Suggested by Authors(s))	18. Distribution Statement
Life-cycle cost, Multi-Disciplinary Design, design criterion, cost sensitivity, attitude control sub-system, structures subsystem, space station	Unclassified - Unlimited

19. Security Classif.(of this report)	20. Security Classif.(of this page)	21. No. of Pages	22. Price
Unclassified	Unclassified	105	

For sale by the National Technical Information Service, Springfield, Virginia 22161